Charles University in Prague

Faculty of Science

Department of Genetics and Microbiology

Study programme: Biology

Branch of study: Genetics, Molecular Biology and Virology

Specialization: Molecular Biology and Genetics of Eukaryotes

Adam Hlaváček

Úloha translačních elongačních faktorů v dynamice stresových granulí

Role of translational elongation factors in dynamics of stress granules

Master's thesis

Supervisors: Ing. Jiří Hašek, Ph.D., Ing. Pavla Vašicová, Ph.D.

Prague 2015

Prohlášení

Prohlašuji, že jsem danou magisterskou práci zpracoval samostatně a že jsem uvedl všechny použité informační zdroje a literaturu. Tato práce ani její podstatná část nebyla předložena k získání jiného nebo stejného akademického titulu.

V Praze, 14.8.2015 ……

Adam Hlaváček

Acknowledgments

I would like to thank to everybody who helped me to get here and supported me thru my study. To my supervisors, Jiří Hašek and Pavla Vašicová, for their patience, advices and guidance. To all the lab members of Laboratory of Cell Reproductionion for a great time I had with them these past two years. Last, but not least, I would like to thank to my friends and family for their support, for without them none of this would be possible. Thank you.

Table of Contents

Abstract

eIF5A seems to be involved in both, translation initiation and elongation. It was also reported to affect assembly of P-bodies. Given similarities of P-bodies with stress granules (SGs) we decided to test the role of eIF5A in dynamics of heat-induced SGs and its implications for the cell recovery. For the evaluation of eIF5A function in SGs formation was used the temperature- sensitive (ts) mutant eIF5A-3 (C39Y/G118D) cultivated under permissive temperature 25°C and Rpg1-GFP fusion protein as a marker of SGs. The cells were exposed to robust heat shock at 46°C for 10 minutes. The ability of the mutant cells to recover was tested by propidium iodine staining and colony forming units plating. We found that the eIF5A-3 mutant forms heat-induced SGs more loosely aggregated, indicating that the fully functional eIF5A is necessary for SGs assembly. However, it does not seem to affect the rate of SGs dissolution. Survival tests indicate that eIF5A-3 mutant cells are susceptible to dying in a similar way as WT cells; nevertheless, their ability to resume proliferation is significantly better. We also observed a loss of the ts phenotype of the eIF5A-3 mutant. This loss cannot be explained by reversion of mutated eIF5A sequence into normal. Probable cause lies in the adaptive evolution. Our results indicate role of eIF5A in actin dynamics. We suggest that role of eIF5A in SGs assembly might help to elucidate its function.

Key words: translation, heat stress granules, actin, elongation, factors

Abstrakt

Translační faktor eIF5A se pravděpodobně podílí na iniciaci i elongaci. Existují také zmínky o jeho roli v tvorbě P-bodies. Vzhledem k podobnosti P-bodies a stressových granulí (SGs) jsme se rozhodli otestovat roli eIF5A v dynamice teplem-navozených SGs a jeho důsledky pro zotavení buněk. Pro hodnocení funkce eIF5A v tvorbě SGs byla použita teplotně citlivá (ts) mutanta eIF5A-3 (C39Y/G188D) kultivovaná za permisivní teploty 25°C, s Rpg1-GFP fúzním proteinem jako značkou SGs. Buňky byly vystaveny robustnímu tepelnému šoku 46°C po 10 minut. Schopnost mutovaných buněk přežít byla testována propidium iodidovým barvením a výsevem jednotek tvořících kolonie (CFU). Zjistili jsme, že mutanta eIF5A-3 tvoří teplem navozené SGs, které agregují volněji. To naznačuje, že pro skládání SGs je nutný plně funkční eIF5A. Nicméně mutace nejeví dopad na míru rozpouštění SGs. Testy přežívání ukazují, že mutanta eIF5A-3 je citlivá vůči buněčné smrti obdobně jako WT buňky, avšak její schopnost znovu nastolit proliferaci je znatelně lepší. Pozorovali jsme také ztrátu ts fenotypu eIF5A-3 mutanty. Tyto změny vlastností nebyly způsobeny zpětnou změnou mutované sekvence genů pro eIF5A. Jejich pravděpodobná příčina leží v adaptivní evoluci. Naše výsledky také naznačují účast eIF5A v aktinové dynamice. Navrhujeme, že účast eIF5A v skládání SGs může pomoci porozumění jeho funkce.

Klíčová slova: translace, teplotní stresové granule, aktin, elongace, faktory

.

List of abrevations

ARE	AU rich element
ABP	Actin-binding protein
ARE-BP	AU rich element - binding protein
AUG	start codone (adenin-uracil-adenin)
CHX	cycloheximide
DNA	deoxyribonucleic acid
eIF	eukaryotic initiation factor
GCN	general control non repressed
GDP	guanosin diphosphate
GEF	GTP exchange factor
GFP	green fluorescent protein
GTP	guanosin triphosphate
HuR	human antigen R
IRES	internal ribosome entry site
Met-tRNAiMet	methionyl initiator tRNA
miRNA	micro RNA
MRE	miRNA response element
mRNA	messenger RNA
rRNA	ribosomal RNA
tRNA	transfer RNA
mTOR	mammalian target of rapamycin
m7G	7-methylguanosine
PABP	poly(A)-binding protein
PIC	pre-initiation complex
PI	Proprium iodine
poly(A)	polyadenosine
P site	peptdyl site
P-body	Processing body
RNA	ribonucleic acid
S	Svedberg, unit of sedimentation coeficient

SG	Stress granule
TC	ternary complex
TIA	T cell inflamatory antigen
TIAR	TIA-related protein
ts	temperature sensitive
UTR	untranslated region
4E-BP	eIF4E-binding protein
40S	eukaryotic small ribosomal subunit
43S	pre-initiation complex
48S	pre-initiation compex with attached mRNA
60S	eukaryotic large ribosomal subunit
80S	assembled ribosome 40S + 60S subunit

1 Introduction

Translational control is a complex process influencing translational rate of cytoplasmic mRNAs. Already as they are transcribed, mRNAs are enveloped in coat of RNA-binding proteins that are correlated with localization, degradation and translational efficiency in cytoplasm. mRNA molecules with their coat proteins and other proteins functionally related to mRNA biology tend to accumulate together and form specialized intracellular compartments that are not surrounded by membrane. These compartments are known as mRNP foci. Cytoplasmic mRNP foci are known for a relatively long time to be a part of translational control mechanisms. Most notorious examples of these cytoplasmic macromolecular aggregates, collectively called RNA granules, are P-bodies and stress granules (SGs).

Translational control gains an increasing attention in recent years, since growing amount of evidence indicates a substantial role of the post-transcriptional regulation in the phenotype of the cell. Within its response time in range of minutes and tens of minutes, it lies between the quickly mediated response executed in matter of seconds by post-translational modifications, like phosphorylation, and considerably slower transcriptional regulations, which often take hours to express themselves in the proteome. Translational control is a mechanism especially suitable for the response to stress conditions, but its usefulness is not restricted only to stress. Mechanisms that are implied in cell development and activation share some significant similarities. For instance the activation of many immune system cells and initial stages of immune response share a substantial similarity with stress response and share many control mechanisms. Other known examples of translational control and its significance are: (i) cells without functional nucleus, such as hematocytes and platelets; (ii) long-term memory storage in neurons; and finally (iii) translational changes accompanying metamorphosis of terminally differentiated cell, the egg, into omnipotent zygote after fertilization.

Stress granules form in cytoplasm of cells exposed to environmental stresses (heat, oxidative conditions, UV irradiation, hypoxia, osmotic shock, low levels of nutrients, etc.). SGs are part of the mRNA metabolism reprogramming under stress. However, their exact role, structure and molecular mechanism are still unknown. This matter is caused partly due to the incredible plethora, around one hundred, of proteins that are reported to localize into SGs and partly due to relatively loose nature of the interactions that prohibits the use of robust biochemical methods.

The research in the Laboratory of Cell Reproduction of the Institute of Microbiology of the CAS focuses on heat stress response of *Saccharomyces cerevisiae* regarding translation and mRNA

metabolism. Understanding of fundamental processes influencing mRNP foci formation in yeast can be of great value. Notwithstanding the obvious value of knowing more about the biology of the cell and it's amazing changeability by itself, better understanding of the stress granule aggregation could ultimately lead to better understanding of many phenomena such as: processes leading to various pathologies, many of them neurological, activation of specific mRNA pool expression and cell survival decisions in cells under stress conditions and at the specific stages of the cell development or differentiation.

2 Aims of the Thesis

Aims of this master's thesis include elucidation of the translation elongation factor eIF5A role in dynamics of heat-induced stress granules and its importance for the ability of *Saccharomyces cerevisiae* cells to recover from the heat shock.

3 Literature Review

3.1 Translation

Translation is a fundamental cellular process and a final step in gene expression. Translational apparatus decodes sequences of ribonucleic acids and catalyzes the formation of peptide bond between aminacids in proteins. Translation can be divided into four distinct phases: initiation, elongation, termination and ribosome recycling. Each of these steps requires specific factors – proteins and protein complexes with vital functions for each and every step. Initiation and elongation are major subjects of study, and are also emphasized in this chapter.

The textbook cap-dependent translation initiation in Eukaryotes is a series of steps beginning with the activation of ribosome, more precisely of small ribosomal subunit 40S, and with the activation of mRNA. Followed by scanning of mRNA by 40S subunit, recognition of START codone AUG, joining of the large ribosomal subunit 60S to form fully functional 80S ribosome bound to mRNA and synthesis of the first peptide bond. Activation of the ribosome starts with the assembly of a ternary complex (TC) from Met-tRNA$_i^{Met}$, eIF2 and GTP bound to eIF2. eIF2 is GTPase protein. In order to associate with Met-tRNA$_i^{Met}$ effectively, eIF2 has to be in its GTP form (eIF2-GTP) (Levin et al. 1973) GTPase activity is increased by eIF5 later on in process of AUG recognition and lock-on (Yamamoto et al. 2005). Ternary complex, 40S subunit and initiation factors eIF1, eIF1A, eIF3 and eIF5 together form the 43S Pre-Initiation Complex (PIC). The eIF3 complex has a crucial role as a scaffold that brings all other eIFs and ribosomal subunits together. The factor eIF1 is required for the AUG codon recognition, eIF1A supports Met-tRNA$_i^{Met}$ binding to 40S subunit and eIF5 stimulates eIF2 GTPase activity after AUG recognition (reviewed in (Valášek 2012). Subsequently the 43S PIC binds to activated mRNA and forms the 48S complex. The activaton of mRNA is conducted by the eIF4F complex, that is composed from eIF4E, eIF4A and eIF4G factors. eIF4E binds the cap structure and can be negatively regulated by phosphorylation or by binding of eIF4E-binding proteins (4E-BPs) that inhibits the eIF4F complex formation and thus strongly represses translation (Haghighat et al. 1995). eIF4A has a helicase function that creates a landing pad for the 40S ribosomal subunit on mRNA. The eIF4A helicase activity is also needed on the 5’ UTRs with a rich secondary structure (Pestova and Kolupaeva 2002).The factor eIF4G serves as a scaffold mediating interaction between eIF3 and the rest of the eIF4F complex.

The next step in initiation is scanning o mRNA molecules by the 48S complex from the cap structure at 5’ end to 3’ end, until recognition of the START codon with proper Kozak consensus. Upon the AUG codon recognition, eIF5 promotes the GTP hydrolyses in eIF2, this leads to

dissociation of initiation factors and joining the large ribosomal 60S subunit, leading to formation of a complete 80S ribosome. Ribosome is bound to mRNA with Met-tRNA$_i^{Met}$ occupying the P-site (peptide site) and ready to receive the fist aminoacyl-tRNA into A-site (amino acid site) and for formation of the first peptide bond.

Elongation is the process of peptide bond formation and transfer of peptidyl-tRNA from A-site to P-site accompanied by movement of the ribosome along the mRNA strand for three nucleotides per step. eEF1A factor catalyses the binding of aminoacyl-tRNA into A-site. eEF1A has internal GTPase activity and affinity to actin. Aminoacyl-tRNA binding is mutually exclusive with F-actin binding. Second elongation factor directly influencing the elongation is the eEF2, GTPase responsible for translocation of peptidyl-tRNA from A-site to P-site and movment of whole ribosome by 3 nucleotides alongside mRNA. Third translational factor promoting the efficiency of elongation is the eIF5A, although not necessary for elongation in general, it is crucial for some specific transcripts. Specifics of the eIF5A role are covered in a separate chapter (reviewed in (Mateyak and Kinzy 2010)).

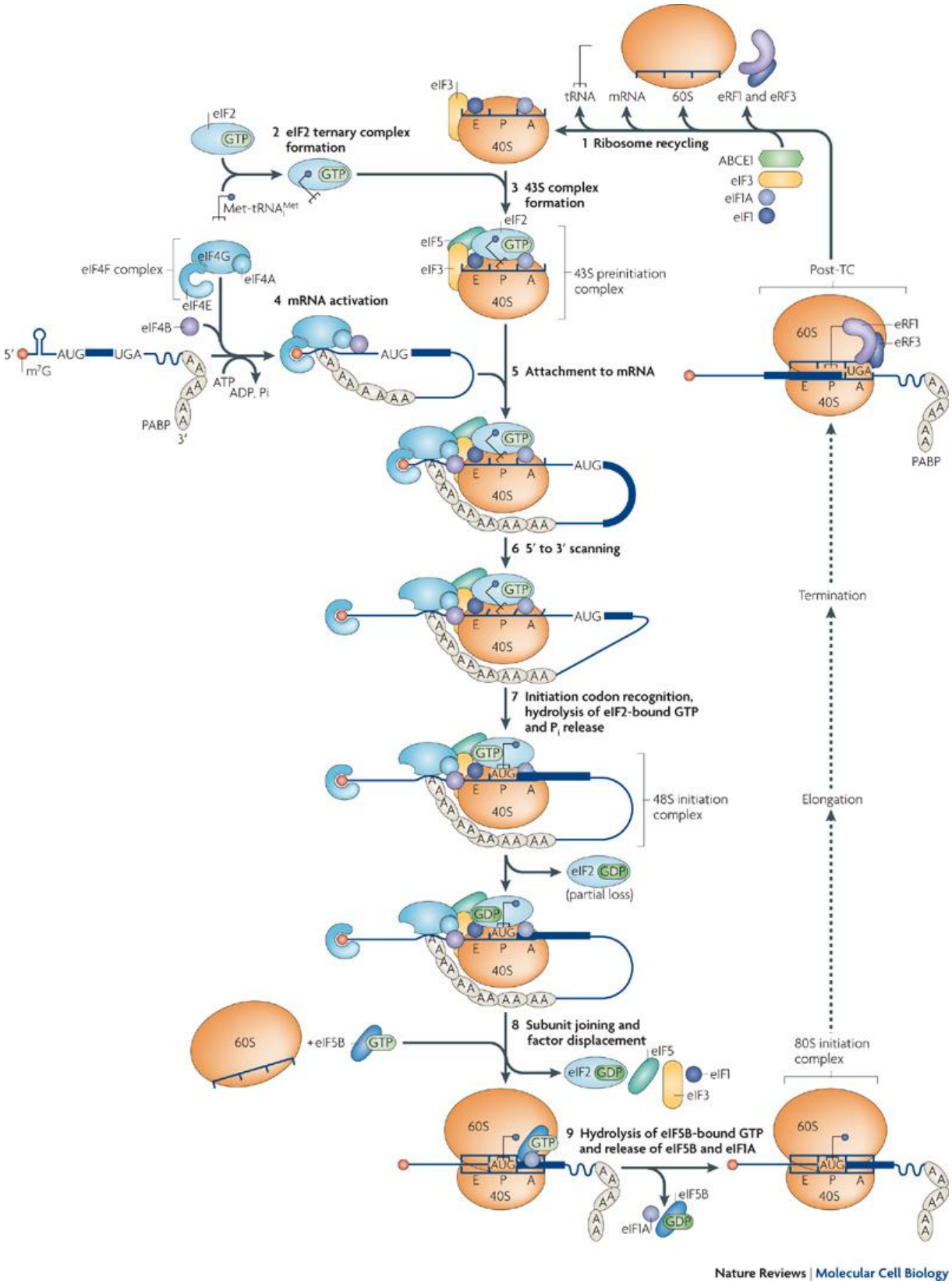

Figure 1. Model of the canonical pathway of eukaryotic translation initiation. Adapted from (Jackson et al. 2010)

3.1.1 Translational controls in *S.cerevisiae* – regulatory mechanisms

The main reasons for the utilization of the translational control in regulation of gene expression are its immediacy, accuracy, efficiency and redundancy. Translational control affects the cellular phenotype in matter of minutes. The translational control can also achieve much more precise regulation and fine tuning at the late stage of the gene expression than transcriptional control at the beginning of gene expression. It can act in combination with the transcriptional control to ensure that expression of toxic or proliferation stimulating proteins is strictly regulated on multiple levels and that they are expressed only when needed (Brant-Zawadzki et al. 2007).

Translational control mechanisms can be viewed as modifications that alter the translation efficiency of both single and multiple mRNA species. The translational efficiency is defined as number of complete protein products per mRNA molecule per unit of time. Under ideal conditions the only limiting factor for translation would be its initiation. This is the reason why it is a critical point for the translation regulation. Proteosyntesis levels are influenced by a number of different mechanisms; some of the most important are mentioned in this chapter.

The effectivity of the protein synthetic machinery is limited by the abundance and activity of the least abundant and active translational component (translation factor). This regulatory mechanism is often based on phosphorylation induced conformational changes and is strongly supported by a high proportion of phosphoproteins in ranks of translation factors. Elongation rate can also substantially influence the efficiency of translation. In order to assembly the ribosome at the 5’ end of mRNA, it requires certain length of free nucleotides as a landing pad for its mounting. If the elongation rate at this segment decreases so does the rate of initiation events on this mRNA.

Other limiting factor for translation is represented by constrains in the amount of mRNA substrate or in the mRNA translational efficiency. mRNA transcripts are subjected to many regulatory steps that ensure their proper cellular spacio-temporal distribution. The amount of mRNA substrates in cytoplasm is governed by their export from the nucleus and their half-life in cytoplasm. The mRNA half-life is often directly linked with the mRNA translational efficiency. Finally, under specific conditions the translation rate can be also limited by the abundance of functional ribosome subunits. mRNA utilization is specifically directed by cis-elements that influence the mRNA on their own or in synergy with trans-acting factors, usually RNA binding proteins, but also small non-coding RNA molecules. Cis-elements are present in both 5’ UTR and 3’ UTR.

The 5’ UTR can contain various cis- acting elements that contribute to both general and specific translational control. 5’ UTR cis-elements are: (i) the 7-methylguanosine (m7G) cap structure,

(ii) primary sequence context of the start codon, (iii) upstream open reading frames (uORFs), (iv) specific secondary structures, (v) internal ribosomal entry sites (IRES) and others. The last but not least important attribute of 5' UTR is simply its length. It has to be sufficient to support ribosome loading as the translation becomes more efficient with increasing length of 5' UTR. In majority of higher eukaryotic mRNAs the 5' UTR length varies from 20 to 60 nucleotides, but 5' UTRs as long as 450 nucleotides are not exceptional (Connor and Lyles 2002).

3' UTR also harbors many structures important for translational control. The most important feature is the polyadenosine (poly(A)) tail at the very 3' end of mRNA. Length of poly(A) tail influences a half-life of mRNA and through its interaction with poly(A) binding protein (PABP) also translational efficiency. There are also other means of translational control operating at 3' UTR. Micro RNAs (miRNAs), although not present in yeast, are small non-coding RNAs, which interfere with translation and destabilize transcripts by binding to partially complementary sequence in the 3' UTR called miRNA response elements (MRE). 3' UTRs contain also various binding sites for proteins with RNA binding domains, for instance AU-rich elements (ARE). These cis-acting elements attract AU rich element binding proteins (ARE-BPs) that can alter the mRNA half-life through interactions with nucleases. And since the mRNA is circularized during translation they can also interact with eIFs at 5' UTR and affect the translational rates (Nakagawa 2008).

3.1.2 Translational controls in stressed cells

Since the translation is a final step of gene expression and also, with consumption of four macroergic bonds per one peptide bond, very energetically demanding, it comes as no surprise that it is subjected to stringent controls, enabling cell to respond to various internal and external stimuli. This controlling process can be divided to specific and general mechanisms based on the pool of mRNAs they affect (Sonenberg and Hinnebusch 2009).

General control mechanisms are regulated by availability of ribosomes, cytoplasmic pool of available and active translation factors, aminoacyl synthetases and tRNAs. Probably the most common and crucial reaction to stress is immediate and general decrease in levels of translation initiation, leading to its shut-down. This process is governed by phosphorylation state of the eIF2α translation initiation factor. The eIF2α is, as mentioned in a previous section, protein with intrinsic GTPase activity. A pool of the eIF2α-GTP is limiting for the initiation step of translation. Exchange of GDP for GTP is provided by the eIF2B factor. Phosphorylated eIF2α has significantly higher affinity for its GTP Exchange Factor (GEF) than its non-phosphorylated form. It effectively inhibits renewal of the eIF2α-GTP pool and translation initiation. Physiologically relevant eIF2α phosphorylation in yeast is

ensured by kinase GCN2 (**G**eneral **C**ontrol **N**on-repressible), in higher eukaryotes there are also other specific kinases PKR, PERK and HRI (reviewed in (Proud 2005)).

Other kinase pathways significant for the translation initiation control and their targets are the MAPK (Mitogen Activated Protein Kinase) pathway leading to phosphorylation of eIF4E and 4E-BP1 via MNK kinase, under conditions permissive for growth (Chang and Karin 2001) (Uesono and Toh-E 2002), and the mTORC1 pathway leading to phosphorylation of the kinase S6K, which phosphorylates the ribosomal protein subunit S6 and other targets, and also to phosphorylation of 4E-BP1 (excellent review in ((Betz and Hall 2013) and (Simpson and Ashe 2012).

Even though, the initiation is the most pronounced point of regulation during translational cycle. It is by no means the only option for the cells to influence their levels of proteosyntesis. The rate of proteosyntesis and ribosome transit time can be heavily modified by changes in availability of active elongation factors. Both factors, eEF1A, bringing the AA-tRNA to A-site, and eEF2, translocating peptidyl-tRNA from A-site to P-site, are subjected to regulatory mechanisms. Translation ready pool of eEF1A can be influenced by both phosphorylation, GEF activity of eIF1B, changes in availability of AA-tRNAs and also by variations in the actin cytoskeleton dynamics (Pittman et al. 2009)(Gross and Kinzy 2005).

Translational controls under stress conditions are not limited to translation factors. They are also influenced by stability, and subcellular localization of translational apparatus and mRNA substrate. Translation under stress condition can be influenced by changes in tRNA and rRNA stability. tRNA is endonucleolytically cleaved in its anticodon loop. This cleavage is no part of cellular tRNA quality control and is substantially increased under stress conditions. Cleavage products effectively decrease translational levels and serve in signaling as messenger molecules (Zhang et al. 2009) (Thompson et al. 2008). tRNA molecules and the proportion of uncharged tRNA to AA-tRNA molecules are interlinked with the eIF2α inactivation, because this balance has also a sensory function due to binding of uncharged tRNA to Gcn2, which is activated by this interaction. tRNA molecules are not only cleaved but also transported back into nucleus in order to prevent translation during stress. Stress conditions also lead to diminished synthesis of ribosome components (Rudra and Warner 2004).

Based on the presence or absence of specific group of elements, mRNAs can be divided into mRNA regulons, which react in similar manner to stimuli. One of these regulons consists from mRNAs that are translated in conditions that lead to inhibition of general translation. Members of this regulon are crucial for overcoming the stress conditions and for decision of cell survival.

Elements present in 5' UTR have major impact on the translation initiation while the elements in 3' UTR influence the mRNA half-life and localization. Heat Shock Protein 70 (Hsp70) is a good example of aforementioned regulatory mechanisms. Since its mRNA localization pattern changes in favor of cytoplasm under stress conditions (Saavedra et al. 1996), the translation efficiency of HSP 70 mRNA increases with a severity of the heat shock, despite the inhibition of normal protheosyntesis. HSPs (small heat shock proteins) are often translated via IRES or ribosomal shunting (Yueh and Schneider 2000). Stability and translation levels of HSP mRNA increase under heat shock conditions.

Many of these regulatory mechanisms lead to localization of mRNAs and components of thanslaitonal machinery into stress granules and other cytoplasmatic RNA foci. Structure and function of these aggregates is discussed more into depth in the next chapter.

3.2 Stress granules

3.2.1 Various cytoplasmic RNA foci – continuous spectrum from P-bodies to SGs

Cells present on many occasions that proteins, and RNPs, specialized in different aspects of RNA metabolism and biology, often gravitate together, to form specialized foci even though they are well functional in their disperse state. Well known examples of this phenomenon can be found in nucleoplasm as nucleolus, center of rRNA metabolism and Cajal bodies, focusing splicing apparatus. Notourious cytoplasmic examples of RNA foci are P-bodies and SGs.

P-bodies and SGs are the most well known mRNP (ribonucleoprotein) foci in cytoplasm, but there is a whole continuum of structures with various compositions in-between them. The function of these foci reflects their composition; main difference is the presence, or absence, of ribosomal subunits and translation initiation factors. These other granules are present predominantly in metazoans, and are not present in yeast, but variation in their function, can approximate variation in function of differently composed SGs and PBs under different stress conditions (see below).

Other, less known mRNP are as follows. Germ cell granules retaining maternal transcripts crucial for germ cell line commitment from translationaly active pool, until embryonic development reaches appropriate stage (Schisa et al. 2001). Neuronal transport granules have similar function, they are responsible for spatially differentiated translation in neurons, granules contain silenced transcripts and both small and large ribosomal subunits. Dendritic P-body-like structures are present in the body of neuron and dendrites, these foci release retained transcripts, after nerve stimuli reaches dendritic membrane (Cougot et al. 2008).

Stress granules also contain mRNPs but differ from P bodies by the presence of factors from the 48S pre-initiation complex. More specifically, stress granules harbour: mRNPs associated with Pab1, translation initiation factors (eIF2, eIF3, eIF4A, eIF4E, eIF4G), in some cases also the 40S ribosomal subunit, RNA binding proteins (Pub1, Ngr1), mRNA decay proteins (Dcp2, Dhh1, Xrn1, Lsm12, Sus1), and a few proteins of unknown function (Pbp1, Pbp4)(Anderson and Kedersha 2006) (Buchan et al. 2008) (Balagopal and Parker 2009) (Swisher and Parker 2010) (Grousl et al. 2009).

Surprisingly, we still do not know with certainty whether the formation of SGs has beneficial or negative effect on physiology of the cell and as many times in biology the answer will be probably strongly influenced by the context. Original concept of the unambiguously positive role of SGs was impaired by the major role of defective dissolution of protein aggregates in numerous pathologies.

3.2.2 SGs assembly

Stress granules (SGs) can be perceived as a part of the mechanism that oversees translational controls and transcript turn-over in a cell. They share these, and many other, traits with another type of cytoplasmic RNA foci – P-bodies. There are however some fundamental differences between SGs and P-bodies. First and foremost difference is in the circumstances of their formation. SGs form as accumulation of translationaly repressed mRNAs, translation factors and ,in some cases, ribosomal subunits during stress, while the P-bodies form continuously in both, normal and stress conditions. Second substantial difference is in the composition of given RNA foci (for more see below). Third difference is in function, while P-bodies are canonically perceived as sites for the mRNA decay and silencing, SGs are connected with transient translational silencing, sequestration and protection of mRNAs, translation factors and ribosomal subunit. SGs also play a key role in translation restart of cells recovering from stress and also in cellular signaling.

SGs are composed mainly from the stalled translation pre-initiation complexes. The best characterized mechanism of the SGs formation is a phosphorylation of the eIF2α factor by any of its kinases, the most notorious, and also the only one of them present in yeast, is the GCN2 kinase. Phosphorylation of eIF2α leads to a decreased pool of translation-ready initiation factors and to lower levels of translation initiation. Formation of SGs can occur independently of the eIF2α phosphorylation by GCN2. An alternative mechanism was discovered in our laboratory. This mechanism is active in formation of SGs in yeast cells under robust heat shock and appears to be driven by state of translation elongation factors (Grousl et al. 2013). Formation of SGs is affected also by the polysome run-off. Major elongation factors are briskly post-translationally modified as a part of the stress response (see above). Hovewer, the hypusinated elongation factor eIF5A retains its

function even during stress, accelerates the polysome run-off and by that, it contributes to a rapid SG formation (Li et al. 2010).

The SGs formation is a gradual process. First, mRNP “seeds” are formed, abundant, microscopically barely visible aggregates that in later stage merge together to bigger stress granules (Grousl et al. 2013). Given the rapid rate of the SGs assembly/disassembly cycle, it is very likely that these processes are governed by the active cytoplasmic transport along the cytoskeleton. These claims are supported by effects of the cytoskeleton disrupting drugs, and anterograde/retrograde microtubular motors on mRNP assembly/disassembly (Loschi et al. 2009). (

Models of mRNP formation are based on phase separation or aggregation, leading to different state of RNP granule (liquid or solid). Molecular basis for mRNP cohesion in yeast SGs lies probably in self-aggregation properties of many resident proteins and mRNAs. These properties can be given by: (i) prion-related domains, as in case of TIAR. These results are disputed by Sup35p (eRF3) experiments with deletion of prion-like domain, which did not impair the accumulation of SGs (Grousl et al. 2013); (ii) domain specific interaction, as in case of proline rich domain in G3BP and SH3 domain;(iii) by promiscuous sticky interactions of misfolded proteins as seen in aggresomes (excellent article (Kroschwald et al. 2015)). Last option is valid especially for SG induced by robust heat shock in yeast cells, since there is spike in demand of chaperones, like Hsp70, and they are effectively titrated by unfolded proteins. Formation and “activation” of SGs could be, in this manner, analogical to other stress response pathway like Ire1, ATF6, or PERK in higher Eukaryotes.

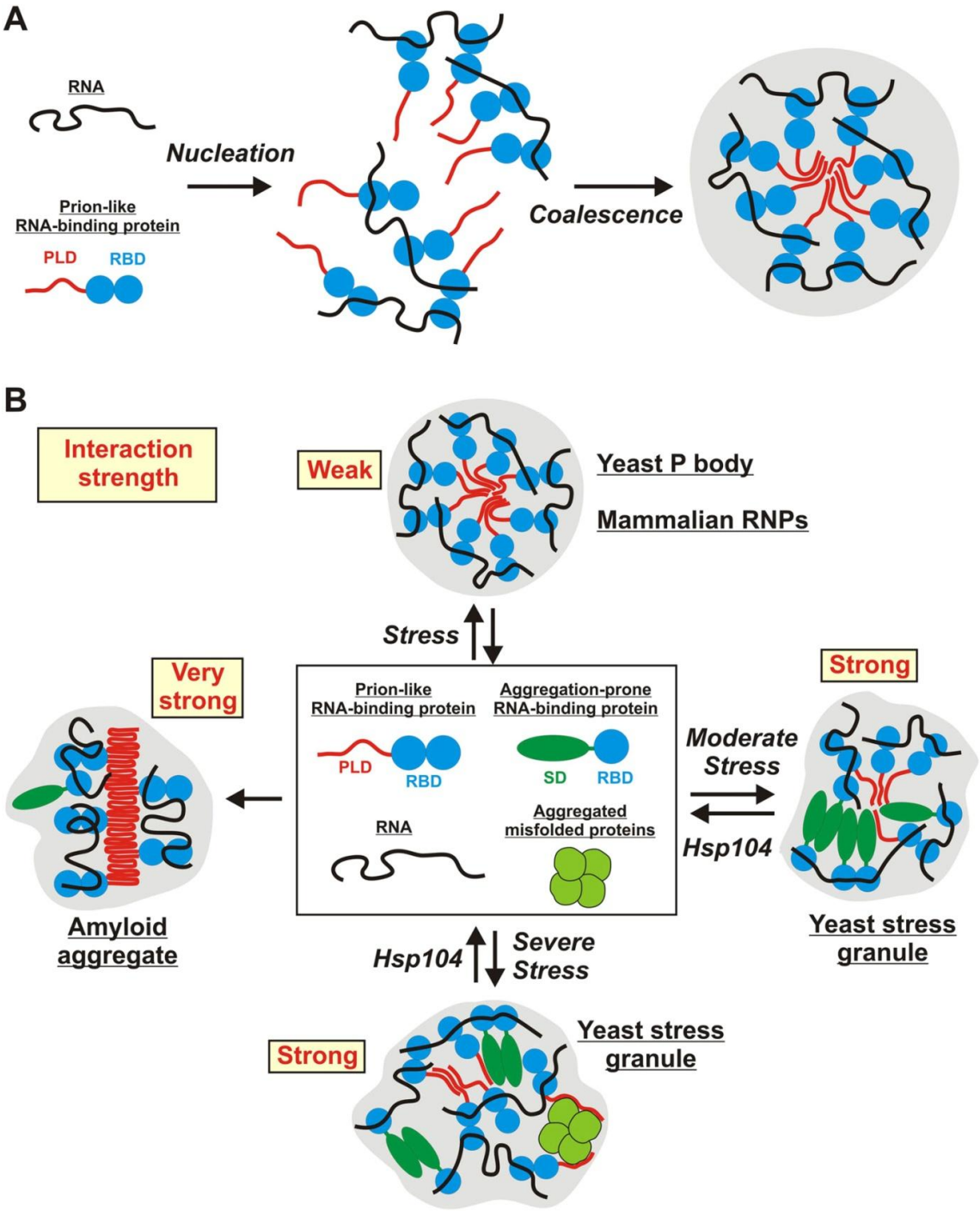

Figure 2. Schematic illustrating the potential molecular mechanisms underlying the formation of stress inducible RNP granules. (A) RNA-protein (RNP) granule formation as a two-step assembly process. In the first step, RNAs and RNA-binding proteins associate to form large RNP complexes (nucleation step). In the second step, these RNP complexes coalesce into larger compartments through additional RNA-mediated interactions, but primarily through PLD-mediated weak binding events (coalescence step). PLDs are indicated in red and RBDs indicated in blue. (B) Stress-inducible RNP granules have different compositions, which affect their dynamic and material properties. The presumed average interaction strength is indicated in red. Weak interactions increase the vulnerability to hexanediol. An aggregation-prone stress sensor domain (SD) is indicated in dark green. (Kroschwald et al. 2015)

3.2.3 Composition of SGs varies based on species, stress, and stage of stress response

mRNP foci refered as stress granules can vary greatly in their compositions. Almost a hundred of proteins, predominantly linked to mRNA metabolism are SGs constituents. Stress granule composition differs significantly between various stresses. SGs forming in response to same stress in different species do also differ in their components. And finally, contents of SGs can change spatially and temporally as cellular response to stress progresses. Proteins localized into SGs are predominantly translation factors and modulators, nucleases, splicing factors and others, often members of signaling pathways, etc (see Table 1).This variation in composition and form of SGs reacting to different stimuli might lead to difference in function. Variation in mRNP foci composition is not limited to proteins, but mRNA composition can also vary substantially (reviewed in (Thomas et al. 2011)). Uniqueness of yeast heat shock SGs lies in their formation independent of eIF2α phosphorylation and also in the involvement of eEFs and eRFs (Grousl et al. 2009) (Grousl et al. 2013).

Table 1. Stress granules and related foci induced upon stress and their variable composition, adapted from (Thomas et al. 2011)**.**

Organism	Stressor	RNA granule*	eIF2α phosphorylation	Kinase	Components Included	Components Excluded
Mammals	Arsenite or ER-stress	SG	YES	HRI or PERK respectively	polyA(+) RNA, PABP, TIA-1/R, eIF3, G3BP, eIF4G, 40S, others.	60S, HSP27, TTP, Dcp-1, Dcp-2, Hedls, GW182, Lsm1–7, others.
	Heat shock	SG	YES		HSP27, polyA(+) RNA, PABP, TIA-1/R	
	Pateamine, Hippuristanol, tiRNA, Energy deprivation	SG	NO		polyA(+) RNA, PABP, TIA-1/R, eIF3, G3BP, 40S, eIF4E, TTP (for energy deprivation), others	Hedls, 60S, Dcp1, Rck/p54
	UV	SG	YES		polyA(+) RNA, PABP, TIA-1/R	HSP27
D. melanogaster	Heat shock	SG	NO		polyA(+) RNA, FMR1, eIF4E, eIF3, PABP, Rox8 (TIA1), 18S rRNA	DCP1, RPL P0
	Arsenite	SG	YES	PEK and GCN2**	polyA(+) RNA, FMR1, eIF4E, eIF3, PABP, Rox8 (TIA1), 18S rRNA	DCP1, RPL P0
T. brucei	Heat shock	SG	NO		eIF4E1 to 4, eIF2A, eIF3B, PABP1/2	DHH1/Rck/, XRNA/XRN1
	Carbon-source starvation	mRNA granules			PABP1, UBP1, polyA(+) RNA	
T. cruzi	Carbon-source starvation	mRNA granules			PABP1/2, eIF4E, TcDhh1/Rck, XRNA/ XRN1, TcUBP1 to 4, 5a and 6b, polyA(+) RNA	eIF3D, TcS15(40S), TCL3 (60S)
	Nutritional stress	Cytoplasmic *foci*			5′ tRNA halves, 3′tRNA halves	polyA(+) RNA
S. pombe	Osmotic or heat shock	Stress-dependent *foci*			tRNA, eIF4E, Sum1/eIF3i, p116/eIF3b, Int6/eIF3e	
S. cerevisiae	Heat shock	SG	NO		eIF3, Pab1p/PABP, eIF4G2, Rps30A (40S), Ngr1/TIAR, Pub1/TIA 1, Dcp2p, Dhh1/Rck	Rp125 (60S), eIF2α
	Glucose starvation	Pab1-containing PBs			polyA(+) RNA, Pab1p/PABP, eIF4E, eIF4G. Partially Dcp2p	eIF3
	Glucose starvation	EGP bodies			eIF4E, eIF4G, Pab1p/PABP	eIF3b, eIF4A1, eIF2α, eIF2Bγ,
	Glucose starvation	SG	YES	Gcn2	Pub1/TIA-1, Ngr1/TIAR, Pbp1/Ataxin-2, Pab1p/PABP, eIF4GI, eIF4GII, eIF4E, Eap1/4EBP, Hrp1, Ygr250c, Gbp2	eIF3, PeIF2α
	Glucose starvation or arsenite	SG			Pbp1(Ataxin-2), Pub1(TIA1), Pbp4p, Lsm12, Dhh1(Rck/p54)	
C. elegans	Heat Shock / sperm depletion in female worms	RNP *foci* (oocytes)			RNA, MEX-3, DCP-2, CAR-1/Rap55, CGH-1/Rck, PABP, TIA1	
C. reinhardtii (chloroplast)	Oxidative stress / High Light / FCCP / UV / Phosphate deprivation	cpSG			cPABP, S21 (40S), mRNA	L12 (60S), L2 (60S)

* names given by the authors. PBs are not included.

** PEK main kinase, GCN2 secondary role.

3.2.4 Possible roles of SGs

Role of SGs can be deduced from circumstances leading to their formation. SGs are formed rapidly in part as an immediate response to various stress conditions and in part due to general translational control mechanisms. Experiments with cycloheximide show that depletion of the polysome pool is crucial for SGs formation. Opinions on SGs function differ, putting the emphasis of different aspects of SGs biology. There are four major themes concerning SGs function.

SGs can be viewed as sites of mRNA triage necessary for shifts in the expressed proteome. This is illustrated by exclusion of HSP mRNAs form SGs during the heat shock response (Kedersha and Anderson 2002). SGs can also play role in IRES dependent translation during stress, since necessary components including eIF3 are present in granules (Roy et al. 2010).Others see the main function of SGs in retention and protection of translational machinery against harmful effects of stress and following protein degradation. SGs contain proteins with broad spectrum of post-translational modifications and ubiquitination is no exception. Inhibition of proteasome leads to increase in SGs formation. Yeast SGs also contain protein Mmi1, yeast ortholog of TCTP (translationally-controlled

tumor protein) which co-localizes with de-ubiquitination machinery and seems to protect some protein substrates from degradation (Rinnerthaler et al. 2013). It is also possible that the main function of SGs does not lie in processes directly ongoing during stresses, but it is more related to the recovery of translation. In this respect, SGs may serve as sites for re-initiation after passage of unfavorable conditions (Kimball et al. 2003).

On the other hand, SGs could influence signaling cascades and apoptosis. SGs may sequester various components of signaling networks. This could have critical impact on cell survival rates and the cell recovery from stress, because of SGs may modify a pool of active components in systems responsible for evaluating stress load severity and its compatibility with further propagation. SGs in metazoans accumulate for instance tumor necrosis factor associated protein 2 by its interaction with eIF4G (Kim et al. 2005). In yeast system was also reported recruitment of TORC1 into SGs under stress conditions and its subsequent signaling reactivation thru SG disassembly. TORC1 is key kinase in proliferative signaling pathway and its sequestration stops cell division and propagation (Takahara and Maeda 2012).

As mentioned above, many proteins in signal and metabolic pathways aggregate together, even though perfectly capable of their function on their own, in order to increase the efficiency of performed process. Formation of mRNP foci shares many similarities with this phenomenon. Additionally, many RNA-binding proteins require oligomerisation, or other forms of aggregation for their proper function.

3.3 eIF5A – initiation factor with influence on elongation

eIF5A is essential protein known for almost 40 years, yet the exact functional and molecular basis of its crucial role still remains to be elucidated. eIF5A is also a sole known eukaryotic protein undergoing hypusination, post-translational modification of lysine by polyamine spermidine to hypusine. Moreover this modification seems to be crucial for correct physiological function of eIF5A. Hypusination is also essential in most model eukaryotes, with the exception of yeasts. eIF5A influences whole plethora of cellular functions and processes. It has been implicated to partake in mRNA turnover and mRNA decay downstream of decapping, actin dynamics, cell cycle progression oriented growth and cell wall integrity maintainence (www.uniprotorg/uniprot/P23301) .

In yeast eIF5A can be expressed from two genes. First gene, HYP2, is expressed universally while second gene, ANB1, is expressed only under the anaerobic conditions. Sequential identity of both proteins is about 90% but they differ in their C-terminal domain. The difference in conditions under which are yeast variants of eIF5A gene expressed bears resemblance to mammalian tissue

specific expression of gene variants eIF5A1 and eIF5A2. While eIF5A1 is present ubiquitously thru whole of body, eIF5A is present only in brain, testes and pathologically in tumors. In yeast model HYP2 variant of the gene is used for majority of studies, this one is no exception. eIF5A is, as most of translation factors, relatively small protein. Yeast eIF5A length is 157 amino acids, molecular weight 17,114 kDa and isoelectric point is 4.56 (http://www.yeastgenome.org/locus/S000000760/overview).

3.3.1 eIF5A hypusination – an unique modification

Hypusination is modification essential for function of eIF5A in higher eukaryotes and severely impacts growth in yeast, plus also effects intracellular localization of eIF5A. Non-hypusinated precursor can be found in both cytoplasm and nucleus, while hypusinated eIF5A localizes only into cytoplasm (Lee et al. 2009). Hypusination is unique post-translational modification since eIF5A is only known substrate undergoing this modification.

Hypusine [Nε-(4-amino-2-hydroxybutyl)-lysine] is a basic amino acid with extraordinarily long side chain. In yeast, side chain of eIF5A lysine 51 (Lys 51) undergoes specific two step modifications in order to be hypusinated. Enzymatic pathway responsible for this post-translational modification composes from two proteins: deoxyhypusine synthase (DHS) and deoxyhypusine hydroxylase (DOHH). In first step of reaction, DHS adds 4-aminobutyl from spermidin onto Nε of lysine side chain and forms deoxyhypusine. This step is essential in all eukaryotes and substitution mutations of Lys51 are lethal. Second step of hypusination is mediated by DOHH, however the hydroxylation and formation of hypusin is not essential in yeast (reviewed in (Park et al. 2010)).

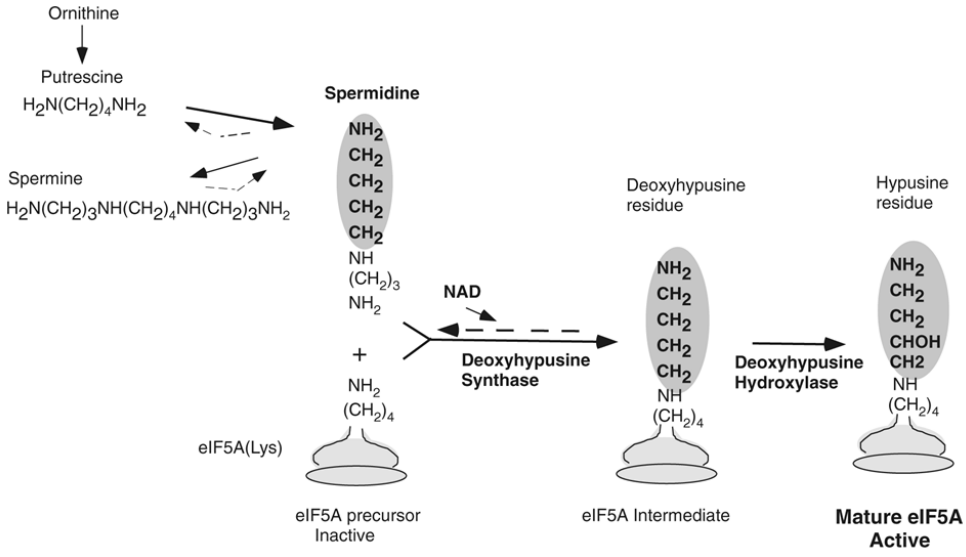

Figure 3. Hypusine biosynthesis in eIF5A, adapted from (Park et al. 2010)**.**

3.3.2 eIF5A structure

The factor eIF5A consisits of two predominantly β-sheet domains. N-terminal domain contains β-strands that form into SH3-like β-barell, present in other translation related proteins, RNA binding KOW motive and of course the hypusine containing loop – flexible, exposed and protruding from the whole of protein. C-terminal domain contains RNA binding OB-fold β-barrel and C-terminal α-helix that is crucial for eIF5A function. Substitutions in eIF5A-3 mutant (C39Y and G118D) lead to structural changes (Dias et al. 2008). Based on the comparison of eIF5A-WT model from X-ray diffraction and eIF5A-3 mutant model based on in sillico structure prediction method (http://zhanglab.ccmb.med.umich.edu/I-TASSER/) we can tell that A-3 mutant exhibits changes in properties of groove between NTD and CTD, narrowing the gap of the groow in vicinity of AA-tRNA and rRNA interacting surface. Based on the structural studies contemplating its function, eIF5A was localized to E-site(exit site) of ribosome(Gutierrez et al. 2013).

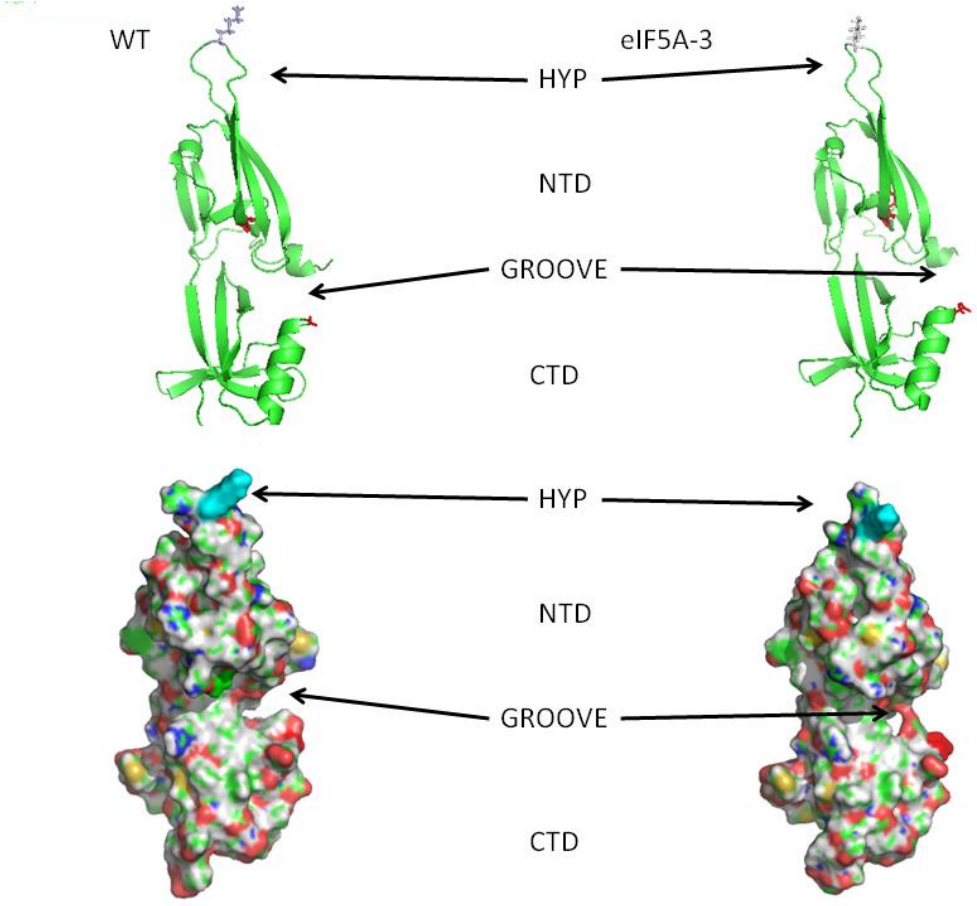

Figure 4. Structural models of eIF5A variants. Upper, ribbon model shows mutated amino acids. Lower, surface model shows impact on conformation. WT is based on PDB entry 3ER0, eIF5-3 is based on I-TASSER model. HYP- hypusine loop, NTD –N-terminal domain, GROOVE – area most noticeably altered in model of eIF5A-3. CTD – C-terminal domain.

3.3.3 eIF5A functions

Even though there has been a substantial progress in last years, exact reasons for the eIF5A essentiality and molecular basis of this phenomenon still remain elusive. eIF5A is a very unique protein acting not only as translational factor affecting both initiation and elongation but also affecting other cellular processes previously mentioned.

It was originally attributed role in translation initiation, as factor supporting formation of the first peptide bond in the rabbit reticulocyte lysate system (under its former designation eIF-4D) (Benne and Hershey 1978). However, later degron mutant studies shifted the view of eIF5A function more towards the translation elongation. Outcome of the polysome profile analyses under the non-permissive conditions resembled results obtained by the treatment of normal cells with cycloheximide (CHX), a translation elongation impairing drug. Mild decrease in incorporation of radioactively labeled amino acids and increase in the ribosome transit time indicated that eIF51A is a general translational factor stimulating elongation by optimizing the interaction between peptidyl-tRNA and amino acyl-tRNA (Saini et al. 2009) (Gregio et al. 2009).

Role of eIF5A in eukaryotic translation can be deduced from the role of its bacterial ortholog EFP. EFP critically influences relieve of ribosomal stalling on polyproline stretches during elongation of bacterial proteins (Ude et al. 2013). Ribosomal stalling on polyprolines is caused by uneven incorporation rates among amino acids. Some amino acids are worse substrates for peptide bond formation than the others and especially a troublesome substrate is cyclic imino acid proline (Pavlov et al. 2009). Slow rate of proline incorporation is more pronounced when transcripts encode three or more proline residues in a row (Pro-Pro-Pro, but also Pro-Pro-Gly). In such case ribosome tends to stall in these regions until rescued by EFP. Length of proline stretch increases severity of stalling. Experiments with eukaryotic ortholog eIF5A in Saccharomyces cerevisiae gave analogical result and confirmed that eIF5A optimize the interaction between peptidyl-tRNA in P-site and aminoacyl-tRNA in A-site and is critical for synthesis of polyproline repeat rich proteins (Gutierrez et al. 2013).

Genome-wide analysis and classification of polyproline rich proteins lead to another interesting conclusion. Proteins containing polyproline stretches in their sequence are non-randomly grouped into functionally specific units (Mandal et al. 2014). These units are mainly involved in six cellular processes: actin cytoskeleton-associated function, DNA binding, replication and transcription, RNA splicing and processing, signal processing, vesicular trafficking and cell cycle and morphology. Proline repeats give rise to a unique structural feature, folding into secondary structure of poly-L-proline type II (PP II) helix. PP II helix is functionally significant not only for its presence in structural

proteins (collagen) but especially for its role in protein-protein and protein-nucleic acid interaction. These non-covalent interactions can form very rapidly, are relatively strong and have low specificity. Good examples of domain interaction based on polyproline interaction is SH3 domain with its ligands, RNA polymerase II complex formation and in metazoans also salivary proteins binding polyphenols (reviewed in (Williamson 1994))

It is tempting to speculate on the involvement of these structural motives in formation of SGs, since proline motives are also present in prion-like proteins and amyloid interactions are suspected to play substantial part in SGs formation (reviewed in (Thomas et al. 2011)). However, data obtained in our lab on the yeast model contradict this notion, at least in the case of heat stress induced SGs and Sup35 (Grousl et al. 2013).

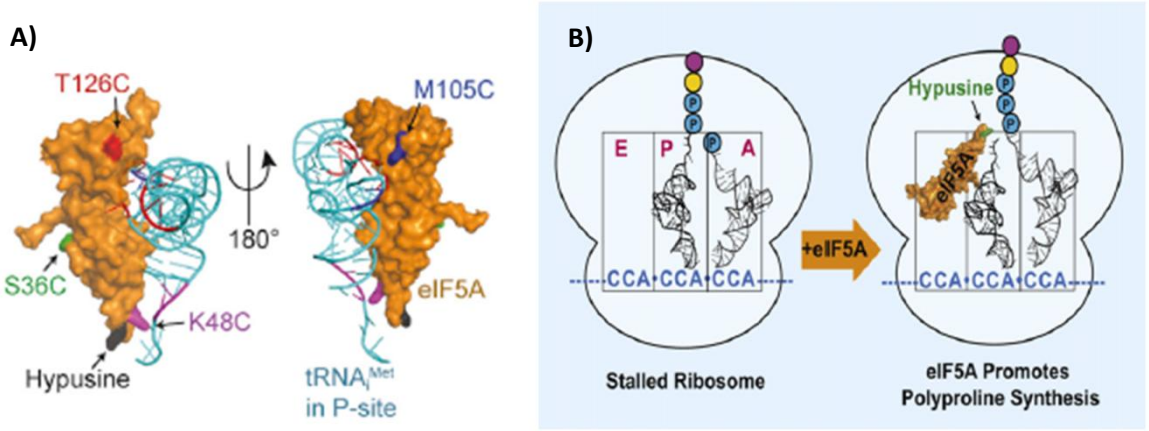

Figure 5. A) Binding of yeast eIF5A with tRNA. Amino acids important for interactions are colored. B) Model of eIF5A role in relief of ribosomal stalling. Adapted from (Mathews and Hershey 2015) **and** (Gutierrez et al. 2013)

4 Materials and Methods

4.1.1 Yeast strains

All strains used in this study are based on the *S. cerevisiae* strains BY4741 and BY4742. The strains used and created in this study are summarized in Table 2.

Table 2. List of all strains of *Sachcaromyces* cerevisiae used in this study.

STRAIN	GENOTYPE	SOURCE
CRY1369	*MATalpha his3 leu2 ura3 trp1 lys2 ABP140GFP::kanMX tif51A::HIS3 [tif51A/URA3/CEN]*	Our laboratory
CRY1372	*MATalpha his3 leu2 ura3 ABP140GFP::kanMX tif51A::HIS3 [tif51A-3/LEU2/CEN]*	Our laboratory
CRY2192	MATalpha his3 leu2 ura3 trp1 *tif51A::HIS3 [tif51A-3/LEU2/CEN] (tif51AC39Y/G118D)*	C. Zanelli, Brazil
CRY2195	MATalpha his3 leu2 ura3 trp1 *tif51A::HIS3 [TIF51A/URA3/CEN]*	C. Zanelli, Brazil
CRY2196	MATalpha can1::STE2pr-SP his5 lyp1 leu2 ura3 his3 met5 *TIF51A::natMX4*	C. Zanelli, Brazil
CRY2198	MATalpha can1::STE2pr-SP his5 lyp1 leu2 ura3 his3 met5 *tif51A-3::natMX4*	C. Zanelli, Brazil
CRY1365	MATalpha his3 leu2 ura3 trp1 lys2 *RPG1-GFP::kanMX tif51A::HIS3 [tif51A/URA3/CEN]*	Our laboratory
CRY1368	MATalpha his3 leu2 ura3 trp1 *RPG1-GFP::kanMX tif51A::HIS3 [tif51A-3/LEU2/CEN]*	Our laboratory
CRY410	MATa his3Δ1 leu2Δ0 met15Δ0 ura3Δ0 */RPG1-Gfp::HIS3MX6*	Our laboratory
CRY2417	MATa can1::STE2pr-SP his5 lyp1 leu2 ura3 met5 *TIF51A::natMX4 /RPG1-Gfp::HIS3MX6*	This study
CRY2418	MATa can1::STE2pr-SP his5 lyp1 leu2 ura3 his3 met5 *tif51A-3::natMX4 /RPG1-Gfp::HIS3MX6*	This study

4.1.2 Plasmids

Plasmids used in this study are derived from yeast centromeric shuttle vectors (Sikorski and Hieter 1989).

Table 3. List of all plasmids used in this study.

Plasmid	Feature	Source
pSV59 (pRS315)	LEU2, CEN	Sikorsky and Hieter, 1989
pSV60 (pRS316)	URA3, CEN	Sikorsky and Hieter, 1989

4.1.3 Oligonucleotides

Table 4. List of all oligonucleotides used in this study.

Oligo	Sequence	Length (bp)
GFPcollcontr	TACATAACCTTCGGGCATGG	20
RPG1ctrl	GACCGTTTCTCCAGATAAAG	20
eIF5A-F	GAACATACCTTTGAAACTGCTGACG	25
eIF5A-R	GCGGCTTCTTCACCCATAGC	20
ABP140 kontrola	CAGATTTTGCTCCAAGAGCC	20
GFP40	GGTCAATTTACCGTAAGTAGC	26

4.1.4 Cultivation media

Yeast cells were either grown in complex medium (YPD) (1% (w/v) yeast extract (Difco), 2% (w/v) peptone(Oxoid) and 2% (w/v) D-glucose) (Lachema) or synthetic complete glucose medium (SC-glucose) (2% (w/v) D- glucose, 0.17% (w/v) yeast nitrogen base without amino acids, 0.5% ammonium sulphate and complete dropout mixture (0.2% Arg, 1,0% Asp, 1.0% Glu, 0.2% His, 0.6% Leu, 0.3% Lys, 0.5% Phe, 0.4% Ser, 2.1% Thr, 0.4% Trp, 0.3% Tyr, 1.6% Val, 0.2% Met, 0.4% Ade, 0.2% Ura, (w/v)) (Serva).

The corresponding solid media contained 2% agar (Serva). To select for auxotrophies, the respective amino acid was omitted from the dropout mix. To select for resistance to antibiotics, the appropriate antibiotic was added to the media (NTC (Biolone) (final concentration 200 μg/ml)).

Sporulating cells were grown on Fowel plates containing 0.1M KAc(Sigma), 0.1% yeast extract, 0.05% glucose and 2% agar

4.1.5 Cultivation

4.1.5.1 Solid media

Cells were smeared by sterile tooth-pick or inoculation loop on the Petri dish with appropriate medium. Cultures grew for 3-4 days at 25°C (due to ts phenotype) or at 37°C, if selecting against the ts mutant. Petri dishes were temporarily (up to one month) stored at 4°C, for long term storage cultures were stored at -80°C in glycerol solution.

4.1.5.2 Liquid media

Cultures were shaken in flasks (maximally 1/10 of total volume), in order to ensure proper aeration at 180rpm. Temperature setting was same as at solid media. Culture growth was measured by CASYton (see below).

4.1.6 Cell counting

Cell counting was conducted by CASY Cell Counter DT, (Schärfe system). Cell culture aliquot was diluted by deionized water, 10x to 20x times, based on concentration (should not exceed 10^7 cells/ml in sample). 10µl of diluted aliquot were then added to 10 ml of CASY ton in CASY cup and sealed by cap. Solution was mixed by gentle shaking and ready for measurement.

Cell counting itself is based on Electrical Current Exclusion principle. Device measures change in voltage field as cells pass from the cup, thru measuring pore to the capillary, enabling not only to measure number of cells, but also sort measured values into groups based on cell volume and diameter (1,4-2 µm; 2-15 µm; 15-40 µm). Measuring capillary was washed thoroughly before each measurement session and after each sample.

Solutions:

- CASY ton – pH = 7.3; 0.743% NaCl (Penta) (w/v); 0.038% Na_2EDTA (Sigma) (w/v); 0.04% KCl (Penta) (w/v); 0.03% NaF (Fluka)(w/v); 0.019% Na_2HPO_4 (w/v); 0.0195% NaH_2PO_4 (w/v)
- CASY clean – precise composition unknown – supplied by Roche

4.1.7 Microscopy

All images were taken by 100x PlanApochromat objective (NA=1.4) using an Olympus IX- 81 inverted microscope equipped with a Hammamatsu Orca/ER digital camera and an Olympus CellR™ detection and analyzing system (GFP filter block U-MGFPHQ, exc. max. 488, em. max. 507; RFP filter block U-MWIY2, exc. max. 545–580, em. max. 610). Images were processed and merged using Olympus Cell R™, FIJI and Adobe CS5 software.

Cell cultures for microscopic observation were taken from the YPD plates, inoculated into liquid YPD medium and cultivated at 28°C overnight. In the next morning, the cultures were transferred into fresh YPD in Erlenmeyer flasks. The cultures were diluted with fresh YPD in such proportion that the concentration of the cells in culture would be around $5*10^6$ cells/ml and cells would undergo at least one, preferably two, cell divisions before the microscopic experiment is started. An appropriate volume of the culture in YPD was centrifuged and pelleted cells were resuspended in 500 ul of the synthetic CM medium, which was pre-heated to appropriate temperature. CM is medium more suited for fluorescence microscopy due to its lower autofluorescence compared to the YPD medium. Moreover, the concentration of cells for

microscopic observations into this small volume enables fast heat exchange between the content of microcentrifuge tube and block heater.

4.1.7.1 Robust heat shock

Cells were heat-shocked in a block heater (Eppendorf) heated for 46°C and shaken at 1050rpm in 500 µl of CM in microcentrifuge tube for 10 minutes (or 30 minutes in prolonged version). After the heat shock, an aliquot of the 150 µl of the culture was transferred to another tube and shortly centrifuged. Most of the supernatant was removed and the pellet was resuspended in approximately 20 ul of the remaining CM medium. An aliquot of 3 µl of this suspension was placed on the covering glass and overlaid with a small square tiny slab of the 1,5% agarose (Appligene) in CM, at room temperature. Control samples were prepared in the same manner, with only exception being the setting of heater temperature at 25°C. These samples were observed and photographed in Nomarski interference contrast, GFP fluorescence, with the exposition time of 1000 ms, and bright field.

4.1.7.2 Robust heat shock with inactivation

Cultures and samples were treated in same way and experimental set-up was identical as in 46°C/10min robust heat shock experiments (see above) with only exception being the 4 hour incubation at 37°C prior to heat shock experiment.

4.1.7.3 Robust heat shock with recovery

Cultures and samples were treated in same way and experimental set-up was identical as in 46°C/10min robust heat shock experiments (see above). Microcetrifuge tubes with heat-shocked cells in CM were transferred into block heater pre-heated to 25°C and let to recover for 2 hour. Samples were taken and observed every 30minutes. Cell viability assay was conducted simultaneously with this experiment.

4.1.7.4 Propidium iodine staining(cell viability)

Cell culture treatment was identical to SG recovery experiments at 46°C. Only exception was the treatment of heat-shocked samples for propitium iodine staining prior to imaging.

Protocol:

- Pellet heat-shocked cells and wash in 100 µl of citrate buffer.
- Resuspend the pellet in 98 µl of citrate buffer and ad 2 µl of propidium iodine solution for the final concentration of 20ng/ml. Incubate in in block heater, in dark, at room temperate for 10 minutes at 550 rpm.

- Pellet stained cells and wash them in 100 µl of citrate buffer.
- Pellet washed cells and remove most of the supernatant.
- Resuspent cell in approximately 20 µl of citrate buffer and place 3 µl aliqote on the coverin glass. Overlay with small slab of 1,5% agarose in CM, at room temperature.
- Photograph samples in Nomarski interference contrast and RFP fluorescence set-up, with exposition time of 500 ms.

Solution:

- Citrate buffer: 0.1M potassium phosphate-citrate buffer, pH 5.9 2.28 % (w/v) $K_2HPO_4.H_2O$ (Sigma); 0.7 % (w/v) citric acid (Lachema)
- Propidium iodine stock solution: 1 ng/ml (Sigma)

4.1.7.5 Robust heat shock and actin recovery

Cell cultivation and treatment was identical to SG assembly experiments. Final image was created by an Olympus CellR^{TM} software as a Z-stack of images covering whole volume of observed cells with step of 0.6 µm between layers. Exposition time for each image was 500 ms.

4.1.8 Used software

Following scientific software is used in this thesis:

- Xcellence RT – imaging software for life science microscopy (http://www.olympus-lifescience.com/)
- FIJI – image editing (http://fiji.sc/Downloads)
- oCellaris – granulometric analysis of fluorescence image (http://www.ocellaris.cz/index.php/en/download)
- GraphPad Prism 6 – basic statistical analysis and graph plotting (http://www.graphpad.com/scientific-software/prism/)
- I-TASSER – prediction of protein structure (http://zhanglab.ccmb.med.umich.edu/I-TASSER/)
- PyMol – visualization of protein structure (https://www.pymol.org/)

4.1.8.1 oCellaris

Images taken under specific conditions with Olympus CellR microscopic system equipped with Xcellence RT software, were subsequently analyzed by oCellaris v0.93. oCellaris is the new

software developed by DEL company for analyses of fluorescence images of living yeast cells. It is based on Hough transformation to identify yeast cells in bright field image and to compute cells contours with active contour algorithm. A set of algorithms enable fitting fluorescence images to cell contours and computing various parameters of fluorescence for each cell. These parameters describing fluorescence image are suitable not only for evaluation of total fluorescence intensity within the cell area but also for comparison of various strains in one parameter either at the single cell level or within the population.

Examples of the compared parameters are: peak brightness, fluorescence intensity in comparison to disperse background signal, peak slope and many others. Possible applications of oCellaris include: (i) estimation of expression levels of tagged protein; (ii) precise computing of cell number; (iii) distinction of fluorescence type; (iv) qualitative evaluation of localized fluorescence; (v) evaluation of quantity of localized fluorescence. Software is capable of graphical presentation of analyzed images and enables export of values calculated for each cell in form of Excel or Matlab table.

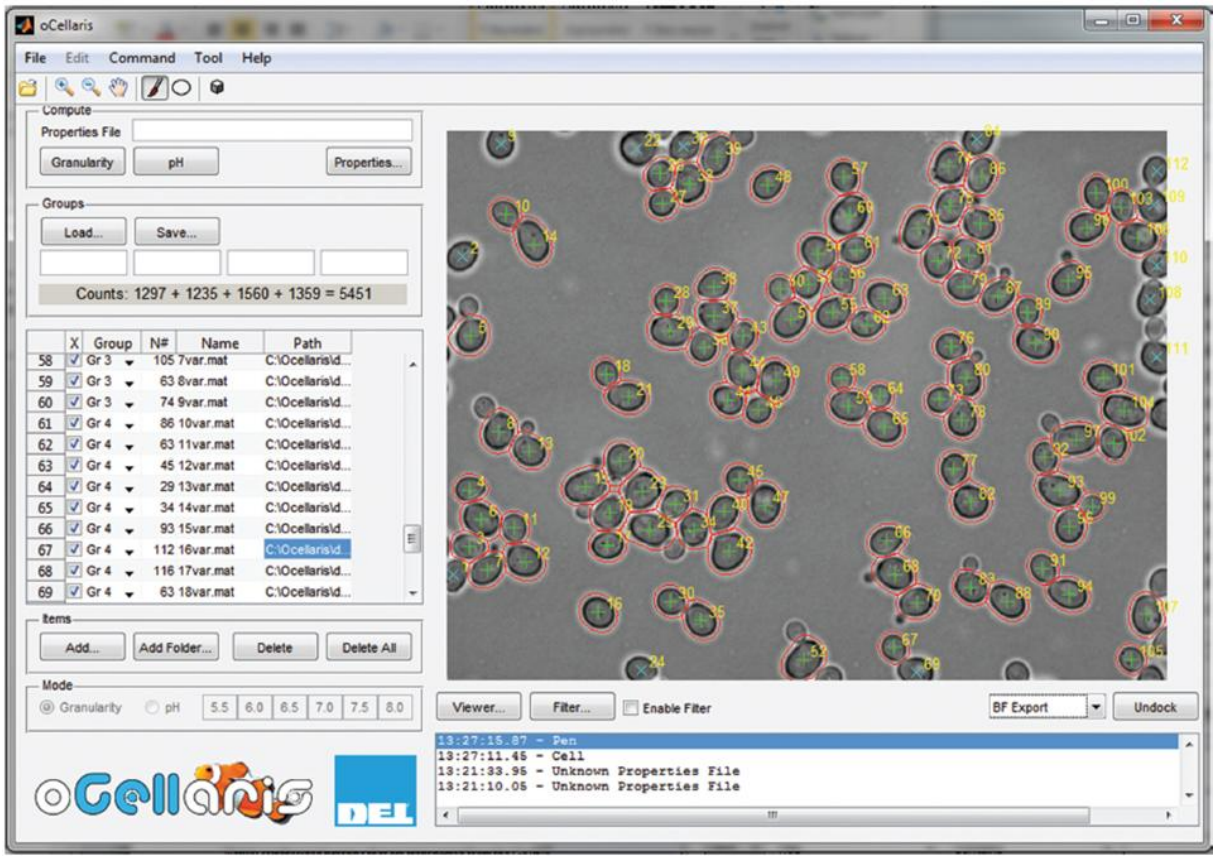

Figure 6. Recognition of cells in bright-field image and interface of oCellaris.

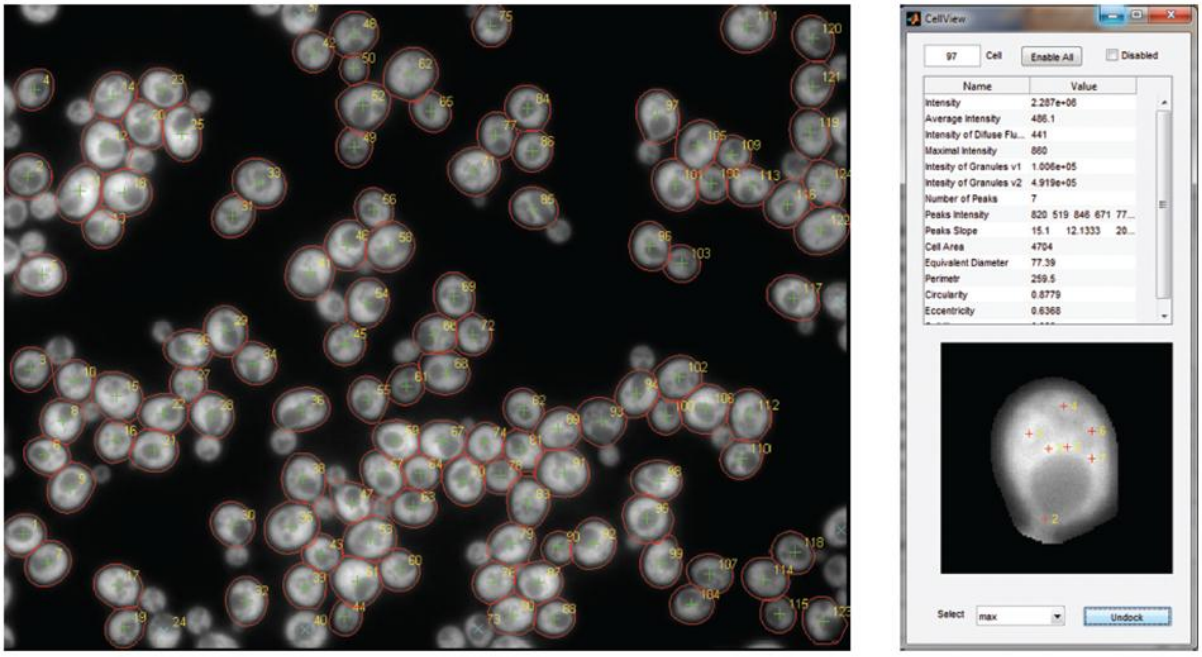

Figure 7. Projection of cell borders on fluorescence image and fluorescence analysis. On the right we can see a detail information about the selected cell. Red crosses in detail picture of the cell represent local maxima of fluorescence marked as peaks. Control sample.

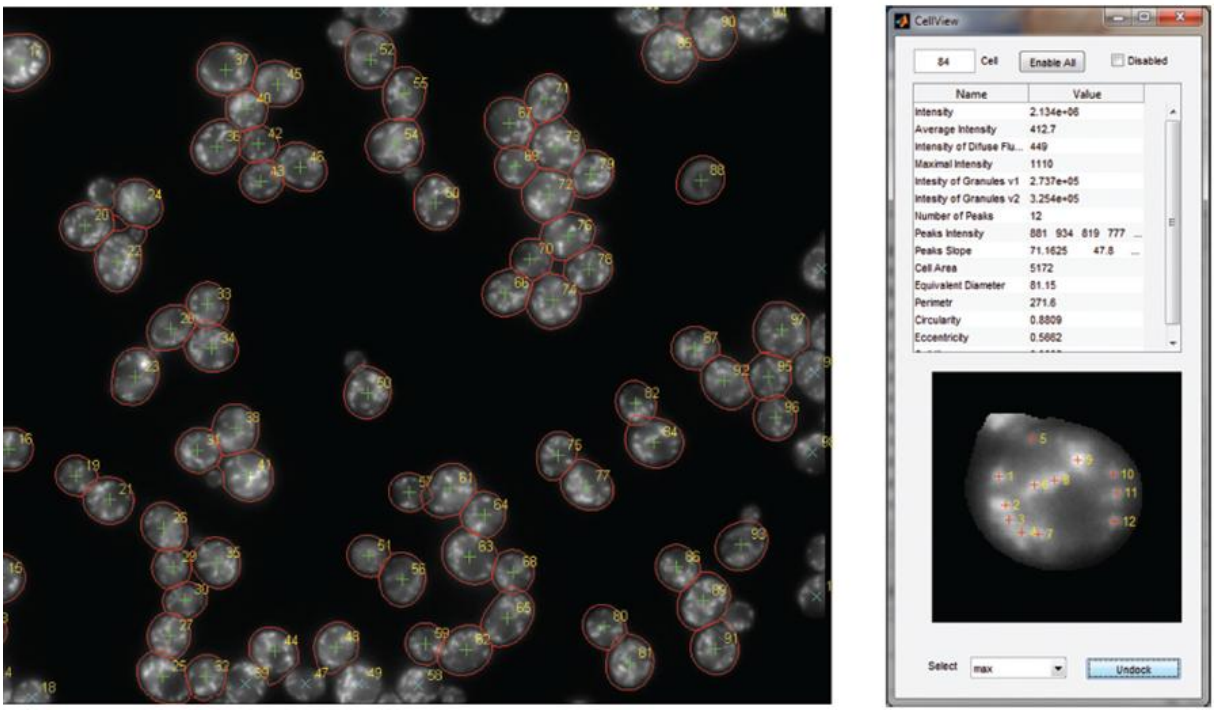

Figure 8. Projection of cell borders on fluorescence image and fluorescence analysis. On the right we can see a detail information about the selected cell. Red crosses in detail picture of the cell represent local maxima of fluorescence marked as peaks. Heat shocked sample.

4.1.8.2 GraphPad Prism 6

Statistical program GrapgPad Prism 6 has been used for statistical analysis and graph plotting of gathered data. Granulometric data gathered for all cells in WT strain at given time point were compared to data from A-3 mutant at the same time point, data sets were statistically analyzed by unpaired t-test method, to be more specific with the Mann-Whitney variant. Data sets from cell survival assay were statistically analyzed by paired t-test method. The significance levels were: * for P ≤ 0.05; ** for P ≤ 0.01; *** for P ≤ 0.001; **** for P ≤ 0.0001.

4.1.9 Doubling time calculation

Doubling time (T) was calculated for specific strains in this study according to formula:

$$T = \frac{\ln 2}{\ln\left(\frac{OD_{END}}{OD_{START}}\right)} * t$$

Where OD_{END} and OD_{START} is optical density and *t* is time of growth.

4.1.10 Spot assay

This method is used for various tests – for instance temperature sensitivity, auxotrophy, cell survival, etc.

Protocol:

- Cultures for spot assay grow over night in a liquid medium.
- Measure concentration of cells and dilute them in the medium in microcentrifuge tubes. Dilute appropriately in order to get desired concentration of cells in spotted volume. First dilution is for the most concentrated spot.
- Pipette 200 µl of suspension from microcentrifuge tube into first well in line of 96-well plastic plate.
- Fill following 5 wells in line with 180 µl of medium, with multichannel pipette.
- Perform 10-fold dilution row by pipetting 20 µl of volume from the first well, the most concentrated one, to the next cell in the row and repeat this step until reaching the last well in the row.

- Spot appropriate volume from each cell onto plate. Spotting is executed by multichannel pipette, spotting simultaneously column with same concentration of cells.
- Let plates briefly dry and soak in the moisture from spots, to avoid cross-contamination.
- Cultivate at an appropriate temperature for 2-3 days.

4.1.11 Cell viability assay

Cell cultures for viability assay were taken from the YPD plates, inoculated into liquid YPD medium and cultivated at 28°C overnight. In the next morning, the cultures were transferred into fresh YPD in Erlenmeyer flasks. The cultures were diluted with fresh YPD in such proportion that the concentration of the cells in culture would be around $5*10^6$ cells/ml and cells would undergo at least one, preferably two, cell divisions before the experiment is started. An appropriate volume of the culture in YPD was centrifuged and pelleted cells were resuspended in 500 ul of YPD medium, Concentration of cells measured by CASY CellCounter at this point was crucial for dilution of the cultures after the shock and prior to plating.

Cells were heat-shocked in a block heater heated for 46°C and shaken at 1050rpm in 500 µl of YPD in microcentrifuge tube for 10 minutes (or 30 minutes in prolonged version). After the heat shock, cells were diluted by water to the concentration of 1500 cell/ml and 100 µl were plated. Control samples were diluted in same manner, resulting in expected value of 150 CFU (Colony Forming Units) to be equal to 100%.

4.1.12 Mating, sporulation and tetrad analysis

4.1.12.1 Mating protocol

- Mix parental strains, with different mating types, by smearing them together with inoculation loop on YPD plate.
- Cultivate for one day at appropriate temperature.
- Check microscopically for presence of zygotes, if present continue to next step, else cultivate for another day and repeat.
- Resuspend culture with zygotes in 1ml of deionized water. Dilute this suspension 1:6 with deionized water. Divide Petri dish in half by marker and plate 150 µl of suspension on right side of plate with/out selection agent.
- Using micromanipulator, pick up 5-10 zygotes and move them to the other half of Petri dish.
- Cultivate diploids for 2-3 days at appropriate temperature on selection plate.

4.1.12.2 Sporulation protocol

- Inoculate diploid colonies onto YPD plate as a smear with aprox. area of 1cm^2
- Cultivate for one day at appropriate temperature
- Transfer all fresh cells onto sporulation Fowel medium as a small glob (3x3x3mm)
- Sporulate for 2-4 day at 25°C.

4.1.12.3 Spore sorting protocol

- Check microscopically for presence of ascus, if present continue to next step, else cultivate for another day and repeat.
- Pick part of sporulated culture by tooth-pick, transfer into deionized water and mix with zymolyaze to final concentration of enzyme 0.05% (w/v). Incubate at room temperature for 10 minutes.
- Briefly centrifuge solution, remove supernatant and wash cells with 1ml of water.
- Resuspend pellet in 1ml of water. Dilute this suspension 1:6 with deionized water. Divide Petri dish in half by marker and plate 150 µl of suspension on right side of YPD plate. Such plate is ready for micromanipulation.
- Using micromanipulator, pick up at least 5 tetrads and move them to the other half of Petri dish and separate them into individual haploid cells.
- Incubate separated spores for 2-3 days.
- Test for selection markers and mating type.

4.1.12.4 Mate type test

- Tested and testing strains for mating type a and alpha were cultivated over night in liquid medium. On the second day measure concentration of cells. Dilute to OD_{600}=0,4 and spread testing strains on YPD plates and let dry out.
- Subsequently Pipette 5µl droplet of tested culture on both plates (with mat a substrate and mat alpha substrate).
- Cultivate for 2-3 days.
- Observe zones around tested droplets that develop, it mating type of tested strain and substrate strains differ.

4.1.13 DNA isolation

4.1.13.1 Plasmid DNA isolation from yeast

Protocol:

- Collect the cells in microcentrifuge tube
- add 230 µl of DNA lysis buffer and resuspend the cell pellet
- add 0.4 g of acid-washed glass beads and 200 µl phenol:chloroform:isoamylalcohol
- vortex at top speed for 2 minutes
- Centrifuge at 16,000g for 5 minutes. Transfer the aqueous phase (top layer) to a new microcentrifuge tube.
- Add 600 µl of cold 95% ethanol to precipitate DNA, and keep the tube at -20°C for 30 minutes. Pellet the DNA by centrifugation at 16,000g for 5 minutes and discard ethanol.
- Resuspend DNA pellet in appropriate volume of TE buffer(50 µl).

Solutions:

- DNA lysis buffer: 2% Triton X-100 (Amersham), 1% sodium dodecyl sulfate (SDS) (Biorad), 0.1 M NaCl,1 mM ethylenediaminetetraacetic acid (EDTA) (Serva), pH 8.0, 10 mM Tris-HC (Serva)l,pH 8.0
- Phenol:chloroform:isoamyl alcohol (25:24:1) (Reactivul, Lachema, Lachema)
- TE: 10 mM Tris-HCl, pH 8.0, 1 mM EDTA, pH 8.0

4.1.13.2 Genome DNA isolation from yeast

Genome DNA isolation technique was based on the protocol for PCR-based applications (Lõoke et al. 2011).

Protocol:

- Pick one yeast colony from the plate or spin down 100-200 µl of liquid yeast culture (OD600=0.4). Suspend cells in 100 µl of 200mM LiOAc, 1 % SDS solution.
- Incubate for 5 minutes at 70°C. 3. Add 300µl of 96-100 % ethanol, vortex.
- Spin down DNA and cell debris at 15 000 g for 3 minutes.
- Wash pellet with 70 % ethanol
- Dissolve pellet in 100 µl of H2O or TE and spin down cell debris for 15 seconds at 15 000 g.
- Use 1 µl of supernatant for PCR.

Solutions:

- 0.2 M Lithium acetate (Sigma) 1% SDS solution.
- Ethanol 96-100 % and 70 %. (Sigma)

4.1.14 DNA amplification by PCR

Polymerase chain reaction was used for amplification of template to verify prsecence of inserts and for sequencing in this study. Typical PCR amplification program is shown below. Annealing temperature was adjusted according to the melting temperature of primers used in the reaction. Elongation time was adjusted according to the length of a fragment being amplified (1 minute/1kb length).

Initial denaturation	95°C	5 minutes	
Denaturation	95°C	1 minute	
Annealing	55°C	1 minute	30x
Elongation	72°C	1 minute	
Final elongation	72°C	5 minutes	
	4°C	hold	

Composition of PCR reactions: 1x ThermoPol Reaction Buffer (NEB), 800 µM dNTP mix (200 µM of each), ~20 ng template DNA, 2 µM primers, 1 Unit Taq® DNA Polymerase (NEB), ddH_2O to a final volume (20 µl).

4.1.15 DNA purification kit – PCR clean-up

QIAquick® PCR Purification kit from QUIAGEN was used to purify PCR products for DNA sequencing.

Protocol:

- Add 5 volumes Buffer PB to 1 volume of the PCR reaction and mix. If the color ofthe mixture is orange or violet, add 10 µl 3 M sodium acetate, pH 5.0, and mix.
- Place columns into collection tubes. To bind the sample to column centrifuge for 30-60 seconds. Discard flow-thru.
- Wash column with 0.75 ml PE buffer and centrifuge for 30-60 seconds. Discard flow-thru. Centrifuge once mor for another 1 minute.
- Add 50 µl of EB buffer onto column and centrifuge for 1 minute in order to elute the DNA into new microcentrifuge tube.

4.1.16 DNA electrophoresis in agarose gel

Agarose gel electrophoresis is a method used to separate DNA or RNA molecules by size. This is achieved by moving negatively charged nucleic acid molecules through an agarose matrix within an electric field. For estimating size and concentration of DNA on the gel were used 1 kb DNA Ladder (New England Biolabs) and 1 kb DNA Ladder (Biosystems)

Protocol:

- Dissolve 0.8 - 2% agarose in 1x (TBE or TAE) buffer by heating in microwave.
- Let cool down below 60°C and pour gel into gel rack with inserted comb.
- After the gel has solidified, remove the comb and the rack with gel into tank with buffer.
- Load ladder and samples mixed with loading buffer for agarose gel electrophoresis.
- Apply electric current, with voltage of 5 V/cm of lenght for approximately 1 hour.
- Stain with GelRed (Biotium) for 15 minutes and wash with distilled water.
- Place gel on UV transiluminator (UVP, San Gabriel, USA) and capture image with program (ScionImage)

Solutions:

- 10x TBE – 10.8% Tris base (w/v) (Serva), 5.5% H_3BO_3 (w/v) (Penta), 0.02 mol/dm^3 EDTA pH 8.0,
- 10x TAE – 4.84% tris base (w/v), 1,15% acetic acid (v/v) (Lachema), 0.749% EDTA(Na_2) (w/v) pH 8.0
- 6x Loading buffer – 10mmol/dm^3 Tris HCl pH 7.6, 60mmol/dm^3 EDTA, 60% glycerol (Lachema) , 0,06% brom-phenol-blue (Sigma)
- GelRed solution(Biotium) – diluted 10 000x from stock; stored in dark

4.1.17 DNA sequencing

All sequencing analysis were conducted at Centre Of DNA Sequencing at Institute of Microbiology, Academy of Science of Czech Republic. For sequencing reaction was used template DNA, prepared by PCR amplification from isolated DNA and purified by kit, and specific primers in concentration 10 pmol/µl. The sequencing data were analyzed with BioEdit software.

5 Results

5.1 Impact of the eIF5A-3 mutant on SGs formation in reaction to robust heat shock

Most of the strains used in our studies of the eIF5A influence on cells were already present in the CRY collection of our laboratory. We used the strains expressing the eIF5A variants eIF5A-WT and mutated eIF5A-3 from the plasmids (pSV60 and pSV59), CRY 2195 and CRY 2192 respectively, in combination with various chromosomally expressed fusion proteins, marked C-terminally for fluorescence microscopy, with GFP. Strains CRY 1365 (WT) and CRY 1368 (A3) expressing Rpg1-GFP were used for study of SGs induced by robust heat shock, since Rpg1 is ortholog of the mammalian eIF3a subunit (Valásek et al. 1998). Later on, our study was extended for the strains expressing eIF5A variants from the cassette integrated into the chromosome, WT (CRY 2196) and A3 (CRY 2198) and by integrated versions of eIF5A coexpresed with Rpg1-GFP (CRY 2417) a (CRY 2418). Integrated strains with Rpg1-GFP were produced as part of this thesis.

5.1.1 Preparation of strains with integrated eIF5A for fluorescence microscopy

We chose to replicate some of our tests in a system that is more faithful to the physiological conditions. Hence the strain coexpressing the integrated version of either WT eIF5A or the eIF5A-3 mutant with Rpg1-GFP were used to analyze the reproducibility of our findings from the plasmid system (see below). These strains were produced by mating, sporulation and dissection of spores by micromanipulation.

Our CRY collection already contain strains with integrated versions of both, WT (CRY 2196) and the eIF5A-3 mutant (CRY 2198) of the mating type α and also a strain from the yeast GFP clone collection expressing Rpg1-GFP (CRY 410) of mating type a (more details in Table 5). MAT α strains were crossed with the MAT a strain and sporulated according to section 4.1.12 Mating, sporulation and tetrad analysis in Materials and methods.

Table 5. Strains crossed for chromosomal version of eIF5A-WT and eIFA-3 and their properties.

Strain	Properties	Trait
2196	MATalpha can1::STE2pr-SP his5 lyp1 leu2 ura3 his3 met5 TIF51A::natMX4	eIF5A-WT
2198	MATalpha can1::STE2pr-SP his5 lyp1 leu2 ura3 his3 met5 tif51A-3::natMX4	eIF5A-3
410	MATa his3Δ1 leu2Δ0 met15Δ0 ura3Δ0 /RPG1-Gfp::HIS3MX6	Rpg1-GFP

At the end of sporulation there were five haploid tetrads from each mating couple. Those haploid strains were subjected to series of tests in order to examine them for the presence of desired selection markers. Newly created strains were assessed for growth on media without histidine (His-), resistance to nourseothricin (NTC+), ts phenotype at 37°C, presence of Rpg1- GFP (by both colony PCR and fluorescence microscopy) and also mating type (MAT).

Table 6. Tetrad analysis after mating and sporulation of CRY 410 with CRY 2196 and CRY 410 with 2198. Symbols:+ present trait, - absent trait, XXX not available;. Dotted columns represent clones with all required traits.

410x2196		HAPLOID			
TETRAD	TRAIT	A	B	C	D
1	His -	+	-	+	-
	NTC +	-	-	+	+
	ts	-	-	-	-
	MAT	a	alfa	a	alfa
	GFP	+	-	+	-
2	His -	+	+	+	-
	NTC +	+	+	-	-
	ts	-	-	-	-
	MAT	alfa	a	a	alfa
	GFP	+	+	-	-
3	His -	XXX	-	+	+
	NTC +	XXX	+	-	+
	ts	XXX	-	-	-
	MAT	XXX	alfa	alfa	alfa
	GFP	XXX	-	+	+
4	His -	-	+	+	-
	NTC +	+	-	+	-
	ts	-	-	-	-
	MAT	a	alfa	a	alfa
	GFP	-	+	+	-
5	His -	+	+	+	+
	NTC +	+	+	+	+
	ts	-	-	-	-
	MAT	XXX	XXX	XXX	XXX
	GFP	XXX	XXX	XXX	XXX

410x2198		HAPLOID			
TETRAD	TRAIT	A	B	C	D
1	His -	-	+	+	+
	NTC +	-	-	+	-
	ts	-	-	+	-
	MAT	a	alfa	a	alfa
	GFP	-	+	-	+
2	His -	+	-	+	-
	NTC +	+	-	+	-
	ts	+	-	+	-
	MAT	a	alfa	a	alfa
	GFP	+	-	+	-
3	His -	+	-	+	-
	NTC +	+	-	-	+
	ts	+	-	-	+
	MAT	alfa	a	a	alfa
	GFP	+	-	+	-
4	His -	+	-	+	-
	NTC +	+	-	+	-
	ts	+	-	+	-
	MAT	a	alfa	a	alfa
	GFP	+	-	+	-
5	His -	-	+	-	+
	NTC +	+	+	-	-
	ts	+	+	-	-
	MAT	alfa	a	a	alfa
	GFP	-	+	-	+

Based on the results summarized in Table 6, cells from assumed tetrad number 5 were removed from further analysis, because they were found to have properties of diploid cells. Haploid strains 2196x410 – 1C, 2B, 4C and 2198x410 – 2A, 4A, 5B were selected for our experiment, however strain '98x410 – 5B was latter cross-contaminated and had to be excluded from analysis. eIF5A-WT haploids were named as CRY 2417 and eIF5A- haploids were named CRY 2418.

5.1.2 Granulometric analysis of strains CRY 1365 and CRY 1368

Previous results published by Zanelli et al. indicated role of eIF5A in the formation of P-bodies in yeast (Gregio et al. 2009). That is why we decided to test whether the aforementioned A3 mutation of eIF5A has any influence on formation of the stress granules (SGs) induced by robust heat shock. Stress granules are, cytoplasmic mRNA foci consisting of relatively loose conglomerates of proteins interlinked with mRNA metabolism, cell survival and apoptosis. One of the protein complexes characteristic for SGs is eIF3. We choose to use the Rpg1, which is subunit of eIF3 (Valásek et al. 1998), as a marker for microscopic observation of SG formation. Rpg1 was C-terminally tagged with GFP and inserted into genome by histidine auxotrophy cassette (Huh et al. 2003).

5.1.2.1 10 minute robust heat shock,

In the first series of experiments, strains with deletion of genomic eIF5A gene copy and coexpressing either eIF5A-WT or eIF5A-3 from the centromeric plasmid with Rpg1-GFP were used (CRY 1365 and CRY 1368 respectively). The exponentially growing cells of these strains were exposed to robust heat shock at 46°C in fresh, preheated CM for 10 minutes and then observed via fluorescence microscope. Cells were imaged in bright-field, Nomarski diffraction and GFP fruorescence. Cells were observed alive under agarose with CM, without any fixation or staining. For more details on sample preparation see section 4.1.7.1.

From GFP images of the central section of the cells, in terms of Z axis, we can see an obvious difference in the fluorescence pattern between eIF5A-WT and eIF5A-3 mutant cells. Rpg1-GFP accumulations in WT cells are more pronounced than in the eIF5A-3 mutant, where the accumulations become much less distinguishable from the background Rpg1-GFP diffused signal in cytoplasm. In WT cells, there is relatively a higher contrast between the accumulations and the diffuse signal in cytoplasm compared to the mutant. For sake of presentation, images were normalized for same values of minimal and maximal brightness, enabling relative comparison between images. This does not hamper peak slope comparison, because it is relative. It measures the difference between brightness values of adjacent pixels, not the absolute value of their brightness, and therefore can be used for comparison.

Nomarski diffraction images show substantial increase in vacuolar size in shocked A-3 mutant cells and also in cell size. On details cropped from original images, with normalized dynamic range is noticeable difference in fluorescence levels of GFP signal caused probably due to lower expression levels of Rpg1-GFP.

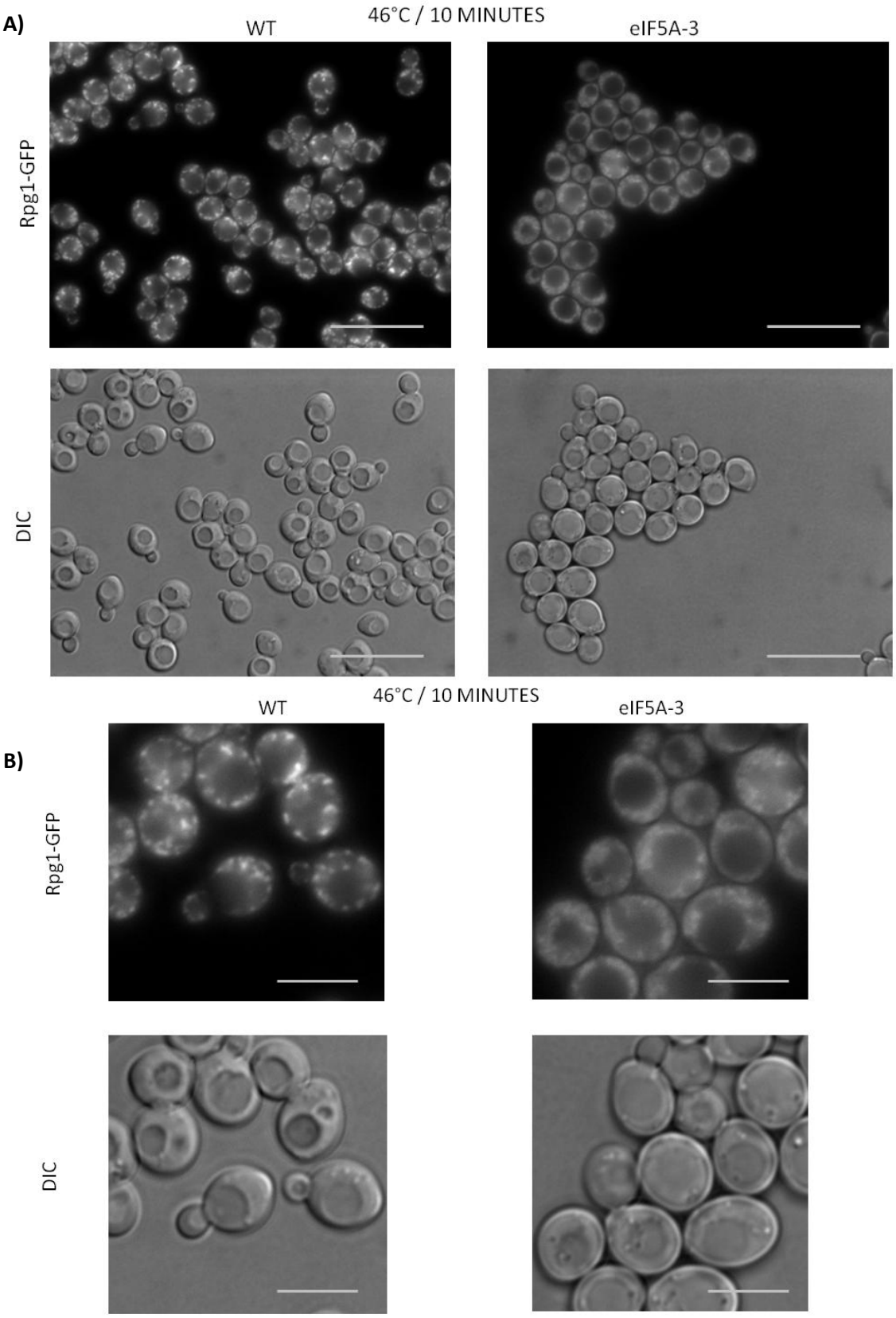

Figure 9. Fluorescence image of Rpg1-GFP and Nomarski diffraction from experiment with 46°C/10min heat shock in plasmid strains CRY 1365(eIF5A-WT) and CRY 1368 (eIF5A-3). (A) Heat shocked samples. Bar 20 µm. (B) Detail of representative cells from heat shocked samples. Bar 4 µm.

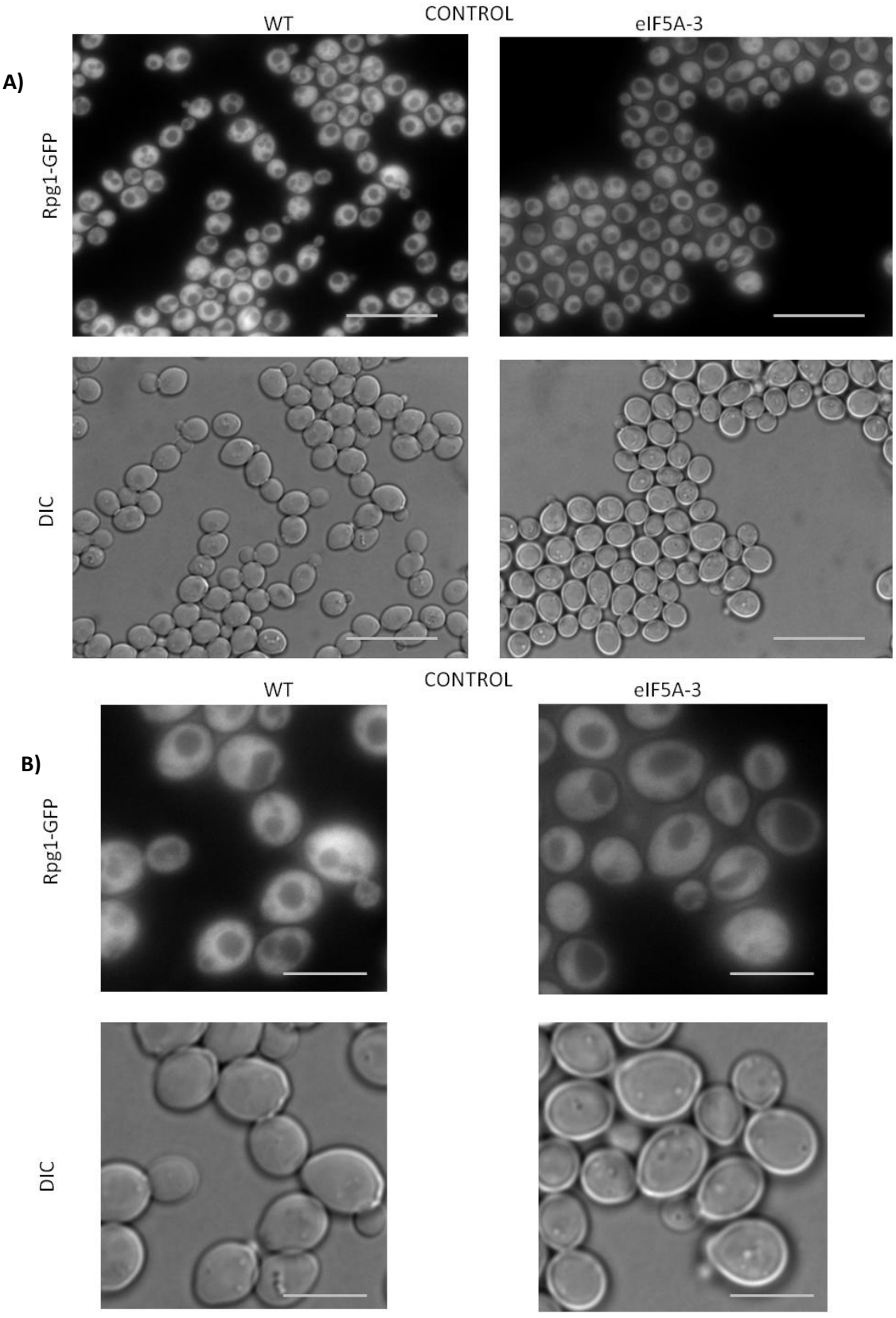

Figure 10. Fluorescence image of Rpg-GFP and Nomarski diffraction from experiment with 46°C/10min heat shock in plasmid strains CRY 1365(eIF5A-WT) and CRY 1368 (eIF5A-3). (A) Control samples for heat shocked cells. Bar 20 µm. (B) Detail of representative cells from control. Bar 4 µm.

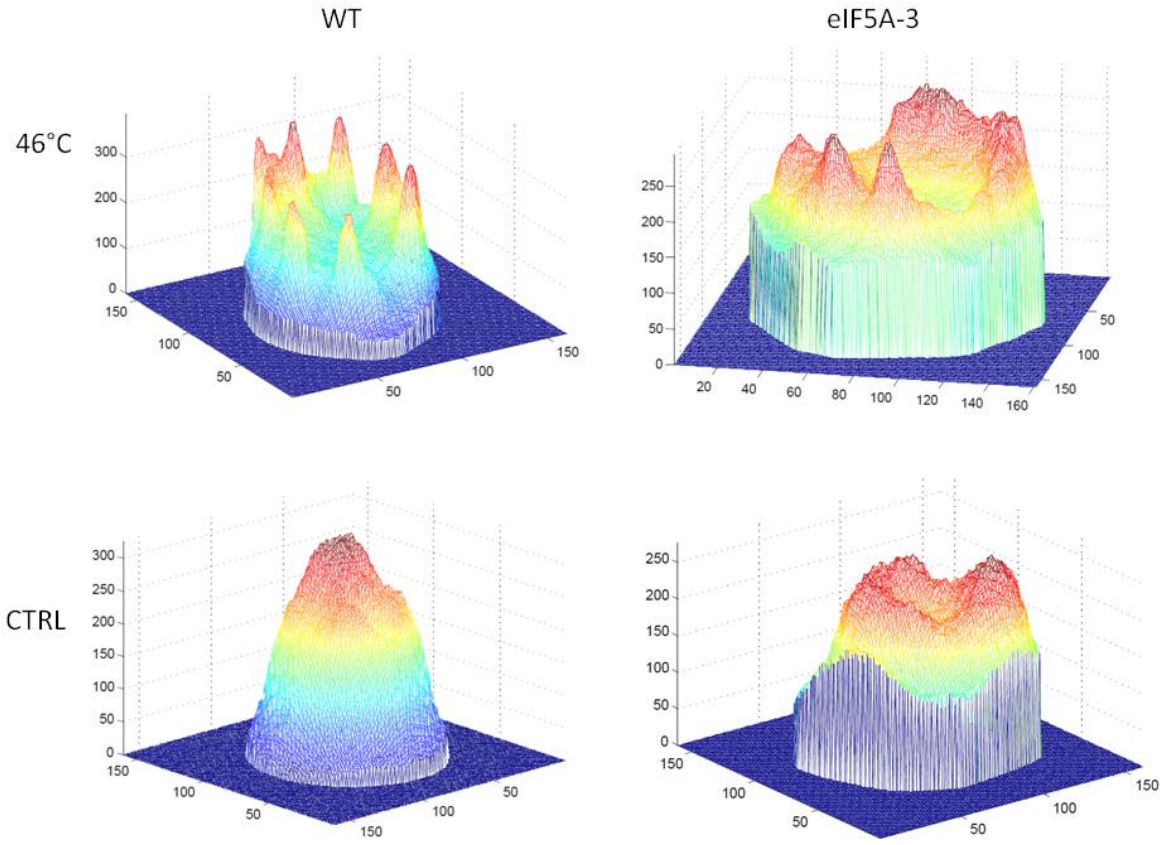

Figure 11. Ocellaris results for 46°C/10min heat shock in plasmid strains CRY 1365 (eIF5A-WT) and CRY 1368 (eIF5A-3). A 3D graph of Rpg1-GFP fluorescence brightness in representative cells from observed population.

In order to quantify the differences between WT cells and the eIF5A-3 mutant cells, images taken under specific conditions with Olympus CellR microscopic system, were analyzed by oCellaris – software specific for granulometric measurements of analyzed images, which has been developed by company Del in colaboration with our laboratory. In addition, the statistical program GrapgPad Prism 6 has been used for statistical analysis and graph plotting. Very briefly, oCellaris is capable to find cell borders automatically in bright field images and project them on corresponding fluorescence images. In the next step it searches for local maxima, evaluates their properties such as peak brightness, fluorescence intensity in comparison to disperse background signal, peak slope and many others. Software is capable of graphical presentation of analyzed images and enables export of values calculated for each cell in form of Excel table.

Graphical 3D representation of fluorescence brightness in a form of surface graph, gives us idea of the shift in SG formation in mutant cells. After the shock, diffuse cytosolic fluorescence from Rpg1-GFP does not clear up to levels observed in wild-type peaks and rises up more gradually.

Observed SGs are less focused than their counterparts in wild-type cells. Scatter plotting number of peaks in cells against the average slope of peaks in given cell illustrates the difference in quality of SGs even better. oCellaris software finds local fluorescence maxima even in disperse signal of control samples. These maxima are mostly ER or cytosolic accumulations of Rpg-1. Identifying trait of these false SGs is that their slope rarely rises over the value of 4.

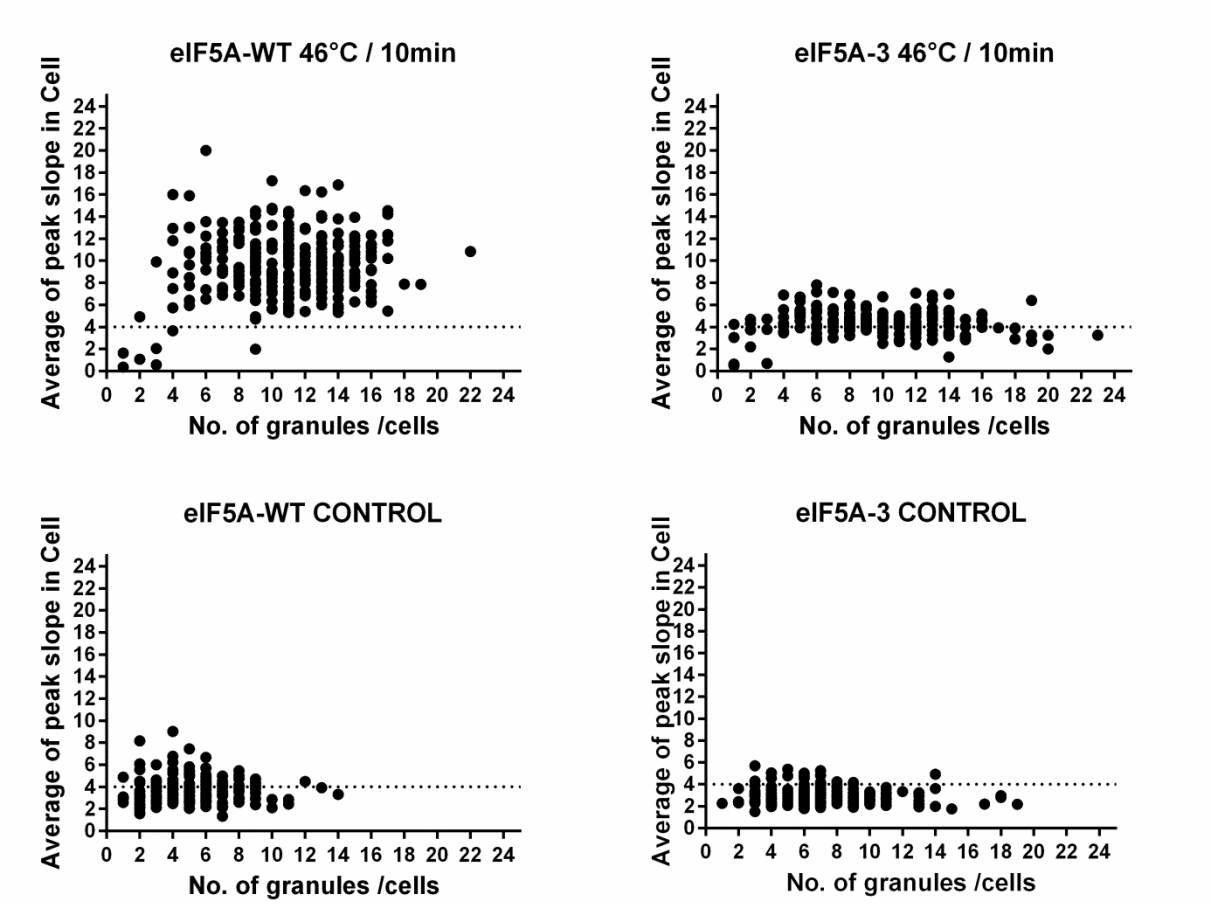

Figure 12. Ocellaris results for 46°C/10min heat shock in plasmid strains CRY 1365 (eIF5A-WT) and CRY 1368 (eIF5A-3). Scatter plot of granularity, each dot represents one cell. Dotted line represents cut-off for local maxima noise in Rgp1-GFP signal.

Results from robust 10minute heat shock clearly indicated that mutation eIF5A-3 has impact in quality of SGs, rendering SGs less focused and Rpg1-GFP signal more dispersed.

5.1.2.2 30 minute robust heat shock

Next, we decided to test whether prolonged heat stress of 46°C for 30 minutes, as used in study of Takahara (Takahara and Maeda 2012), can yield higher levels of granularity in eIF5A-3 mutants, that would reach to levels observed in eIF5A-WT upon 10 minute robust heat shock. Prolonged head stress did not change the trend in relation of WT and mutated strain granularity. eIF5A-3 mutants did still exhibit lower slope in comparison to WT. Nomarski diffraction images did however show us another interesting difference between those strains. The eIF5A-3 mutant cells showed vacuoles with increased size and seemed to be more resistant to death induced by the heat stress compare to the WT cells.

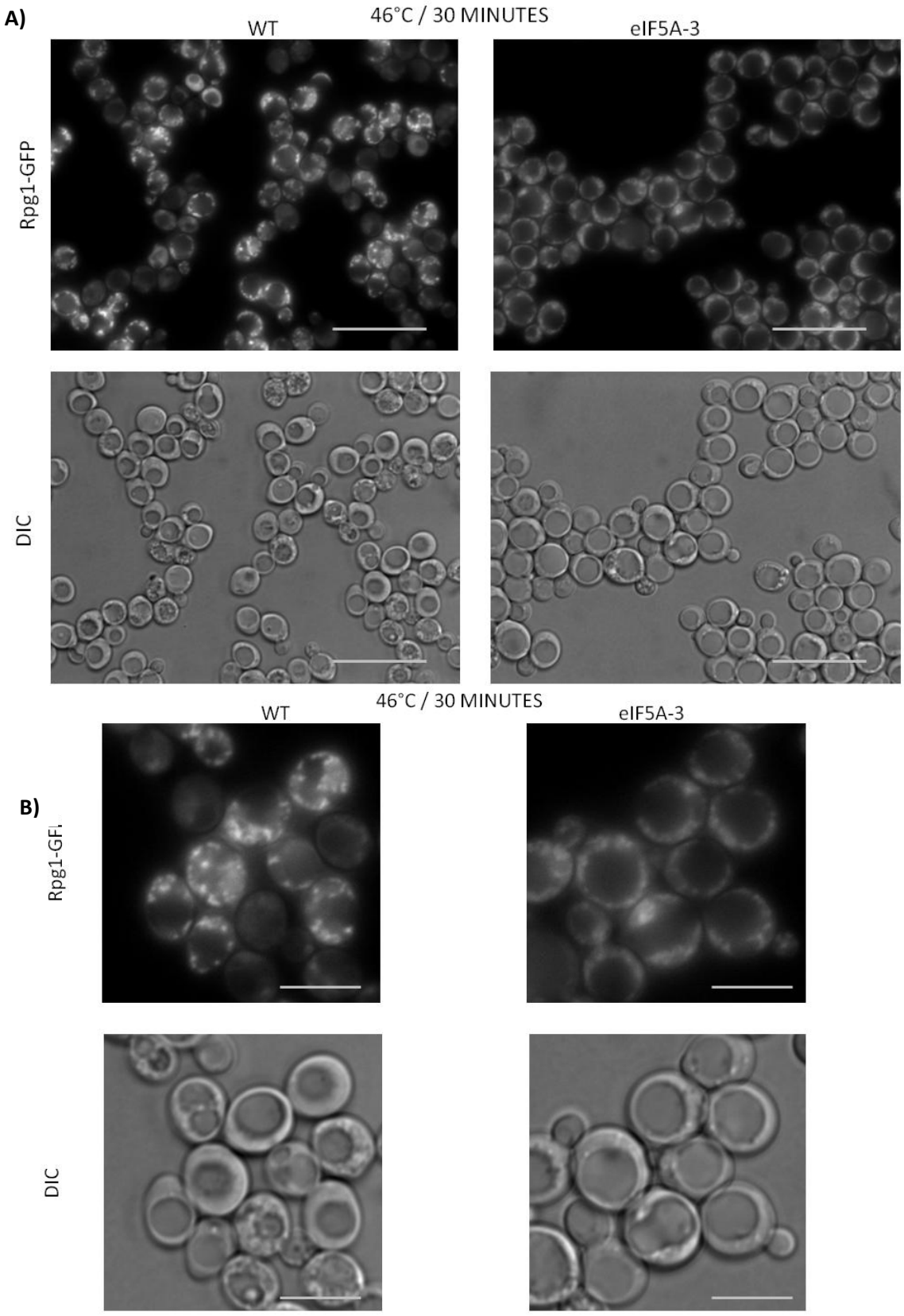

Figure 13. Fluorescence image of Rpg1-GFP and Nomarski diffraction (DIC) from experiment with 46°C/30min heat shock in plasmid strains CRY 1365(eIF5A-WT) and CRY 1368 (eIF5A-3). (A) Heat shocked samples. Bar 20 µm. (B) Detail of representative cells from heat shocked samples. Bar 4 µm.

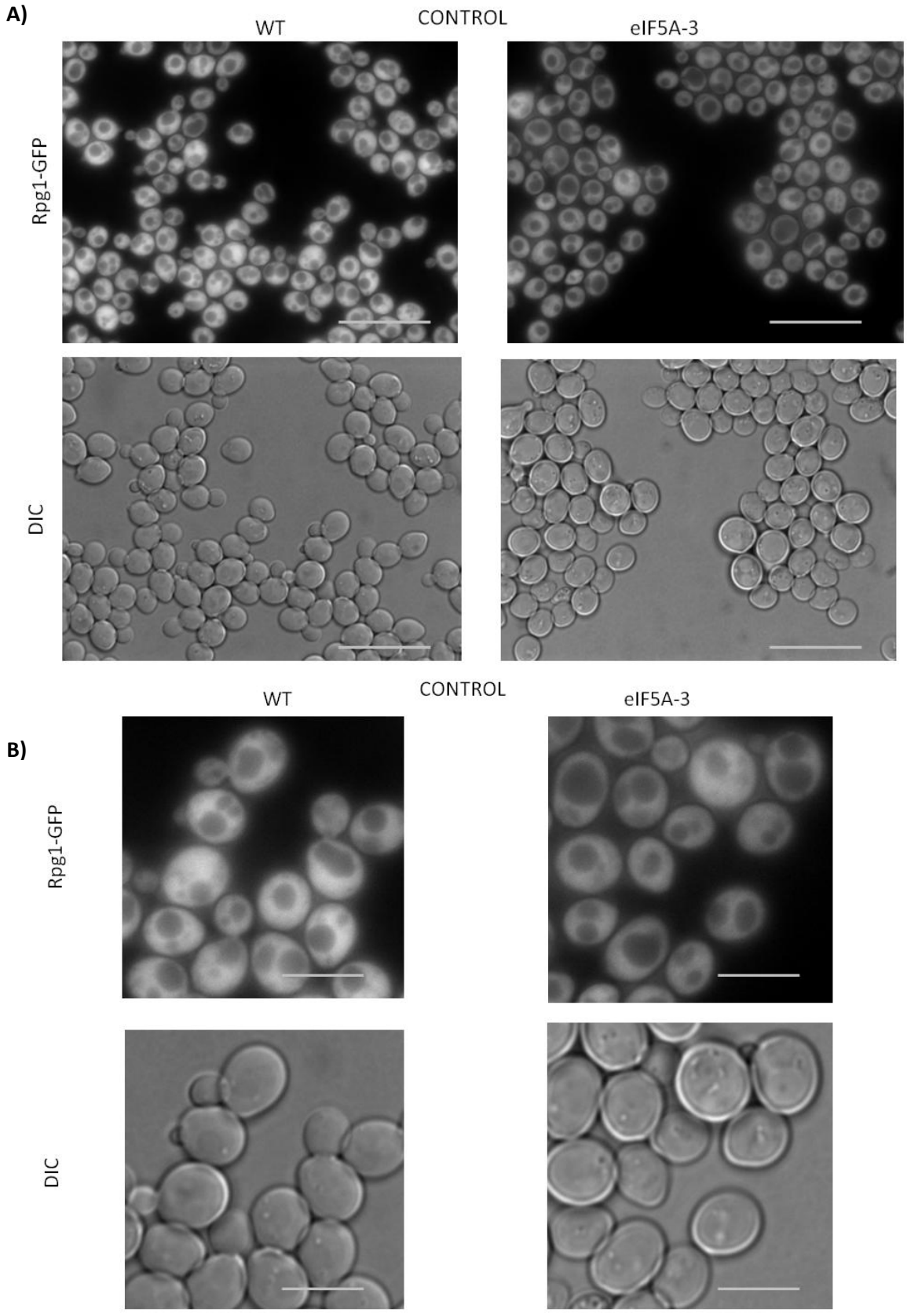

Figure 14. Fluorescence image of Rpg1-GFP and Nomarski diffraction from experiment with 46°C/30min heat shock in plasmid strains CRY 1365(eIF5A-WT) and CRY 1368 (eIF5A-3). (A) Control samples cells. Bar 20 µm. (B) Detail of representative cells from control sample. Bar 4 µm.

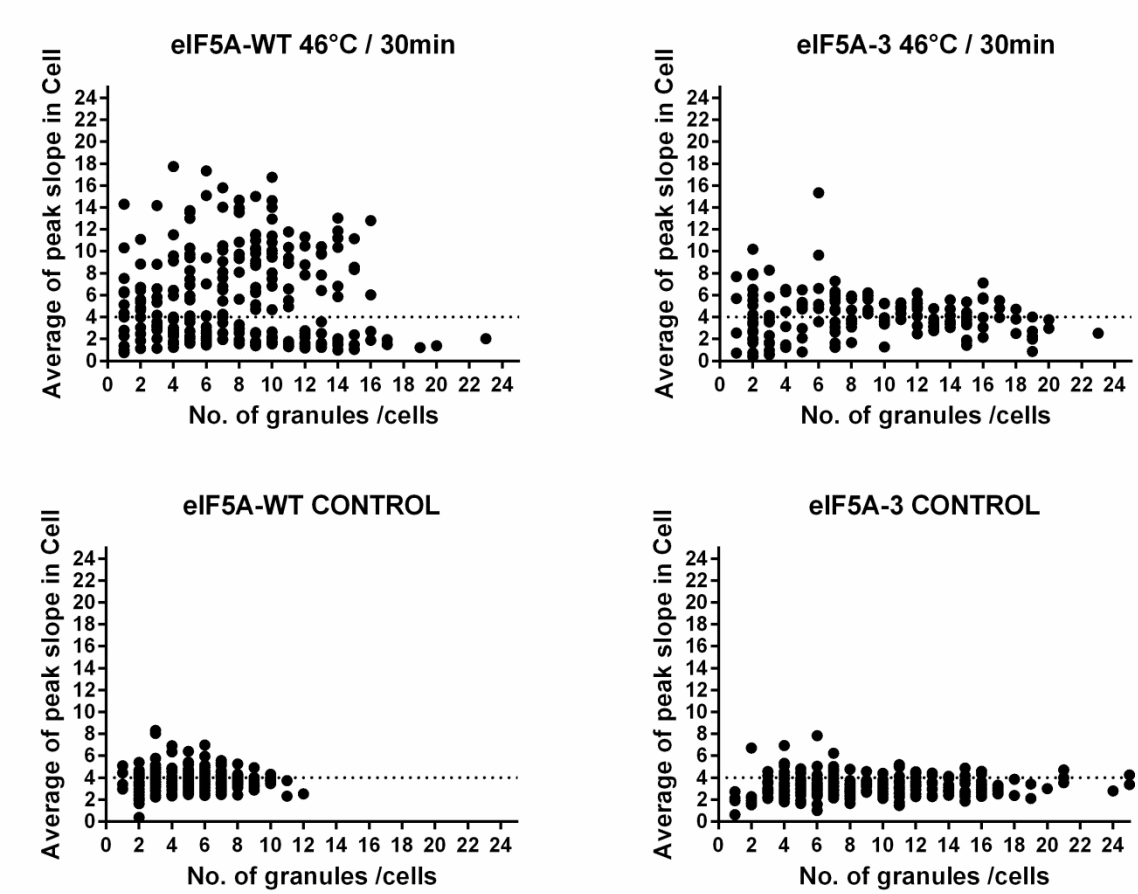

Figure 15. Ocellaris results for 46°C/30min heat shock in plasmid strains CRY 1365(eIF5A-WT) and CRY 1368 (eIF5A-3). Scatter plot of granularity, each dot represents one cell. Dotted line represents cut-off for local maxima noise in Rgp1-GFP signal.

On the scatter plot of heat shocked WT cells are visible two distinct populations; viable cells with high peak slope and dead cells with high number of low local maxima. This is however the only difference from previous experiment. Neither density of SGs accumulations nor the amount of a dispersed signal did change after prolonged 30 minute robust heat shock and the trend stayed the same as in case of 10 minute heat shock. The diminished effect of the robust heat stress on SGs formation in the eIF5A-3 mutant cannot be compensated by the prolonged duration of stress conditions. This suggests that the eIF5A-3 mutant probably influences quality of SGs as a whole and not only the SG aggregation rate and dynamics.

5.1.2.3 10 minute robust heat shock with prior inactivation

Given the temperature sensitivity of the mutant eIF5A-3 we decided to investigate if the inactivation of this protein in cells before the heat shock leads to any observed change in granularity.

Both, wild-type and mutant cells, were cultivated at 37°C in YPD for 4 hours prior to heat shock. Cultivation at this temperature for the respective time has been reported to be sufficient for depletion of the temperature sensitive eIF5A-3 protein in cells (Dias et al. 2008). Captured fluorescence images did not differ significantly from the ones obtained upon heat shock at 46°C for 10 minutes without inactivation.

This result suggests two possible conclusions about the effect of eIF5A-3 mutant on granularity in heat-shocked cells. First, if the eIF5A affects the formation of SGs directly, the A-3 mutations in eIF5A are so severe for SG formation, that cells containing the active form of this protein do express the same SGs formation pattern as the cells that do not contain any eIF5A-3 protein after inactivation. Second, if the eIF5A affect the formation of SGs indirectly, presence or absence of eIF5A at times of stress does not change the SG formation pattern. This might be explained by the fact that expression levels of proteins that may have direct influence on the SGs formation are already affected in the eIF5A-3 mutant (see below).

Recent papers supporting both notions can be found. A direct role of the eIF5A factor in SGs formation, under arsenite-induced stress in mammalian cells has been attributed to its contribution to the polysome disassembly, which is critical for SGs assembly (Li et al. 2010). The polysome profile of the eIF5A-3 mutant under robust heat shock observed in our lab (Avaca-Cusca, upublished) do strongly resemble the polysome profiles of the eIF5A knock-downs under arsenite-indcuced stress in aforementioned paper. Another direct reason might be in reported localization of eIF5A into SGs, which is influenced in eIF5A-3 cells (Avaca-Cusca, upublished). An indirect role of eIF5A on SGs formation might be caused by its important role in translation of proteins rich in poly-proline motive (Gutierrez et al. 2013). Since the poly-proline motive is contained in functionally related groups of proteins (Mandal et al. 2014), and some of them contain proteins important for mRNA metabolism such as eIF4E binding protein (Eap1) and proteins important for SGs formation such as TIA-1 and TIAR (Kimball et al. 2003).

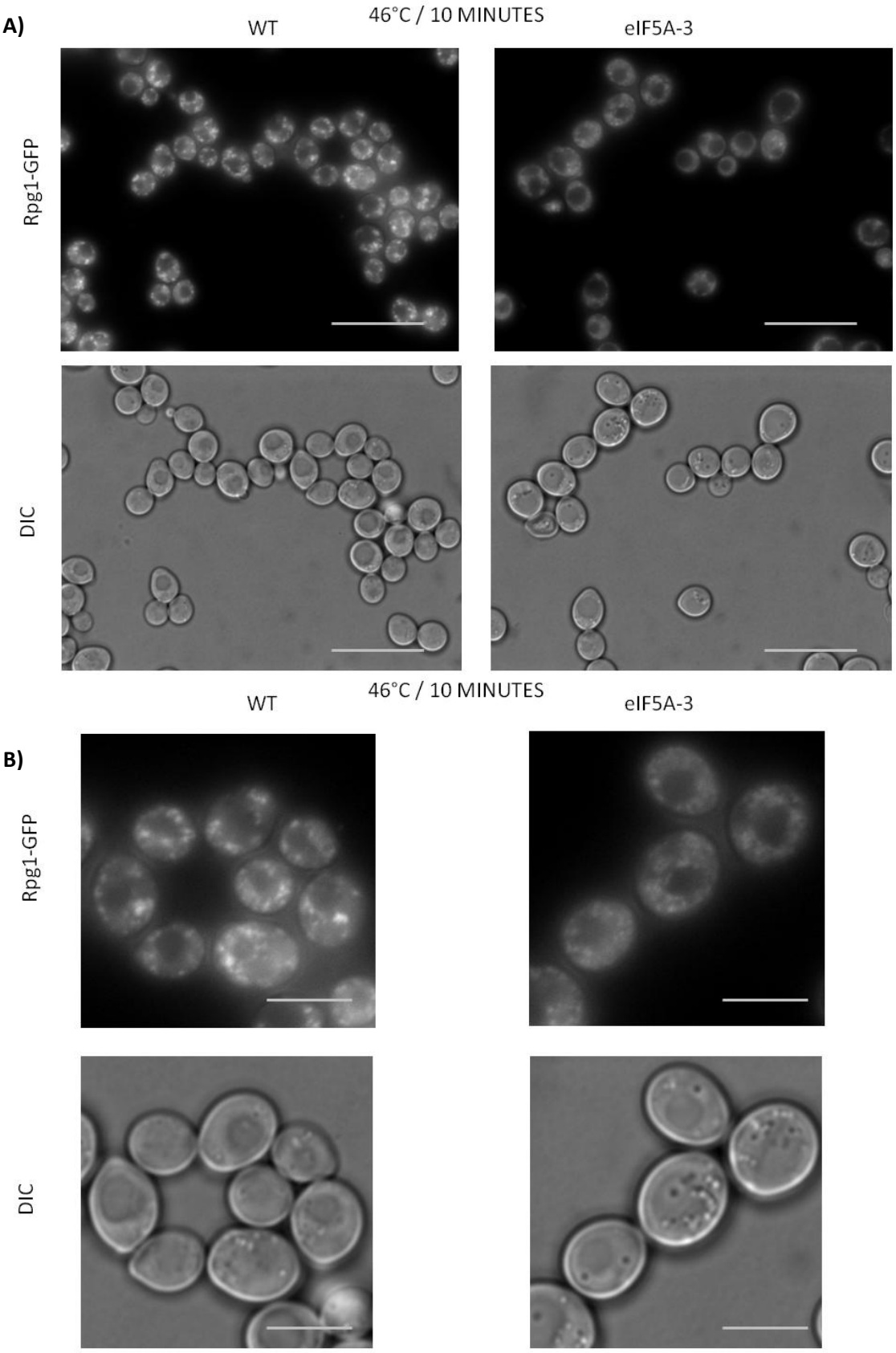

Figure 16. Fluorescence images of cells expressing Rpg1-GFP and Nomarski diffraction (DIC) image of the same cells from the experiment with 46°C/10min heat shock with prior inactivation in plasmid strains CRY 1365(eIF5A-WT) and CRY 1368 (eIF5A-3). (A) Heat shocked samples. Bar 20 µm. (B) Details of representative cells from heat-shocked samples. Bar 4 µm.

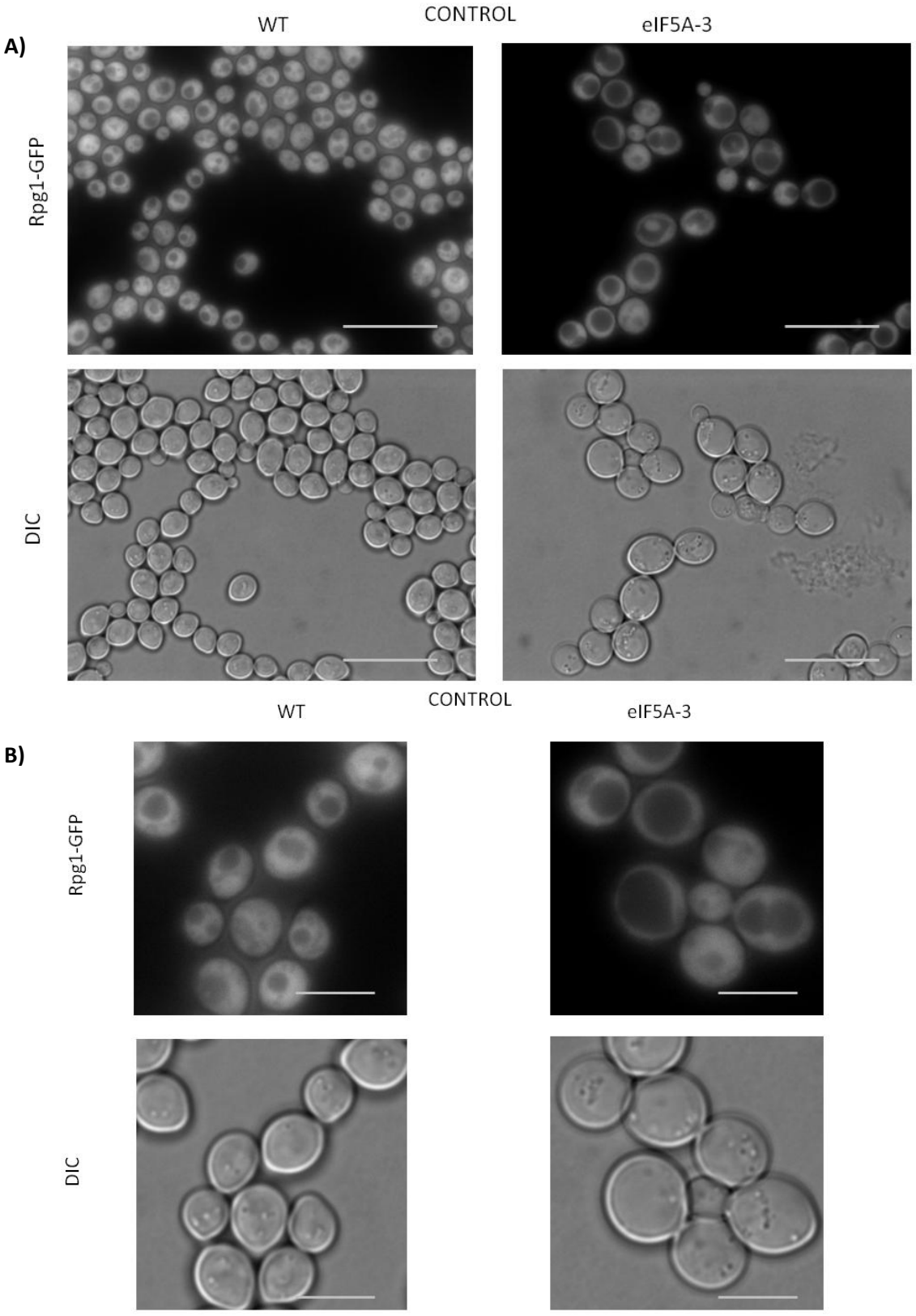

Figure 17. Fluorescence images of cells expressing Rpg1-GFP and Nomarski diffraction (DIC) images of the same cells from the experiment with 46°C/10min heat shock with prior inactivation in plasmid strains CRY 1365(eIF5A-WT) and CRY 1368 (eIF5A-3 mutant). (A) Control samples for heat shocked cells. Bar 20 µm. (B) Detail of representative cells from control samples. Bar 4 µm.

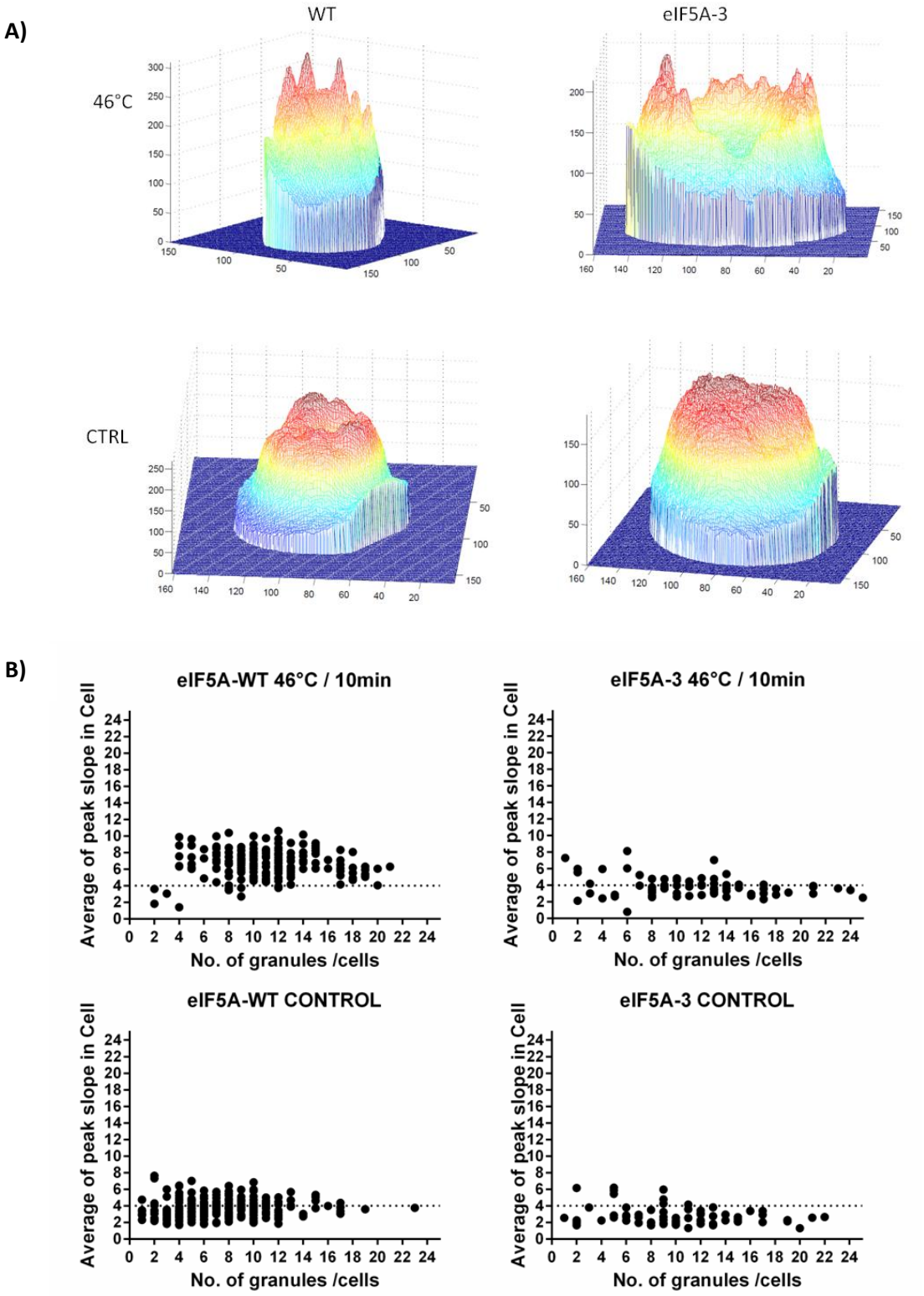

Figure 18. Ocellaris results for 46°C/10min heat shock with prior inactivation in plasmid strains CRY 1365(eIF5A-WT) and CRY 1368 (eIF5A-3). (A) 3D graph of Rpg1-GFP fluorescence brightness in representative cells from observed population. (B) Scatter plot of granularity, each dot represents one cell. Dotted line represents cut-off for local maxima noise in Rgp1-GFP signal.

5.1.3 Granulometric analysis of strains CRY 2417 and CRY 2418

Strains CRY 2417 (WT) and CRY 2418 (A-3) were subjected to the same robust heat shock as the strains co-expressing chromosome-derived Rpg1-GFP with plasmid-derived variants of eIF5A-WT and eIF5A-3. Granulometric properties were compared not just between WT and the mutant, but also between different haploid clones of both groups. Microscopic experiments dealing with the formation of SGs were extended for the SGs recovery observations. Recovery experiments were combined with the cell viability assay by propidiuim iodine. Our results support the trends observed in strains with plasmid-derived variants.

5.1.3.1 Comparison of clones CRY 2417-1C, 2B and 2418-2A, 4A

Before the microscopic experiments with newly created strains could proceed, it was necessary to test whether their phenotypes are uniform and clone independent. Granulometric parameters (we used again the 10 minute robust heat shock in CM) were measured for clones 2196x410 – 1C, 2B and 2198x410 – 2A, 4A. Variations between the clones were statistically insignificant. The rest of the microscopic experiments was performed with clones CRY 2417 –2B and CRY 2418 – 4A.

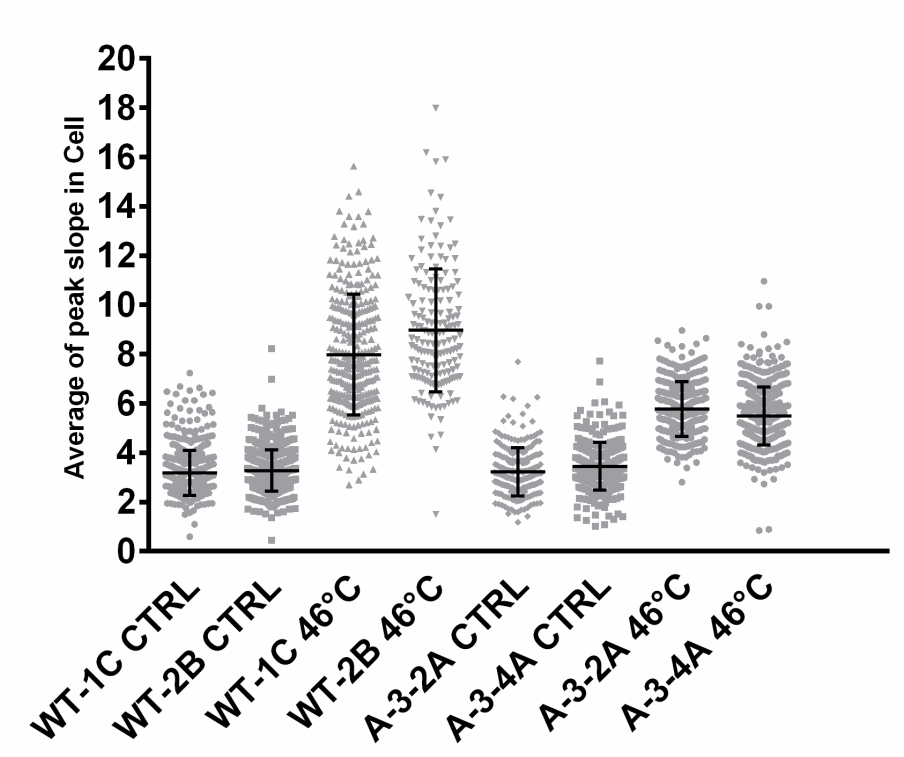

Figure 19. Comparison of SG slope after robust heat shock of 46°C/10min, between different clones of WT (CRY 2417) and A-3 (CRY 2418) in chromosomal versions.

5.1.3.2 10 minute robust heat shock

The fluorescence pattern of eIF5A-WT clearly differs from eIF5A-3 mutant cells, in accordance with trend that was present also in the strain bearing the plasmid versions. Rpg1-GFP accumulations in WT images are more pronounced than in the cells of the eIF5A-3 Peaks in WT cells were more focused and rose more sharply than in the A-3 mutant, while the levels of diffuse fluorescence were relatively higher in A-3 mutant.

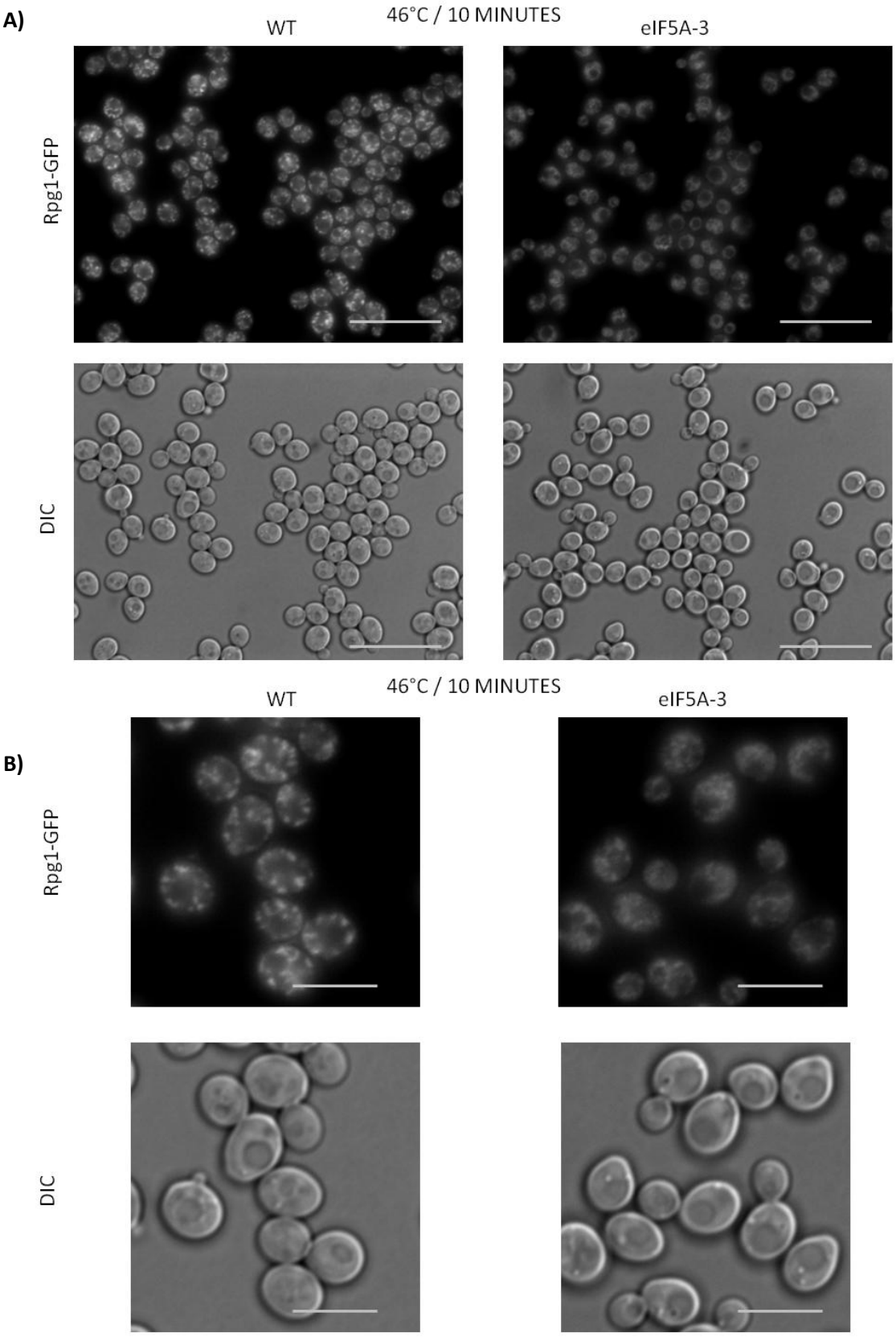

Figure 20. Fluorescence images of cells expressing Rpg1-GFP and Nomarski diffraction (DIC image) of the same cells from the experiment with 46°C/10min heat shock in chromosomal strains CRY 2417 (eIF5A-WT) and CRY 2418 (eIF5A-3). (A) Heat shocked samples. Bar 20 µm. (B) Details of representative cells from heat shocked samples. Bar 4 µm.

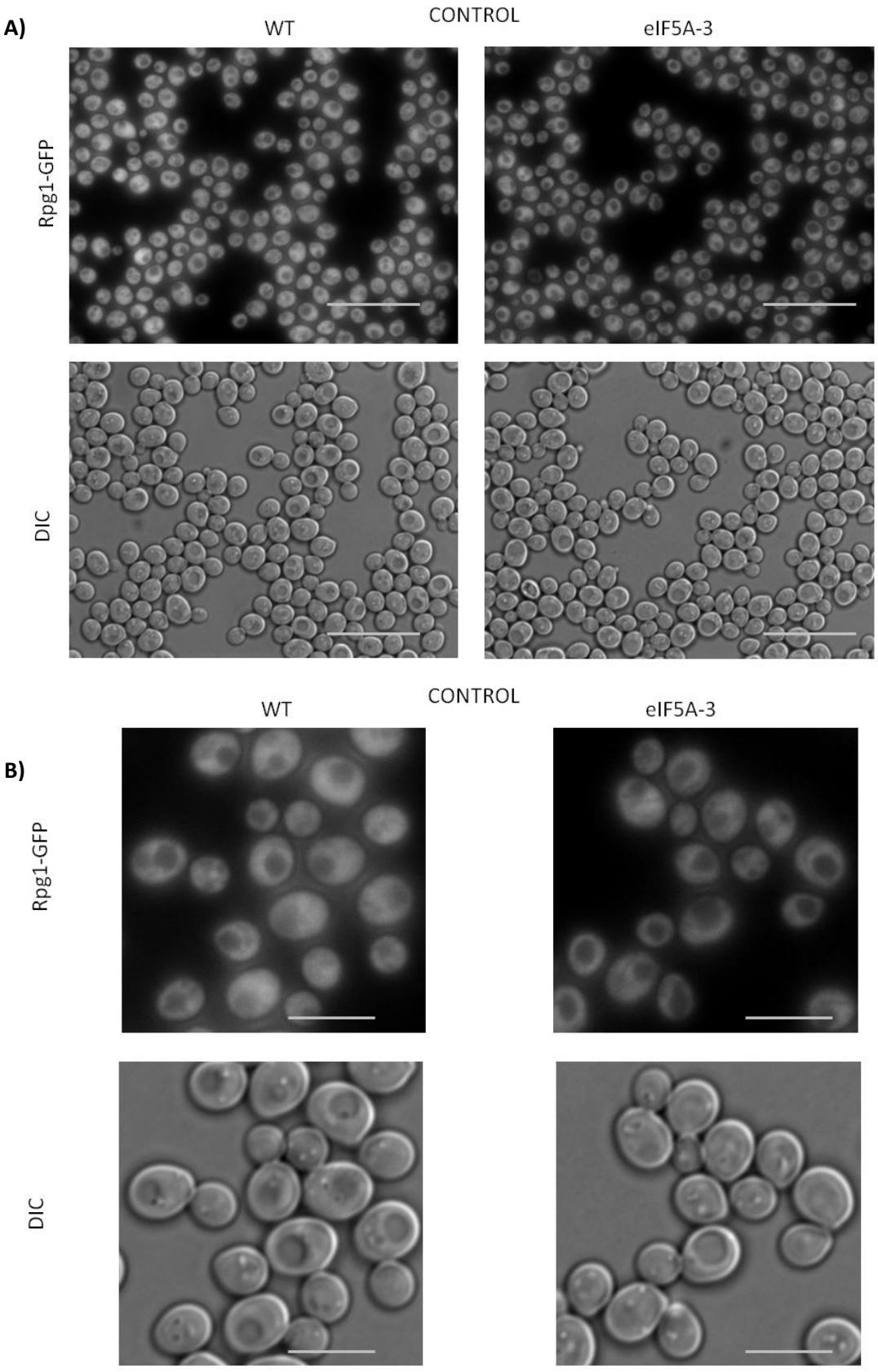

Figure 21. Fluorescence images of cells expressing Rpg1-GFP and Nomarski diffraction (DIC images) from the experiment with 46°C/10min heat shock in chromosomal strains CRY 2417 (eIF5A-WT) and CRY 2418 (eIF5A-3). (A) Control samples for heat shocked cells. Bar 20 µm. (B) Detail of representative cells from control samples. Bar 4 µm.

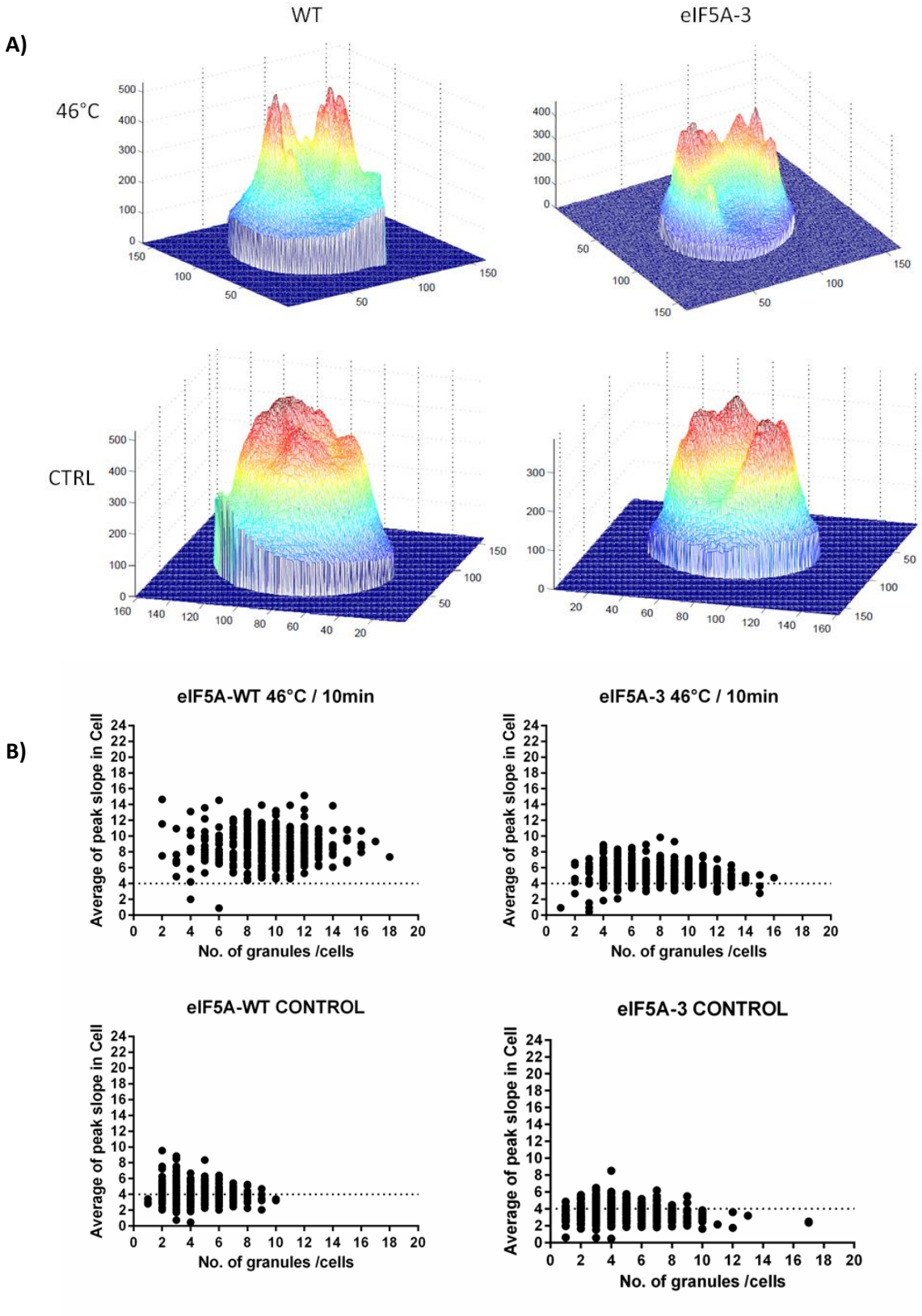

Figure 22. Ocellaris results for 46°C/10min heat shock in chromosomal strains CRY 2417 (eIF5A-WT) and CRY 2418 (eIF5A-3). ((A) 3D graph of Rpg1-GFP fluorescence brightness in representative cells from observed population. (B) Scatter plot of granularity, each dot represents one cell. Dotted line represents cut-off for local maxima noise in Rgp1-GFP signal.

5.1.3.3 Recovery after 10 minutes of robust heat shock and propidium iodine staining of cells

Cells were grown into the exponential phase and exposed to robust heat shock at 46°C for 10 minutes. The aliquots of cells were taken from the culture at 30 minutes time points for two and half hour after the robust heat shock and the cells were inspected microscopically. Surprisingly, given the lower slope of fluorescence, SGs dissolution in eIF5A-3 strains occurred at the same time point as in wild-type strain - at the two hour time point. This result indicates that SGs dynamic during recovery remains same in spite of the A-3 mutation and lower slope of granules accompanying it.

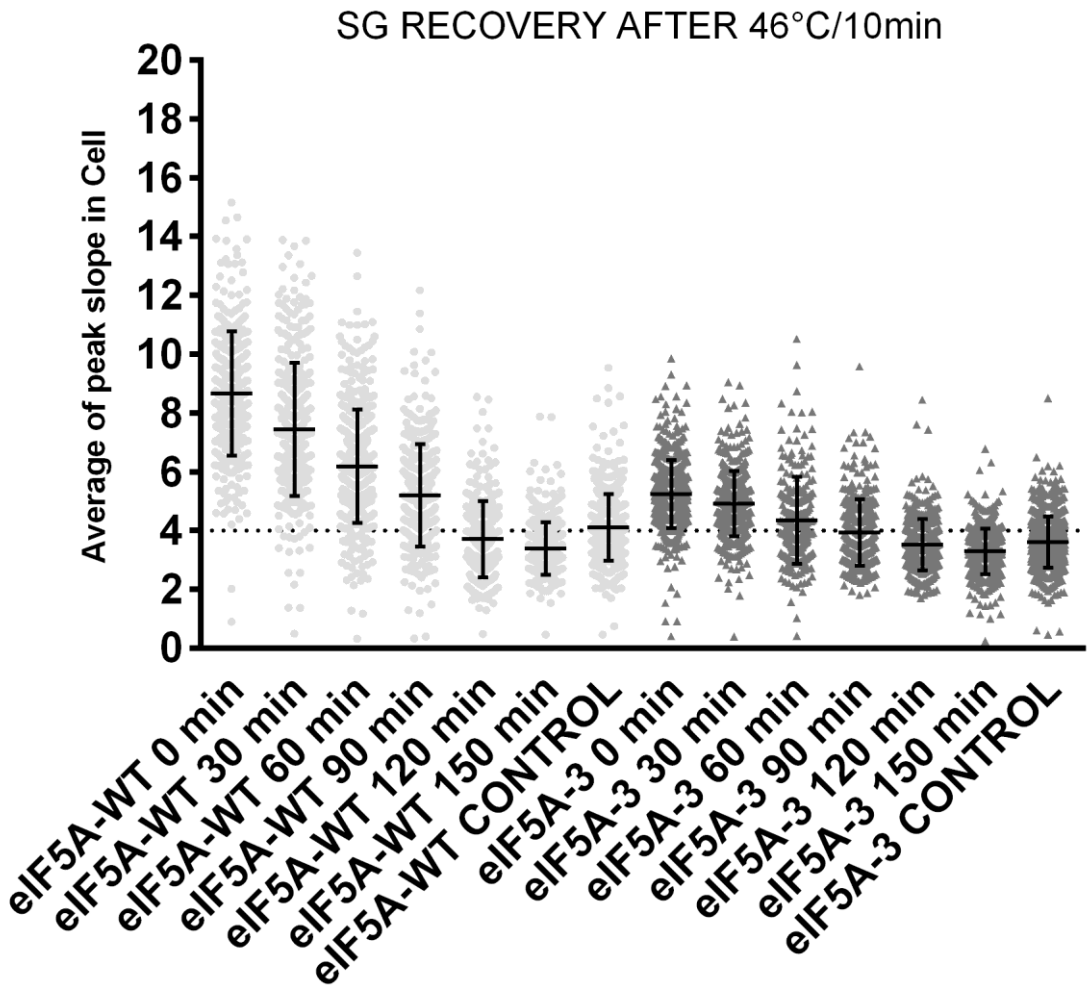

Figure 23. SG slope recovery and dissolution after robust heat shock of 46°C/10min, in chromosomal versions. Dotted line represents cut-off for local maxima noise in Rgp1-GFP signal.

SG recovery experiments were conducted simultaneously with propidium iodine staining. Propidium iodine accumulates in dead cells. Samples were washed in citrate buffer before and after propidium staining. Fluorescence images of both strains did show only a minor fraction of dead cells

after 10 minutes of the robust heat shock and during the recovery. The fraction of dead cells did not exceed 10% of the inspected population. Trend in proportion of stained cells was not statistically reproducible between these experiments. However, in both strains the proportion of stained cells decreases after 120 minutes. This indicates that both cells resumed proliferation after 2 hours.

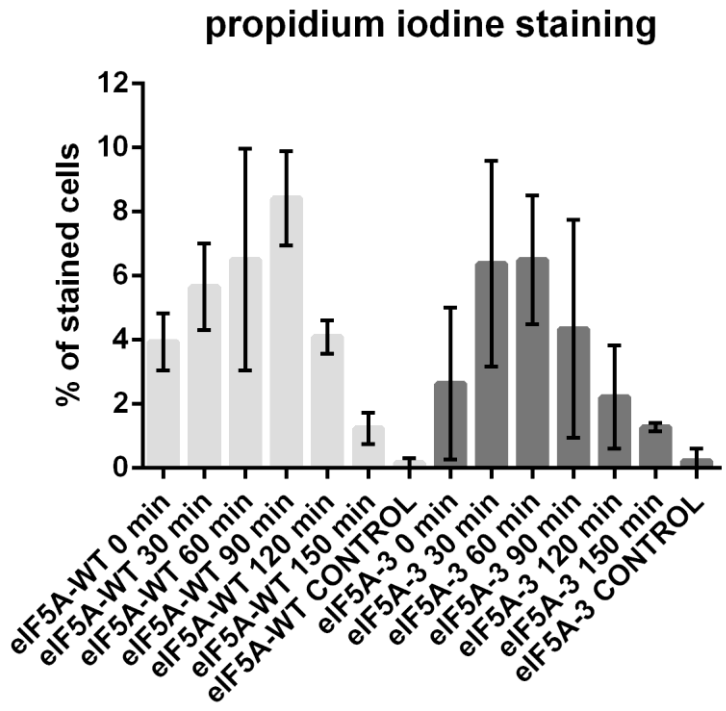

Figure 24. Propidium iodine staining of cells during recovery from 46°C/10min robust heat shock in chromosomal version of eIF5A-WT and eIF5A-3.

5.2 The influence of the eIF5A-3 ts mutation on growth

The factor eIF5A and its hypusination were reported to have a key role in cell proliferation and growth (Chattopadhyay et al. 2008). Plus, the eIF5A-3 mutant cells exhibit temperature-sensitive phenotype. Because of aforementioned reasons, we decided to test also traits important for proliferation in strains used for this study (see Table 2), These tests include the doubling time characterization, spot assay for the ts phenotype and the cell viability assay by plating.

5.2.1 The eIF5A-3 mutation increases doubling time

The protein eIF5A was reported to be an important factor for the cell proliferation (Kang and Hershey 1994). Hence, we decided to measure and quantify the effect of the eIF5A-3 mutation on doubling time. Measurements were conducted by Tecan Infinite 200Pro, with software Tecan i-

control (v 1.7.1.7). Cells were cultivated in 6-well plastic plates, in YDP medium at 28°C. Absorbance at 600nm wavelength was measured every 15 minutes, for 16 hours. The culture was diluted to OD 0,1 at the beginning of the experiment. Measurements were saved in a form of Excel file and doubling times of given strains were calculated (based on the equation in Materials and methods section 4.1.9).

The cells expressing eIF5A-3 (CRY 2192) from the plasmid showed doubling time of approximately 3 hour and 35 minutes that is approximately 1.5x times longer than the 2 hours and 20 minutes of eIF5A-WT expressed in the same manner (CRY2195). Effects diminishing the growth rate in the eIF5A-3 mutant were further amplified by implementation of the fused proteins Rpg1-GFP and Abp140-GFP in strains, which were used for microscopic observation of SGs and actin cytoskeleton. While the cells of the WT strain expressing Rpg1-GFP (CRY 1365) decreased their doubling time to 2 hours and 10 minutes, the eIF5A-3 mutants expressing Rpg1-GFP (CRY 1368) showed increase in doubling time for up to 4 hours, raising the ratio to 1.9x. The same trend was present in variants expressing Abp140-GFP. Wild-type cells (CRY 1369) divided in 2 hours and eIF5A-3 mutant (CRY 1372) in 3 hours and 40 minutes, bringing the ratio to 1.8x.

In accordance with trends observed in the plasmid system the cells expressing eIF5A-3 from the chromosome (CRY 2198) had doubling time of approximately 4 hours and 40 minutes that is approximately 2.4x times longer than the 2 hours of eIF5A-WT cells cultivated in the same manner (CRY 2196). Effects diminishing the growth rate of the eIF5A-3 mutant cells were surprisingly decreased with implementation of the fusion protein Rpg1-GFP by mating the mutant strain with the strain CRY 410. While the WT strain expressing eIF5A from the chromosome preserved it’s doubling time of approximately 2 hours, the eIF5A-3 mutant expressing Rpg1-GFP from the chromosome showed decrease in doubling time to 4 hours and 10 minutes, lowering the ratio to 2x. Increased doubling time in A-3 mutant variants is in line with previous studies.

Table 7. Doubling times of used strains.

STRAIN		DOUBLING TIME		RATIO
		MINUTES	HOURS	3:W
2195	WT-plasmid	139	2:20	1,54
2192	A-3 - plasmid	215	3:35	
1365	WT - plasmid Rpg1-GFP	128	2:08	1,88
1368	A-3 - plasmid Rpg1-GFP	240	4:00	
2196	WT - integ.	116	1:56	2,4
2198	A-3 - integ.	279	4:39	
2417	WT - integ. Rpg1-GFP	124	2:04	2
2418	A-3 - integ. Rpg1-GFP	248	4:08	
1369	WT - plasmid Abp140-GFP	123	2:03	1,8
1372	A-3 - plasmid Abp140-GFP	220	3:40	

5.2.2 Temperature sensitive phenotype of eIF5A-3 mutant

The spot assay was performed in order to verify temperature-sensitive phenotype of the mutants. Cells were diluted in 10 fold serial dilution row in YPD medium and spotted on YPD plates. Concentration ranged from 10^6 to 10^1 cells per spot and pipetted volume per spot was 3µl. YPD plates were incubated at 25°C as control and at 37°C to test the ts phenotype of the mutants. Plates were photographed after 3 days of incubation at appropriate temperatures.

The Figure 25 shows that, our experiment confirmed the ts phenotype of the eIF5A-3 mutant. In both chromosomal (CRY 2198 and CRY 2418) and all plasmid variants used in our previous experiments. That is strain CRY 2192 for heat-shock survival tests, the strain CRY 1368 for microscopic inspection of SGs and CRY 1372 for actin recovery observations. None of the mutant strains cultivated in 37°C did survive these conditions.

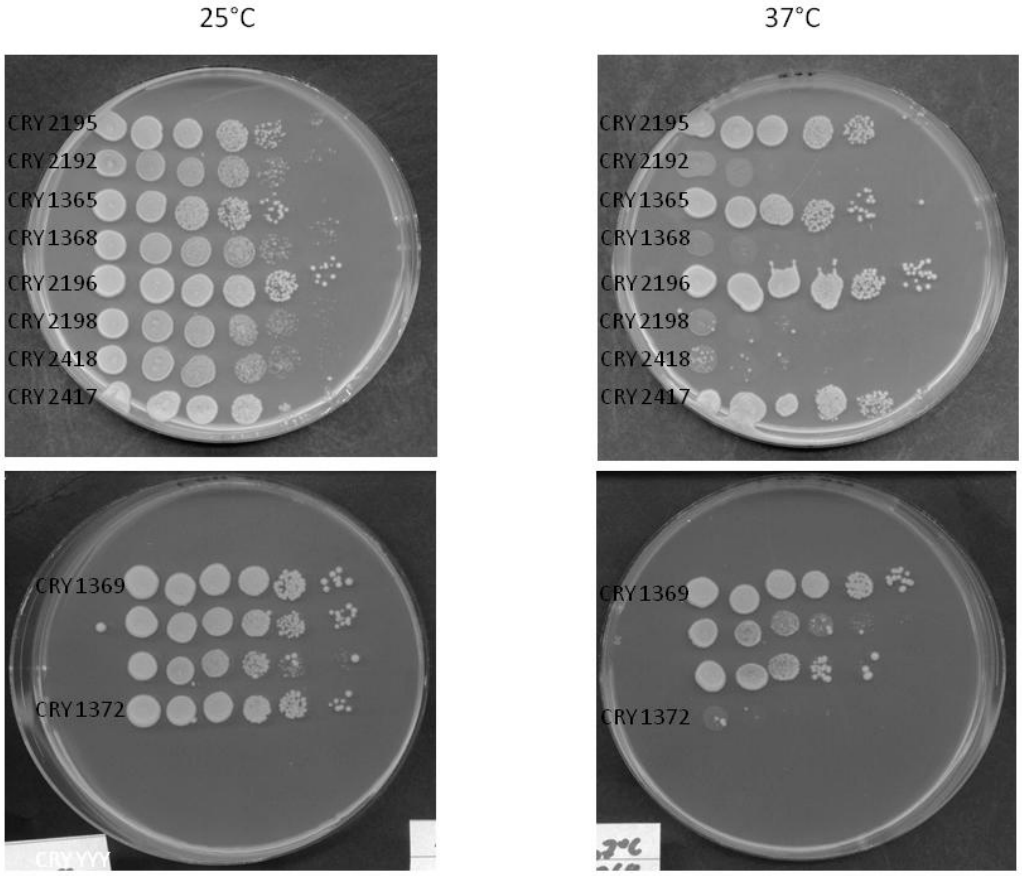

Figure 25. Spot assay for the temperature sensitive phenotype.

5.2.2.1 eIF5A-3 mutant loses its ts phenotype after prolonged cultivation at 25°C

Interestingly, the observation made on chromosomal variants of eIF5A-3 mutants, CRY 2198 and the strains that were created as a result of mating with the strain CRY 2198, indicate that the ts phenotype is reversible (Figure 26). Cells passaged and cultivated for six weeks at 25°C on YPD plates were subjected to the spot assay for the ts phenotype analyses. Surprisingly, the eIF5A-3 mutants reverted and supressed their ts phenotype and grew at 37°C. Majority of clones grew at the same extend or only 10 fold less than the WT strains, with only difference being the slower growth of macroscopically visible colonies. Revertants were sequenced with the primers specific for mutations in eIF5A-3 (primers eIF5A-F and eIF5A-R). Sequence of the mutated eIF5A gene in revertans remained mutated. Therefore they probably developed other compensational mutations, which enabled them to overcome the ts phenotype of the original strain containing the eIF5A-3 mutation, as suggested in works on yeast genome stability (Teng et al. 2013)(Stirling et al. 2014)(Serero et al. 2014) .

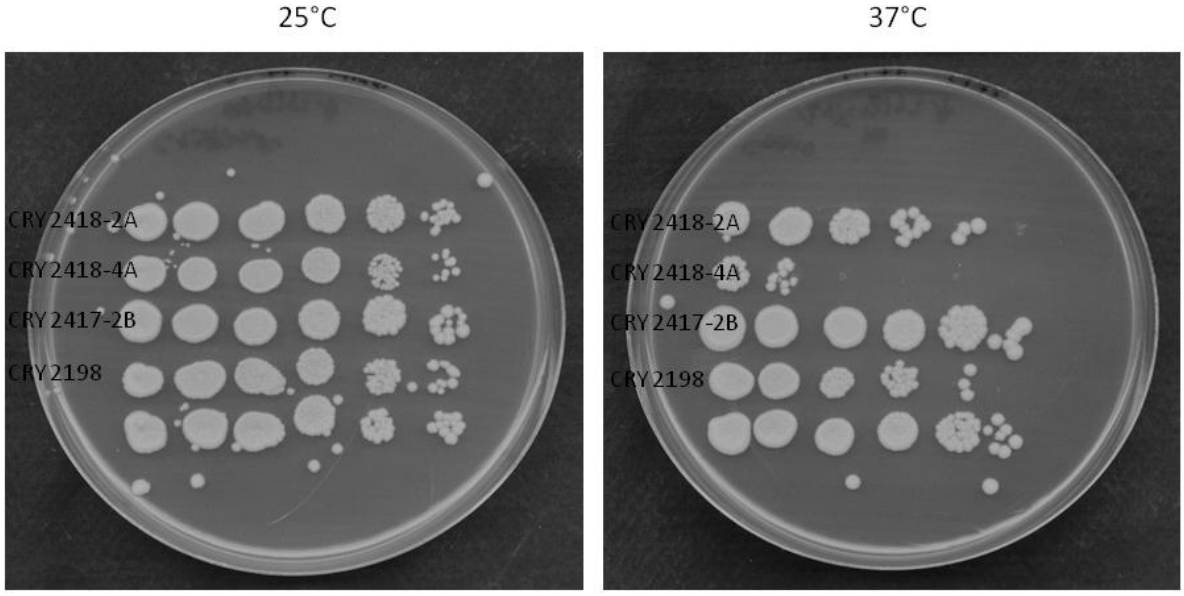

Figure 26. Spot assay for the temperature sensitive phenotype in clones cultivated at 25°C for 6 weeks before the experiment. eIF5A-3 clones exhibit loss of ts phenotype.

5.3 The eIF5A-3 mutation impacts viability of heat shocked cell

Based on the observation from the experiments with the 30 minute heat shock, where the eIF5A-3 seemed to tolerate the heat shock better than the WT strain, the survival rates of these strains were tested by plating and counting colony forming units (CFUs). Cells were cultivated in the YPD media to exponential phase, counted via CASY CellCounter, exposed to robust heat shock, diluted to appropriate concentration in order to plate 150 cells per plate and inoculated on YPD agar plates.

Results of the cell viability assay for the 30 minute lasting heat shock at 46°C indicate that in cells with fusion Rpg1-GFP and plasmid version of eIF5A the mutant eIF5A-3 (CRY 1368) endures heat shock better than the wild-type strain. While the WT cells (CRY 1365) survival rate was 49%, the numbers for the eIF5A-3 mutant cells were significantly higher at 88%.

In order to investigate further the influence of the eIF5A-3 mutation on ability of cells to survive the heat stress, we extended our assay for the plasmid strains that do not contain the Rpg1-GFP fusion protein and also for the heat shock at 46°C lasting for 10 minutes. Strains without fluorescent tags served as a control for cumulative effects of the translation elongation factor mutant and the translation initiation factor subunit eIF3a/Rpg1 fused at the C-terminal end with GFP. Finally, we tested also integrated versions of eIF5A-WT and eIF5A-3, without fluorescent markets (see Figure 27).

Results of the survival assay for strains without Rpg1-GFP, exposed to 46°C for 30 minutes, showed the same trend as observed in strains expressing Rpg1-GFP. Survival rates of the eIF5A-3 mutant (CRY 2192), with 65%, were significantly better compared to WT cells (CRY 2195), with 48%, even if ratio was slightly lower in comparison to values in strains coexpressing eIF5A-3 with Rpg1-GFP.

Outcome of the 10 minute heat shock survival assay, for CRY 1365 and CRY 1368, revealed even more remarkable facts. Surprisingly, the proportion of surviving cells followed the same trend as numbers obtained in the 30 minute heat shock experiment and the trend of higher eIF5A-3 survival rate still continued. The strain eIF5A-3 displayed 85% CFUs, compared to the WT cells where only 52% of expected CFUs on the plates were detected.

To examine the effect of the integrated version of eIF5A-3 mutant on cell survival upon 10 minutes of robust heat shock the survival rates of the strains CRY 2196 and CRY 2198 were tested by plating and counting colony forming units (CFUs). Results of survival assay for integrated strains without Rpg1-GFP showed the same trend as observed in the plasmid strains – survival rates of eIF5A-3 mutant, with approximately 100% CFUs, were significantly better when compared to WT cells, with 75% CFUs.

It is very tempting to assume that the differences in survival rates might be interconnected with differences in SGs formation observed previously, since SGs are well known to sequester proteins that are key factors in cell survival decision making process. It might also affect dissolution of SGs and re-initiation of translation upon release of cells from unfavorable conditions. Reasoning behind this assumption is further explained in both literature review and discussion (see below).

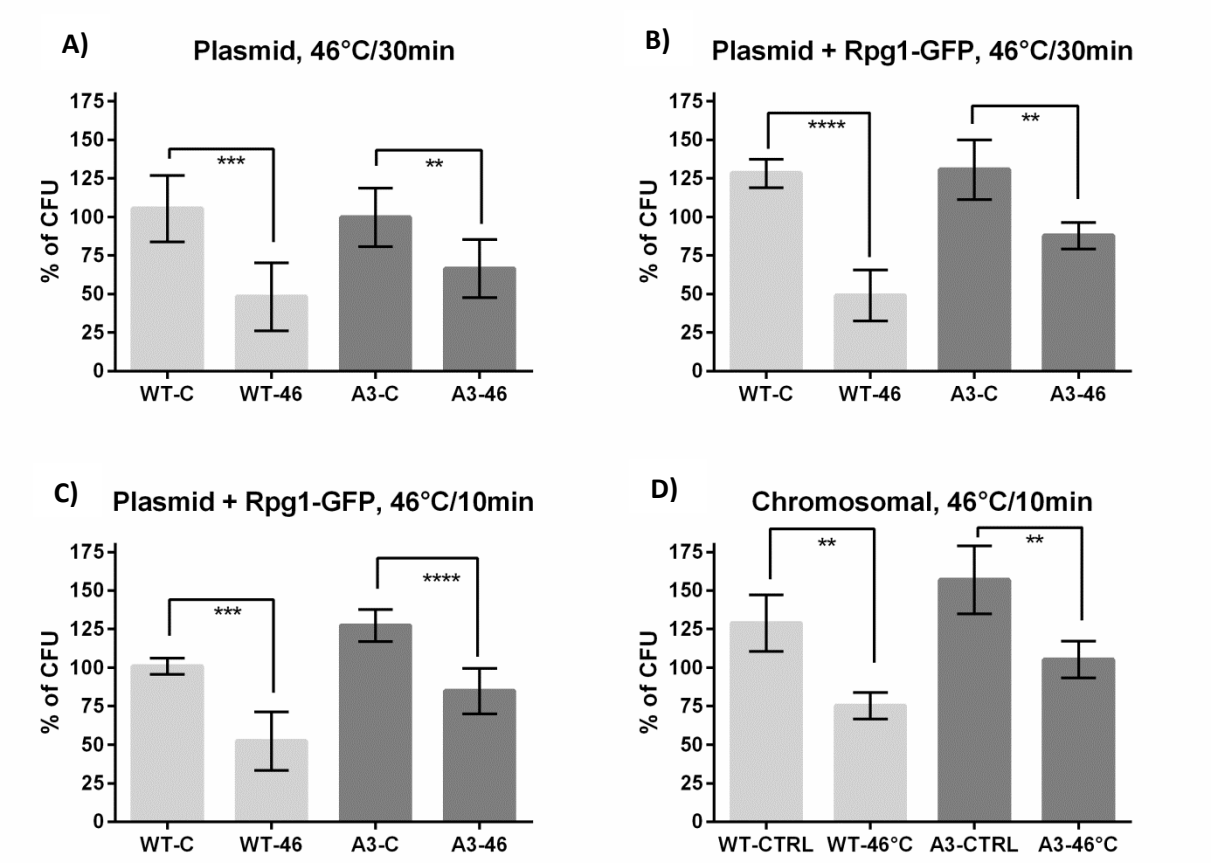

Figure 27. Viability assay of cells exposed to robust heat shock. A) for CRY 2195 (WT) and CRY 2192 (A-3); B) and C) for CRY 1365 (WT) and 1368 (A-3); D) for CRY 2196 (WT) and CRY 2198 (A-3).

5.3.1 Discrepancy of viability assays by plating and by PI staining

Percentage of CFUs surviving the heat shock, which ranges from 49% to 100%, depending on strain, does not match with the 10% of cells in the population that were stained with propidium iodine during the recovery experiments. Propidium iodine staining was tested on chromosomal system in which are the differences between CFU and PI assay smallest from all setups, yet they are still substantial. This discrepancy might suggest that yeast cells robustly heat-shocked for 10minutes do not undergo necrosis, or apoptosis, but their progression through cell cycle is arrested and they do no more undergo cell division and therefore do not give rise to visible CFUs. Higher fraction of visible CFU might indicate that the eIF5A-3 mutation positively influences the escape of cells from the cell cycle arrest after the relief of stress conditions.

5.3.2 Higher than expected growth in controls

Control samples, especially in chromosomal version, showed higher than expected growth of CFU. Main reason for this might be in time delay between measurement of culture concentration and plating of samples. While the heat-shocked cells are arrested in cell division, control samples can

finish their cell cycles. Cells in final stages of budding are still counted as one cell by CASY CellCounter. Some of the cells might finish their division.in the time gap befor plating and by that increase number of CFU to number higher than previously measured. Other reason might be that the volume of some dividing cells, or recently divided cells might have been higher or lower than the volume set up in measurement specifications for yeast cells, giving rise to a fraction of CFU that was not accounted for (see Methods section 4.1.6.).

5.4 Actin cytoskeleton after heat shock – preliminary data

Strains CRY 1369 and CRY 1372 with Abp140-GFP (Actin Binding Protein 140) enabled us to observe changes in actin cytoskeleton recovering from heat shock. Actin cytoskeleton is very dynamic structe. It is sensitive to changes in environmental conditions, notwithstanding stresses. Actin is also intercontected with translation state because many translation factors, most notably eIF1A, have actin binding domins and changes in their free and ribosome bound pool can be linked to changes in state of actin(Kandl et al. 2002) (Gross and Kinzy 2007) (Pittman et al. 2009) (Chatterjee et al. 2006) (Sattlegger et al. 2004)(Gross and Kinzy 2005) (Kim and Coulombe 2010). In adition, many proteins crucial for actin dynamics include poly-proline stretches. As mentioned previously, proline motives are suitable for fast and relatively strong interactions and they are also present in FH domains typical for formins (Li et al. 2014). Five of the S. cerevisiae proteins with highest poly-proline content are: VRP1 (Proline-rich actin associated protein, 9P, 8P, 6P, 4x5P, 3x4P, 2x3P), LAS17 (Actin assembly factor, 6P, 8x5P), AIM3 (Protein that inhibits barbed-end actin filament elongation, 5P, 2x4P, 6x3P), BNI1 (formin, 12P, 10P, 5P) and BNR1 (formin, nucleates the formation of linear actin filaments, 11P, 8P, 2x3P)(Mandal et al. 2014). These two facts were main reasons for our investigation of actin recovery dynamics after heat-shock in eIF5A-3 mutant. For actin visualization in vivo were used strains CRY 1369 (eIF5A-WT) and CRY 1372 (eIF5A-3) expressing eIF5A variants from plasmid and Abp140-GFP (Actin Binding Protein 140) from chromosomal cassette. Cell cultivation and treatment was identical to SG assembly experiments. Final image was created by an Olympus CellR^{TM} software as a Z-stack of images covering whole volume of observed cells with step of 0.6 µm between layers. Presented results are preliminary.

5.4.1.1 Actin recovery after robust heat shock of 46°C for 10 minutes

Cells were grown to exponential phase in YPD medium, and transferred into CM for treatment and experiment. Cells were exposed to robust heat shock of 46°C for 10 minutes and then mounted on cover glass, overlayed with CM agarose and let to recover in room temperature. In order to standardize our experimental setup and to account for variation in handling and mounting time for samples, sample taken directly after heat shock was left to recover for 4 minutes before it

was photographed. Mounted samples were photographed every 2 minutes at different location for 10 minutes, leading to total recovery time of 14minutes.

Directly after robust heat shock, actin cytoskeleton is collapsed into patches of F-actin in both wild-type and A-3 mutant cells. However, after 14 minutes of recovery A-3 mutant's fluorescence images show that considerable portion, about 40%, of observed cells recovered their F-actin into cables. While at the same time point only 4% of wild type cells recovered their actin cables. This preliminary result might indicate change beneficial for actin recovery dynamic, caused by eIF5A-3 mutation. Mutant cells also exhibit an increased vacuolar volume and a higher cell volume in general.

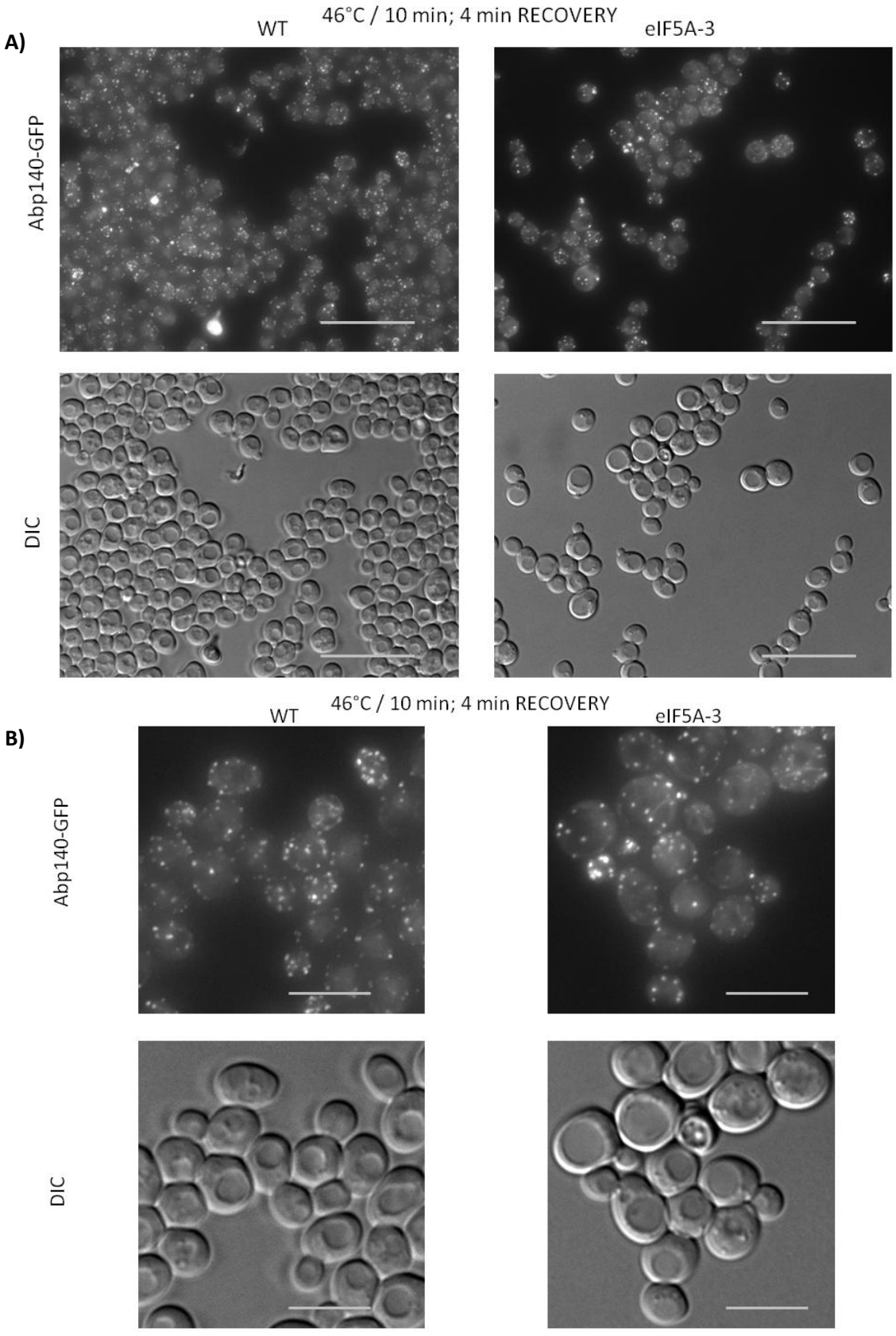

Figure 28. Fluorescence image of Abp140-GFP and Nomarski diffraction from experiment with 46°C/10min heat shock in plasmid strains CRY 1369 (eIF5A-WT) and CRY 1372 (eIF5A-3) after 4 minutes of recovery. (A) Heat shocked samples. Bar 20 µm. (B) Detail of representative cells from heat shocked samples. Bar 4 µm.

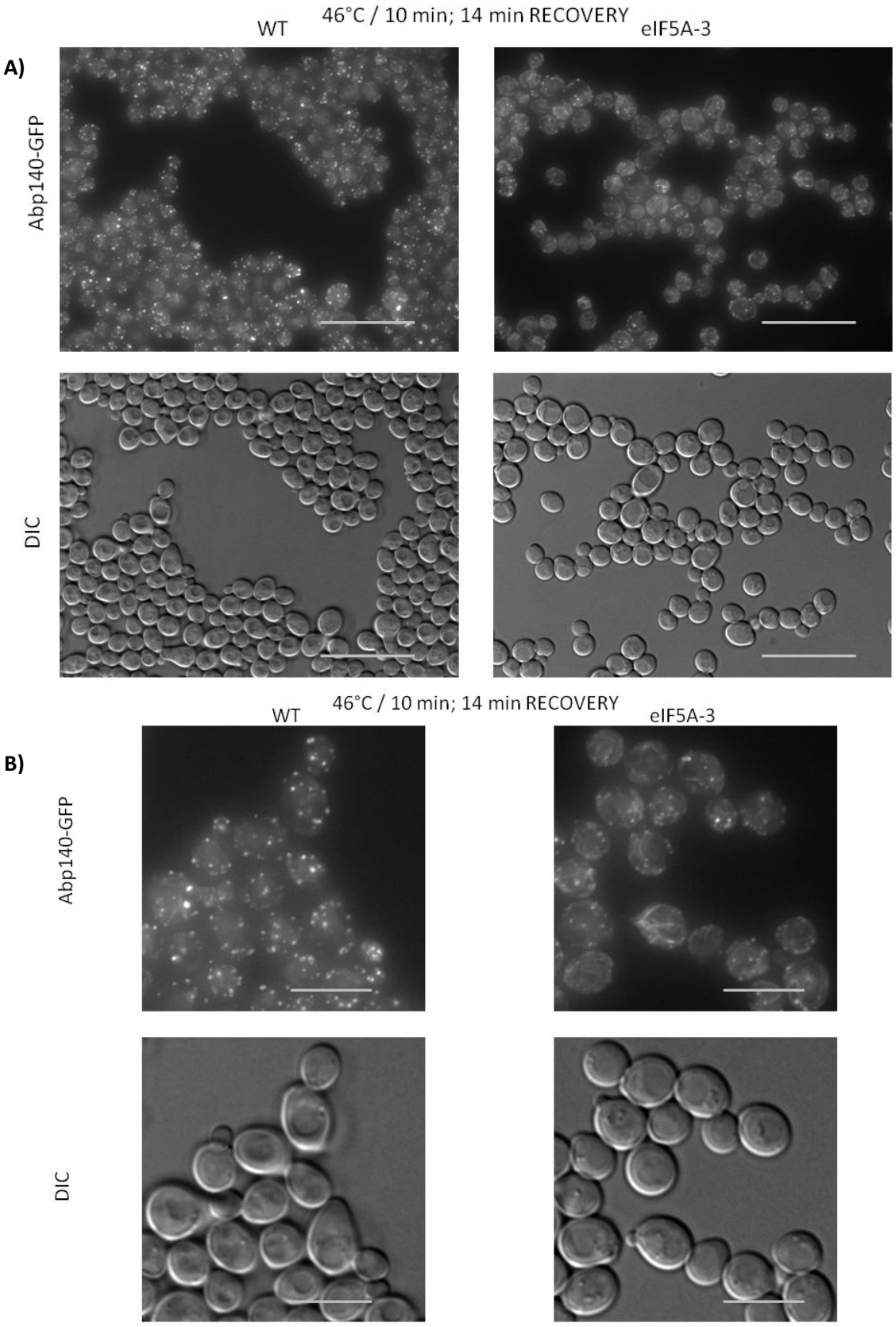

Figure 29. Fluorescence image of Abp140-GFP and Nomarski diffraction from experiment with 46°C/10min heat shock in plasmid strains CRY 1369 (eIF5A-WT) and CRY 1372 (eIF5A-3) after 14 minutes of recovery. (A) Heat shocked samples. Bar 20 µm. (B) Detail of representative cells from heat shocked samples. Bar 4 µm.

5.4.1.2 Actin recovery after heat shock of 42°C for 10 minutes - patches x cables

Experiment was conducted according to same microscopic protocol as in previous test, with only exception being lower temperature of heat shock, 42°C. Effect of eIF5A-3 mutant was visible already at 4 minutes of recovery, while in the wild type population about 52% of cells presented cables as a dominant form of F-actin, In eIF5A-3 population it was approximately 95% of cells with cables, with no visible patches. After 14 minutes of recovery about 95% of cells in both WT and mutant population contain actin in form of cables.

Bearing in mind that these data are only preliminary results, eIF5A-3 mutant appears to have strong influence on actin dynamics, during recovery from heat shock induced stress. Precise mechanism still remains obscure. Possible direct mechanism might include altered levels of poly proline containing formins. However, drop in formine levels would probably have effect opposite to observed phenotype, hindering recovery of cables rather than increasing their dynamics. Indirect effect of eIF5A-3 might be mediated by change in SG formation and its possible consequences for cell signaling, including signals for actin recovery.

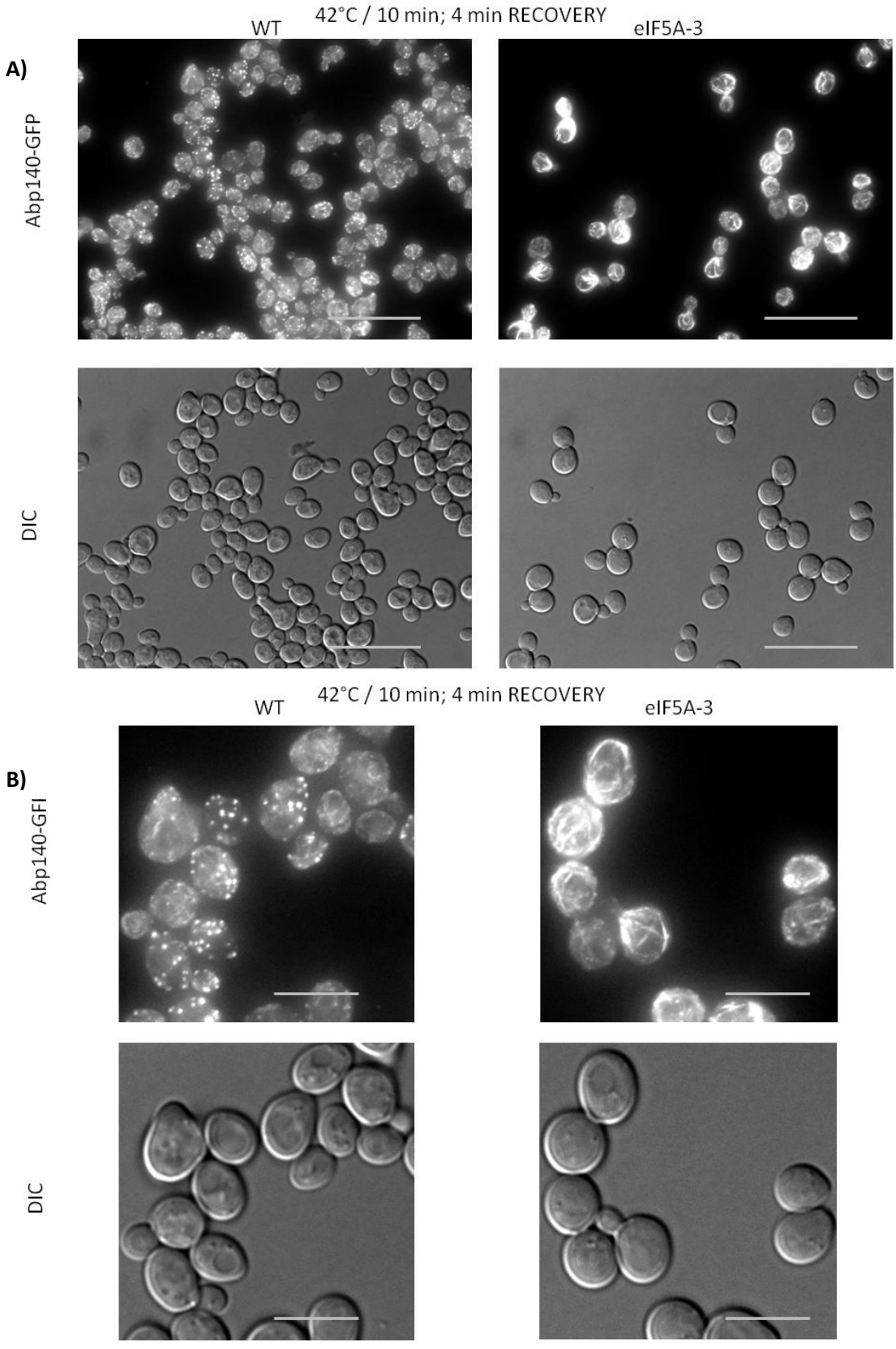

Figure 30. Fluorescence image of Abp140-GFP and Nomarski diffraction from experiment with 42°C/10min heat shock in plasmid strains CRY 1369 (eIF5A-WT) and CRY 1372 (eIF5A-3) after 4 minutes of recovery. (A) Heat shocked samples. Bar 20 µm. (B) Detail of representative cells from heat shocked samples. Bar 4 µm.

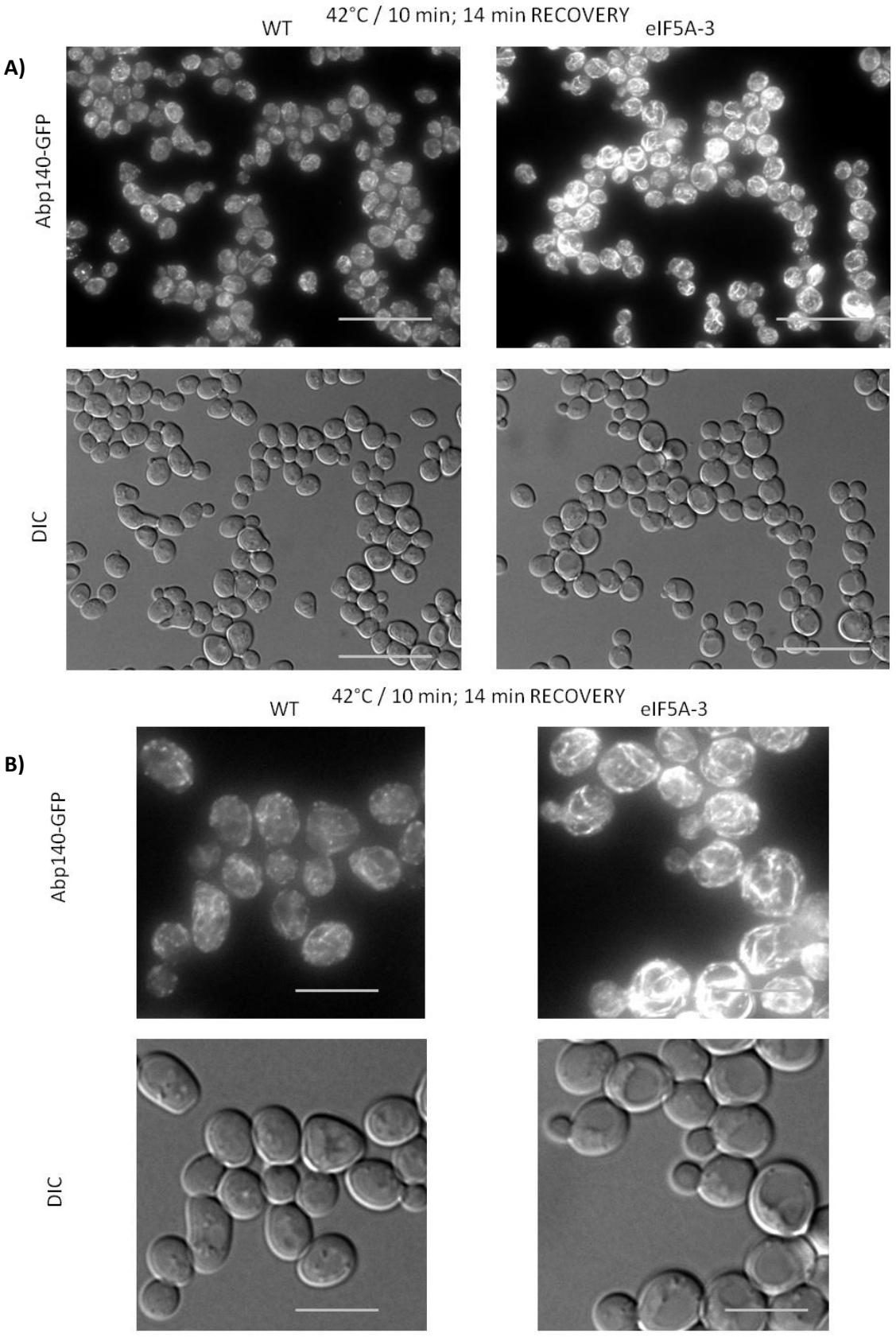

Figure 31. Fluorescence image of Abp140-GFP and Nomarski diffraction from experiment with 42°C/10min heat shock in plasmid strains CRY 1369 (eIF5A-WT) and CRY 1372 (eIF5A-3) after 14 minutes of recovery. (A) Heat shocked samples. Bar 20 µm. (B) Detail of representative cells from heat shocked samples. Bar 4 µm.

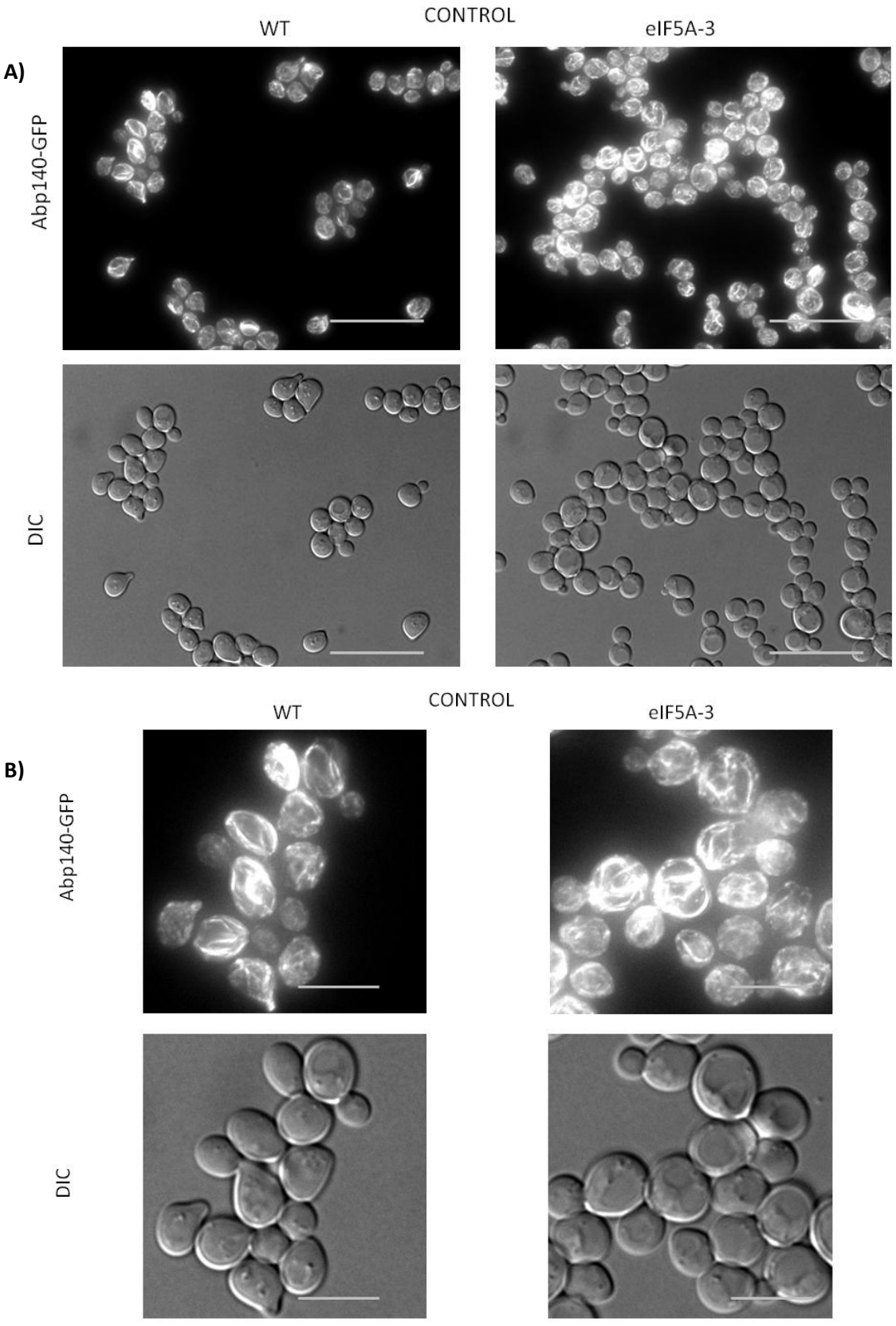

Figure 32. Fluorescence image of Abp140-GFP and Nomarski diffraction from control experiment in plasmid strains CRY 1369 (eIF5A-WT) and CRY 1372 (eIF5A-3). (A) control samples. Bar 20 µm. (B) Detail of representative cells from control samples. Bar 4 µm.

6 Discussion

Working hypothesis of this master's thesis was based on the effects of mutation eIF5A-3 on translation. Temperature-sensitive eIF5A-3 mutant cultivated under restrictive conditions was shown to exhibit increase in the polysome fraction, a similar polysome profile as the cells treated with Cycloheximide (CHX) (Gregio et al. 2009). This similarity indicates a role of eIF5A in translation elongation. Polysome profiles of the eIF5A-3 mutant pre-cultivated under permissive conditions and exposed to robust heat shock indicated changes in polysome profile as well. This change suggested slower polysome run-off in the mutant (Avaca-Cusca, unpublished data). We hypothesized that the mutant eIF5A-3, exhibiting change in the polysome run-off upon robust heat shock, will also affect the formation of SGs under these conditions.

6.1 Impact of the eIF5A-3 mutant on SGs formation in reaction to robust heat shock

The eIF5A is documented to be essential protein, with direct role in translation initiation, elongation and with critical impact on actin dynamics, polarity of cellular growth and progression of cell cycle. However, the exact reason for its essentiality remains long hidden.

Results of our study on effects of eIF5A-3 mutant on SGs formation did show stable trend reproducible between the plasmid and the chromosomal system. The mutant eIF5A-3 exhibits significantly lower granularity. Stress granules formed in the eIF5A-3 strain slope approximately to 0.66x fold of WT granules and this effect can't be reversed by prolonged exposure to stress conditions. The heat induced granularity in the eIF5A-3 mutant cells cultivated at permissive temperature did not differ significantly from values obtained in cells precultivated under the non-permissive conditions. This indicates a critical role of mutated amino acids, and surrounding regions, for the eIF5A function in SGs formation. A broad spectrum of reported eIF5A functions lets us speculate on many possible direct and indirect ways by which can this mutation affect processes leading to SGs formation.

Direct effects are probably represented by the eIF5A role in the polysome run-off and eIF5A incorporation into SGs (Avaca-Cusca, unpublished data) While the indirect role of eIF5A in SGs formation can be related to its role in translation of polyproline-rich proteins; proline motive is present in many protein-protein and protein-nucleic acid interaction domains. It is also present in prions and prion-like proteins, which contain self-organising amyloid structure (Rauscher et al. 2006) (Ziegler et al. 2006). Amyloid interaction of prion-like proteins is suggested to play a major role in

protein aggregation into SGs, as was documented in mammals in case of TIA-1 and TIAR proteins (Gilks et al. 2004).

Diminished SGs formation under the robust heat shock might be also caused by a decrease in disassembly of polysomes. Results of the eIF5A knock-down experiment with arsenite stress on mammalian cell lines showed analogical results. This paper highlighted the importance of the fully functional eIF5A for a rapid ribosomal run-off under stress condition (Li et al. 2010). Given the unfavorable phosphorylation state of other elongation factors during stress, non-functional eIF5A led to increasing ribosomal run time and to ribosome stalling which prevents to polysome run-off. Polysome run-off is critical for mRNP foci formation under stress (Grousl et al. 2009) (reviewed in (Mitchell and Parker 2014)). In this respect, the effect of eIF5A-3 mutation on SGs assembly in *S. cerevisiae* might be explained by this alteration of polysomes which is typical for the CHX treatment and translation arrest in elongation phase.

eIF5A-3 mutant might also alter expression of poly-Pro-proteins in a manner similar to experiment with eIF5A-S149 ts strain in semi-permissive conditions, which led to decrease in proline-rich protein levels (Gutierrez et al. 2013). One of the proteins that might be influenced by this change is Eap1 (EIF4E-Associated Protein 1), which contains two motives of six proline stretches. Eap1 competes with eIF4G for binding to eIF4E, effectively inhibiting cap-dependent translation initiation during stress response. This might have effect on SG formation. Other indirect effect of eIF5A-3 mutant on aggregation of SGs might lie in aforementioned prione-like proteins and their promiscuous interaction with other misfolded proteins, which promote SGs formation (Kroschwald et al. 2015).

Results of our microscopic observations and subsequent image analyses indicate clear and significant link between the eIF5A-3 mutant and decrease in granularity of cells during exposure to robust heat shock and throughout recovery. Recovery experiments also suggest that, even though SGs formation in the mutant is impaired, SGs dynamics, or at least dynamics during recovery, remain similar to wild-type cells. An average granularity slope in cells reach values comparable with control samples after two hours of recovery in both WT and A-3 mutant cells. However, exact principal of eIF5A influence on SG formation remains to be elucidated.

6.2 The influence of the eIF5A-3 ts mutation on growth and viability

We found that the strains expressing the eIF5A-3 mutant exhibited increased doubling times. The time required for cell population to double varied between the expression systems and

was also affected by expression of fluorescent tags. Cell division in mutated strains took approximately from 1,5x to 2,4x more time than in WT cells. This result is in line with the observations about the effects of eIF5A degron line on cell proliferation (Kang and Hershey 1994) and with the importance of functional hypusinated eIF5A for cell growth (Park et al. 1993).

Ability of cells to endure and survive robust heat shock was tested in two independent experimental set-ups, with propidium iodine staining and with cell viability assay by plating and CFU (Colony Forming Units) counting. Propidium iodine tests were conducted alongside with SG recovery tests on chromosomal version of our system. The fraction of dead cells after 10 minutes of robust heat shock did not exceed 10% of the inspected populations in both wild-type and A-3 mutant strains. Number of dead cells peaked at 90 minutes, and then it started to drop at 120 minutes in both WT and A-3, presumably as recovering cells re-entered cell cycle, increasing their number and relatively decreasing proportion of dead cells.Viability assay by plating brought different results, varying substantially from propidium iodine staining. Viability of eIF5A-WT strains ranged from 48% to 75%, based on the expression system and duration of shock. While the viability of eIF5A-3 varied between 65% and 100%. Same trend was present in all experimental set-ups of viability testing by CFU counting. eIF5A-3 mutant cells exhibited higher CFU counts than WT cells, with the difference fluctuating from 17% to 39% in favor of mutant cells.

Number of plated CFU in control samples exceeded expected values, especially in the integrated version of the eIF5A-3 mutant. This can be explained by several possible reasons. Control samples, unlike the heat shocked samples, were not arrested in their cell cycle progression and fraction of the cells finished their division in time gap between sample measurement and plating. Other cells might finish their division due to physical strain put on them during plating. Some of the plated cells were not accounted for in concentration measurement by CASY Cell counter, due to their abnormal size. This could be true for the case of cells in final stage of cell division or small recently divided daughter cells (for more details refer to Materials and methods section Cell counting – CASY Cell Counter).

Seeming discrepancy between propidium iodine staining and CFU analysis results might in fact hide clues for probable impact of the eIF5A-3 mutant on cell viability. Data indicate that wild-type cells don’t undergo necrosis or apoptosis immediately, but rather stop their progression thru cell cycle and then probably slowly wither, without forming visible CFU, while the eIF5A-3 mutants continue to proliferate, in spite of stress, and form visible colonies. Plausible cause of eIF5A-3 mutant cell proliferation might be linked to their altered SG formation. Lower slope in brightness of the accumulated Rpg1-GFP signal, which is sign of less focused and more disperse SGs, is observed in SGs

of the eIF5A-3 mutant and could have several effects promoting progression in cell cycle after relive of stress conditions. One of the positive effects might be an increased pro-growth signaling in the mutant. MTORC1 one of the major players in signaling for growth is reported to be sequestered into SGs under robust heat shock as a part of stress response including the cell cycle arrest to protect cells from the DNA damage (Takahara and Maeda 2012). Qualitative changes in SGs of eIF5A-3 mutant cells might lead to lower retention of MTORC1 into SGs, effectively boosting pro-growth signaling. However SGs do also sequester some of the pro-apoptotic proteins, and decreased SG formation might also positively influence pro apoptotic signaling. Whole problem is probably more complex than the simple retention of mTORC1 and might include kinetics of movement in and out of granules (reviewed in (Kedersha et al. 2013)).

Loss of eIF5A-3 mutant's temperature-sensitive phenotype after a long-term cultivation is probably the most surprising result of this study. There are however many examples of gene deletions and mutations that lead to an adaptive response in the cell. This response often results in substantial changes in genome and gene expression (Teng et al. 2013). Chance of adaptive genomic changes, which would lead to restoration of fitness, increases with severity of deleterious mutation. Strong impact of eIF5A-3 mutant on cell doubling time might be sufficient to induce such changes in 6 weeks of cultivation. Compensational mutations lead to similar adaptation in terms of function; however they can differ significantly in their molecular nature and mechanism in between subpopulations. Moreover, adaptive mutations accumulated to compensate for mutation are conditional to environment, with other possible positive or negative hidden effects that manifest themselves in new conditions (Szamecz et al. 2014). Compensational changes arising in the eIF5A-3 mutant to compensate its fitness in normal conditions had also positive impact on reversion of the ts phenotype at 37°C. Difference in ts suppression and growth rate among clones of eIF5-3 mutant can be attributed to different molecular mechanism of adapted compensational mutations.

6.3 Actin cytoskeleton after heat shock – preliminary data

Actin cytoskeleton is very dynamic structure, sensitive to various extracellular and intracellular stimuli. State of actin is functionally intertwined with state of translation. As mentioned in literature review functional eIF5A is protein crucial for proper translation and prevention of stalling on polyproline stretches. In this respect, the eIF5A-3 mutation appears to have a significant impact on the rate of the actin network rearrangement in cells recovering from the robust heat shock at 46°C and the heat shock at 42°C for 10 minutes. Actin cables in the mutant cells recovered and formed again at a faster rate than in wild-type cells. After the 42°C heat shock there were visible cables in both, WT and A-3 strains as soon as 4 minutes of recovery and the mutant cells showed

much higher proportion of cells with cables. Difference in dynamics became even more prominent in cells recovering from robust heat shock at 46°C. At 4 minutes of recovery did both WT and A-3 mutant exhibit F-actin collapsed in patches. However, A-3 mutant already recovered actin cables in part of observed cells after 14 minutes of recovery, while wild-type cells still retained F-actin in patches. Possible reasons for the observed phenotype are not fully elucidated, but likely candidates affected by the eIF5A-3 mutation are listed below since many proteins crucial for actin organization are rich in polyproline motives. In fact five of *S. cerevisiae* proteins with highest poly-proline content are functionally intercontected with actin organization: VRP1 (Proline-rich actin associated protein, 9P, 8P, 6P, 4x5P, 3x4P, 2x3P), LAS17 (Actin assembly factor, 6P, 8x5P), AIM3 (Protein that inhibits barbed-end actin filament elongation, 5P, 2x4P, 6x3P), BNI1 (formin, 12P, 10P, 5P) and BNR1 (formin, nucleates the formation of linear actin filaments, 11P, 8P, 2x3P)(Mandal et al. 2014).

Mutant eIF5A-3 might influence the expression levels of formins crucial for elongation of actin cables more severally than other eIF5A mutants (Li et al. 2014). But isolated direct effect of decreased formin levels would probably have effect opposite to observed phenotype, hindering recovery of cables rather than increasing their dynamics (Evangelista et al. 2003). Final phenotype might be result of change in dynamics and stechiometry in interactions among various Actin Binding Proteins (ABPs) affecting dynamics and structure of actin network.

Indirect effect of eIFA-3 mutation on actin dynamics might be linked to difference in their SG formation. SGs sequester many proteins active in signaling network, for instance mTORC1 (Takahara and Maeda 2012). Lower slope of SGs in A-3 mutants cells might cause lesser sequestration of signaling proteins leading to increased pro-growth signaling during the recovery from stress, which also positively stimulates actin cytoskeleton. mTORC2 signaling pathway is responsible for remodelating of the actin cytoskeleton, although mTORC2 does not sequester into SGs, in mammals some of its downstream effectors such as RhoA GTPase localize into SGs, it is tempting to speculate that the yeast Rho-like GTPase RHO1 and RHO2 localize into SGs in similar manner (Tsai and Wei 2010).

7 Conclusions

In previous studies on yeast, eIF5A was determined to play substantial role in formation of P-bodies. Goals of this thesis were to elucidate whether the influence of translation factor eIF5A on mRNP foci formation extends to heat stress granules and their assembly. Second goal was to evaluate importance of SGs in recovery of cells from the heat stress. In this work, we used eIF5A-WT and eIF5A-3 variants of eIF5A gene to study the effect of impaired eIF5A function on assembly of stress granules under robust heat shock of 46°C.

Microscopic observations indicate that eIF5A also affects formation of SGs under robust heat shock. The eIF5A-3 mutant phenotype shows a substantial drop in the SGs slope, in both plasmid and chromosomal version, with approximately 0,66x of values observed in the case of eIF5A-WT. This indicates a decreased density of SG accumulations. The effect of eIF5A-3 mutant can't be reversed by a prolonged exposure to stress conditions. In addition, granularity of eIF5A-3 mutant did not differ significantly from values obtained under the non-permissive conditions, which lead to depletion of eIF5A in cells. Overall these results indicate critical role of eIF5A protein in SGs formation and importance of the mutated amino acids, and surrounding regions, for the eIF5A function in SG formation. Role of eIF5A in dynamics of SGs formation is still disputable, since granularity of both WT and A-3 mutant recovered to basal values around two hours after the release of cells from the stress.

The cell viability was assessed by propidium iodine (PI) staining and CFU assays. While the PI stained fraction of dead cells in both WT and A-3 was similar and 2 hours after shock did not exceed 10% of cells. CFU assay showed higher effect of heat shock on colony growth with considerable better survival rates for eIF5A-3. This seeming discrepancy in data might indicate that WT cells do not undergo necrosis or apoptosis immediately, but rather stop their progression thru cell cycle and then probably slowly wither, without forming visible CFU, while the eIF5A-3 mutants, with aberrant SGs, continue to proliferate, in spite of stress, and form visible colonies.

We also characterized impact of eIF5A-3 mutation on proliferation. The cell growth rate is substantially affected by eIF5A-3 mutation increasing doubling time to range from 1.5 to 2.4 fold of wild-type cells, based on expression system. eIF5A-3 mutation was reported and indeed it is temperature sensitive. That is why probably the most surprising result of our experiments was the observed reversion of temperature sensitive phenotype of eIF5A-3 mutant, after 6 weeks of continuous cultivation on YPD plates at 25°C.

Preliminary results also suggest that eIF5A-3 influences the dynamics of actin, visibly increasing actin cables recovery after robust heat shock.

8 References

Anderson, P., and N. Kedersha. (2006). RNA granules. The Journal of cell biology 172:803–8.

Balagopal, V., and R. Parker. (2009). Polysomes, P bodies and stress granules: states and fates of eukaryotic mRNAs. Current opinion in cell biology 21:403–8.

Benne, R., and J. Hershey. (1978). The mechanism of action of protein synthesis initiation factors from rabbit reticulocytes. Journal of Biological Chemistry 253:3078–87.

Betz, C., and M. N. Hall. (2013). Where is mTOR and what is it doing there? The Journal of cell biology 203:563–74.

Brant-Zawadzki, P. B., D. I. Schmid, H. Jiang, A. S. Weyrich, G. A. Zimmerman, and L. W. Kraiss. (2007). Translational control in endothelial cells. Journal of vascular surgery 45 Suppl A:A8–14.

Buchan, J. R., D. Muhlrad, and R. Parker. (2008). P bodies promote stress granule assembly in Saccharomyces cerevisiae. The Journal of cell biology 183:441–55.

Connor, J. H., and D. S. Lyles. (2002). Vesicular stomatitis virus infection alters the eIF4F translation initiation complex and causes dephosphorylation of the eIF4E binding protein 4E-BP1. Journal of virology 76:10177–87.

Cougot, N., S. N. Bhattacharyya, L. Tapia-Arancibia, R. Bordonne, W. Filipowicz, E. Bertrand, and F. Rage. (2008). Dendrites of Mammalian Neurons Contain Specialized P-Body-Like Structures That Respond to Neuronal Activation. Journal of Neuroscience 28:13793–13804.

Dias, C. a O., V. S. P. Cano, S. M. Rangel, L. H. Apponi, M. C. Frigieri, J. R. C. Muniz, W. Garcia, et al. (2008). Structural modeling and mutational analysis of yeast eukaryotic translation initiation factor 5A reveal new critical residues and reinforce its involvement in protein synthesis. The FEBS journal 275:1874–88.

Evangelista, M., S. Zigmond, and C. Boone. (2003). Formins: signaling effectors for assembly and polarization of actin filaments. Journal of cell science 116:2603–11.

Gilks, N., N. Kedersha, M. Ayodele, L. Shen, G. Stoecklin, L. M. Dember, and P. Anderson. (2004). Stress granule assembly is mediated by prion-like aggregation of TIA-1. Molecular biology of the cell 15:5383–98.

Gregio, A. P. B., V. P. S. Cano, J. S. Avaca, S. R. Valentini, and C. F. Zanelli. (2009). eIF5A has a function in the elongation step of translation in yeast. Biochemical and biophysical research communications 380:785–90.

Gross, S. R., and T. G. Kinzy. (2005). Translation elongation factor 1A is essential for regulation of the actin cytoskeleton and cell morphology. Nature structural & molecular biology 12:772–8.

Gross, S. R., and T. G. Kinzy. (2007). Improper organization of the actin cytoskeleton affects protein synthesis at initiation. Molecular and cellular biology 27:1974–89.

Grousl, T., P. Ivanov, I. Frýdlová, P. Vasicová, F. Janda, J. Vojtová, K. Malínská, et al. (2009). Robust heat shock induces eIF2alpha-phosphorylation-independent assembly of stress granules containing eIF3 and 40S ribosomal subunits in budding yeast, Saccharomyces cerevisiae. Journal of cell science 122:2078–88.

Grousl, T., P. Ivanov, I. Malcova, P. Pompach, I. Frydlova, R. Slaba, L. Senohrabkova, et al. (2013). Heat shock-induced accumulation of translation elongation and termination factors precedes assembly of stress granules in S. cerevisiae. PloS one 8:e57083.

Gutierrez, E., B.-S. Shin, C. J. Woolstenhulme, J.-R. Kim, P. Saini, A. R. Buskirk, and T. E. Dever. (2013). eIF5A promotes translation of polyproline motifs. Molecular cell 51:35–45.

Haghighat, a, S. Mader, a Pause, and N. Sonenberg. (1995). Repression of cap-dependent translation by 4E-binding protein 1: competition with p220 for binding to eukaryotic initiation factor-4E. The EMBO journal 14:5701–9.

Huh, W.-K., J. V Falvo, L. C. Gerke, A. S. Carroll, R. W. Howson, J. S. Weissman, and E. K. O'Shea. (2003). Global analysis of protein localization in budding yeast. Nature 425:686–91.

Chang, L., and M. Karin. (2001). Mammalian MAP kinase signalling cascades. Nature 410:37–40.

Chatterjee, I., S. R. Gross, T. G. Kinzy, and K. Y. Chen. (2006). Rapid depletion of mutant eukaryotic initiation factor 5A at restrictive temperature reveals connections to actin cytoskeleton and cell cycle progression. Molecular genetics and genomics : MGG 275:264–76.

Chattopadhyay, M. K., M. H. Park, and H. Tabor. (2008). Hypusine modification for growth is the major function of spermidine in Saccharomyces cerevisiae polyamine auxotrophs grown in limiting spermidine. Proceedings of the National Academy of Sciences of the United States of America 105:6554–9.

Jackson, R. J., C. U. T. Hellen, and T. V Pestova. (2010). The mechanism of eukaryotic translation initiation and principles of its regulation. Nature reviews. Molecular cell biology 11:113–27.

Kandl, K. a, R. Munshi, P. a Ortiz, G. R. Andersen, T. G. Kinzy, and a E. M. Adams. (2002). Identification of a role for actin in translational fidelity in yeast. Molecular genetics and genomics : MGG 268:10–8.

Kang, H. A., and J. W. Hershey. (1994). Effect of initiation factor eIF-5A depletion on protein synthesis and proliferation of Saccharomyces cerevisiae. The Journal of biological chemistry 269:3934–40.

Kedersha, N., and P. Anderson. (2002). Stress granules: sites of mRNA triage that regulate mRNA stability and translatability. Biochemical Society transactions 30:963–9.

Kedersha, N., P. Ivanov, and P. Anderson. (2013). Stress granules and cell signaling: more than just a passing phase? Trends in biochemical sciences 38:494–506.

Kim, S., and P. A. Coulombe. (2010). Emerging role for the cytoskeleton as an organizer and regulator of translation. Nature reviews. Molecular cell biology 11:75–81.

Kim, W. J., S. H. Back, V. Kim, I. Ryu, and S. K. Jang. (2005). Sequestration of TRAF2 into stress granules interrupts tumor necrosis factor signaling under stress conditions. Molecular and cellular biology 25:2450–62.

Kimball, S. R., R. L. Horetsky, D. Ron, L. S. Jefferson, and H. P. Harding. (2003). Mammalian stress granules represent sites of accumulation of stalled translation initiation complexes. American journal of physiology. Cell physiology 284:C273–84.

Kroschwald, S., S. Maharana, D. Mateju, L. Malinovska, E. Nüske, I. Poser, D. Richter, et al. (2015). Promiscuous interactions and protein disaggregases determine the material state of stress-inducible RNP granules. eLife 4:1–32.

Lee, S. B., J. H. Park, J. Kaevel, M. Sramkova, R. Weigert, and M. H. Park. (2009). The effect of hypusine modification on the intracellular localization of eIF5A. Biochemical and biophysical research communications 383:497–502.

Levin, D. H., D. Kyner, and G. Acs. (1973). Protein initiation in eukaryotes: formation and function of a ternary complex composed of a partially purified ribosomal factor, methionyl transfer RNA, and

guanosine triphosphate. Proceedings of the National Academy of Sciences of the United States of America 70:41–5.

Li, C. H., T. Ohn, P. Ivanov, S. Tisdale, and P. Anderson. (2010). eIF5A promotes translation elongation, polysome disassembly and stress granule assembly. PloS one 5:e9942.

Li, T., B. Belda-Palazón, A. Ferrando, and P. Alepuz. (2014). Fertility and Polarized Cell Growth Depends on eIF5A for Translation of Polyproline-Rich Formins in Saccharomyces cerevisiae. Genetics.

Lõoke, M., K. Kristjuhan, and A. Kristjuhan. (2011). Extraction of genomic DNA from yeasts for PCR-based applications. Biotechniques 50:325–328.

Loschi, M., C. C. Leishman, N. Berardone, and G. L. Boccaccio. (2009). Dynein and kinesin regulate stress-granule and P-body dynamics. Journal of cell science 122:3973–82.

Mandal, A., S. Mandal, and M. H. Park. (2014). Genome-Wide Analyses and Functional Classification of Proline Repeat-Rich Proteins: Potential Role of eIF5A in Eukaryotic Evolution. PloS one 9:e111800.

Mateyak, M. K., and T. G. Kinzy. (2010). eEF1A: thinking outside the ribosome. The Journal of biological chemistry 285:21209–13.

Mathews, M. B., and J. W. B. Hershey. (2015). The translation factor eIF5A and human cancer. Biochimica et biophysica acta 1849:836–44.

Mitchell, S. F., and R. Parker. (2014). Principles and properties of eukaryotic mRNPs. Molecular cell 54:547–58.

Nakagawa, J. (2008). Transient responses via regulation of mRNA stability as an immuno-logical strategy for countering infectious diseases. Infectious disorders drug targets 8:232–40.

Park, M. H., K. Nishimura, C. F. Zanelli, and S. R. Valentini. (2010). Functional significance of eIF5A and its hypusine modification in eukaryotes. Amino acids 38:491–500.

Park, M. H., E. C. Wolff, and J. E. Folk. (1993). Is hypusine essential for eukaryotic cell proliferation? Trends in Biochemical Sciences 18:475–479.

Pavlov, M. Y., R. E. Watts, Z. Tan, V. W. Cornish, M. Ehrenberg, and A. C. Forster. (2009). Slow peptide bond formation by proline and other N-alkylamino acids in translation. Proceedings of the National Academy of Sciences of the United States of America 106:50–4.

Pestova, T. V, and V. G. Kolupaeva. (2002). The roles of individual eukaryotic translation initiation factors in ribosomal scanning and initiation codon selection. Genes & development 16:2906–22.

Pittman, Y. R., K. Kandl, M. Lewis, L. Valente, and T. G. Kinzy. (2009). Coordination of eukaryotic translation elongation factor 1A (eEF1A) function in actin organization and translation elongation by the guanine nucleotide exchange factor eEF1Balpha. The Journal of biological chemistry 284:4739–47.

Proud, C. G. (2005). eIF2 and the control of cell physiology. Seminars in cell & developmental biology 16:3–12.

Rauscher, S., S. Baud, M. Miao, F. W. Keeley, and R. Pomès. (2006). Proline and glycine control protein self-organization into elastomeric or amyloid fibrils. Structure (London, England : 1993) 14:1667–76.

Rinnerthaler, M., R. Lejskova, T. Grousl, V. Stradalova, G. Heeren, K. Richter, L. Breitenbach-Koller, et al. (2013). Mmi1, the yeast homologue of mammalian TCTP, associates with stress granules in heat-shocked cells and modulates proteasome activity. PloS one 8:e77791.

Roy, B., J. N. Vaughn, B. Kim, F. Zhou, M. A. Gilchrist, and A. G. V. O. N. Arnim. (2010). The h subunit of eIF3 promotes reinitiation competence during translation of mRNAs harboring upstream open reading frames 748–761.

Rudra, D., and J. R. Warner. (2004). What better measure than ribosome synthesis? Genes & development 18:2431–6.

Saavedra, C., K. S. Tung, D. C. Amberg, A. K. Hopper, and C. N. Cole. (1996). Regulation of mRNA export in response to stress in Saccharomyces cerevisiae. Genes & development 10:1608–20.

Saini, P., D. E. Eyler, R. Green, and T. E. Dever. (2009). Hypusine-containing protein eIF5A promotes translation elongation. Nature 459:118–21.

Sattlegger, E., M. J. Swanson, E. a Ashcraft, J. L. Jennings, R. a Fekete, A. J. Link, and A. G. Hinnebusch. (2004). YIH1 is an actin-binding protein that inhibits protein kinase GCN2 and impairs general amino acid control when overexpressed. The Journal of biological chemistry 279:29952–62.

Serero, A., C. Jubin, S. Loeillet, P. Legoix-Né, and A. G. Nicolas. (2014). Mutational landscape of yeast mutator strains. Proceedings of the National Academy of Sciences of the United States of America 111:1897–902.

Schisa, J. A., J. N. Pitt, and J. R. Priess. (2001). Analysis of RNA associated with P granules in germ cells of C . elegans adults 1298:1287–1298.

Sikorski, R. S., and P. Hieter. (1989). A system of shuttle vectors and yeast host strains designed for efficient manipulation of DNA in Saccharomyces cerevisiae. Genetics 122:19–27.

Simpson, C. E., and M. P. Ashe. (2012). Adaptation to stress in yeast: to translate or not? Biochemical Society transactions 40:794–9.

Sonenberg, N., and A. G. Hinnebusch. (2009). Regulation of translation initiation in eukaryotes: mechanisms and biological targets. Cell 136:731–45.

Stirling, P. C., Y. Shen, R. Corbett, S. J. M. Jones, and P. Hieter. (2014). Genome destabilizing mutator alleles drive specific mutational trajectories in Saccharomyces cerevisiae. Genetics 196:403–12.

Swisher, K. D., and R. Parker. (2010). Localization to, and effects of Pbp1, Pbp4, Lsm12, Dhh1, and Pab1 on stress granules in Saccharomyces cerevisiae. PloS one 5:e10006.

Szamecz, B., G. Boross, D. Kalapis, K. Kovács, G. Fekete, Z. Farkas, V. Lázár, et al. (2014). The genomic landscape of compensatory evolution. PLoS biology 12:e1001935.

Takahara, T., and T. Maeda. (2012). Transient sequestration of TORC1 into stress granules during heat stress. Molecular cell 47:242–52.

Teng, X., M. Dayhoff-Brannigan, W.-C. Cheng, C. E. Gilbert, C. N. Sing, N. L. Diny, S. J. Wheelan, et al. (2013). Genome-wide consequences of deleting any single gene. Molecular cell 52:485–94.

Thomas, M. G., M. Loschi, M. A. Desbats, and G. L. Boccaccio. (2011). RNA granules: the good, the bad and the ugly. Cellular signalling 23:324–34.

Thompson, D. M., C. Lu, P. J. Green, and R. Parker. (2008). tRNA cleavage is a conserved response to oxidative stress in eukaryotes. RNA (New York, N.Y.) 14:2095–103.

Tsai, N.-P., and L.-N. Wei. (2010). RhoA/ROCK1 signaling regulates stress granule formation and apoptosis. Cellular signalling 22:668–75.

Ude, S., J. Lassak, A. L. Starosta, T. Kraxenberger, D. N. Wilson, and K. Jung. (2013). Translation elongation factor EF-P alleviates ribosome stalling at polyproline stretches. Science (New York, N.Y.) 339:82–5.

Uesono, Y., and A. Toh-E. (2002). Transient inhibition of translation initiation by osmotic stress. The Journal of biological chemistry 277:13848–55.

Valásek, L., H. Trachsel, J. Hasek, and H. Ruis. (1998). Rpg1, the Saccharomyces cerevisiae homologue of the largest subunit of mammalian translation initiation factor 3, is required for translational activity. The Journal of biological chemistry 273:21253–60.

Valášek, L. S. (2012). "Ribozoomin"--translation initiation from the perspective of the ribosome-bound eukaryotic initiation factors (eIFs). Current protein & peptide science 13:305–30.

Williamson, M. P. (1994). The structure and function of proline-rich regions in proteins. The Biochemical journal 297 (Pt 2:249–60.

Yamamoto, Y., C. R. Singh, A. Marintchev, N. S. Hall, E. M. Hannig, G. Wagner, and K. Asano. (2005). The eukaryotic initiation factor (eIF) 5 HEAT domain mediates multifactor assembly and scanning with distinct interfaces to eIF1, eIF2, eIF3, and eIF4G. Proceedings of the National Academy of Sciences of the United States of America 102:16164–9.

Yueh, A., and R. J. Schneider. (2000). Translation by ribosome shunting on adenovirus and hsp70 mRNAs facilitated by complementarity to 18S rRNA. Genes & development 14:414–21.

Zhang, S., L. Sun, and F. Kragler. (2009). The phloem-delivered RNA pool contains small noncoding RNAs and interferes with translation. Plant physiology 150:378–87.

Ziegler, J., C. Viehrig, S. Geimer, P. Rösch, and S. Schwarzinger. (2006). Putative aggregation initiation sites in prion protein. FEBS letters 580:2033–40.